Global and Planetary Change 201 (2021) 103475

Contents lists available at ScienceDirect

Global and Planetary Change

journal homepage: www.elsevier.com/locate/gloplacha

Research article

Crustal exhumation and depocenter migration from the Alpine orogenic margin towards the Pannonian extensional back-arc basin controlled by inheritance

László Fodor [a,b,*], Attila Balázs [c], Gábor Csillag [b,d], István Dunkl [e], Gábor Héja [f], Bogomir Jelen [g], Péter Kelemen [e,h], Szilvia Kövér [a,b], András Németh [i], Dániel Nyíri [i], Ildikó Selmeczi [f], Mirka Trajanova [g], Marko Vrabec [j], Mirijam Vrabec [j]

[a] Department of Geology, Eötvös University, Pázmány Péter sétány 1/C, 1117 Budapest, Hungary
[b] ELKH-ELTE Geological, Geophysical and Space Science Research Group at Eötvös University, Hungary
[c] ETH Zürich, Geophysical Fluid Dynamics Group, Institute of Geophysics, Zürich, Switzerland
[d] Research Centre for Astronomy and Earth Sciences, Institute for Geological and Geochemical Research, Budaörsi út 45, 1112 Budapest, Hungary
[e] Sedimentology, Environmental Geology, Geoscience Center, University of Göttingen, Goldschmidtstrasse 3, D-37077 Göttingen, Germany
[f] Mining and Geological Survey of Hungary, Stefánia út 14, 1143 Budapest, Hungary
[g] Geological Survey of Slovenia, Dimičeva 14, Ljubljana, Slovenia
[h] Department of Petrology and Geochemistry, Eötvös University, Budapest, Hungary
[i] MOL Plc., Október 23. u. 18, 1117 Budapest, Hungary
[j] Department of Geology, University of Ljubljana, Faculty of Natural Sciences and Engineering, Aškerčeva 12, 1000 Ljubljana, Slovenia

ARTICLE INFO

Keywords:
Extension
Exhumation
Thermochronology
Thermomechanical modelling
Inheritance
Pannonian Basin

ABSTRACT

The formation and deformation history of back-arc basins play a critical role in understanding the tectonics of plate interactions. Furthermore, opening of extensional back-arc basins during the overall convergence between Africa and Europe is a fundamental process in the overall tectonic evolution of the Mediterranean and adjacent areas. In this frame, Miocene tectonic evolution of the western Pannonian Basin of Central Europe and its connection to inherited Cretaceous structures of the Eastern Alpine nappes are presented.

Revision of published and addition of new structural and thermochronological data, as well as seismic profiles from the western Pannonian Basin is complemented by high-resolution thermo-mechanical numerical modeling in order to propose a new physically consistent tectono-sedimentary model for the basin evolution. The onset of extension is dated as ~25–23 Ma, and higher rates are inferred between 19 and 15 Ma at the south-western part of the area (Pohorje, Kozjak Domes, Murska Sobota Ridge, and Mura-Zala Basin). Rift initiation involved the exhumation of the middle part of the Austroalpine nappe pile along low-angle detachment faults and mylonite zones. The Miocene low-angle shear zones could reactivate major Cretaceous thrust boundaries, the exhumation channel of ultra-high-pressure rocks of the Pohorje Dome, or Late Cretaceous extensional structures. Miocene extension was associated with granodiorite and dacite intrusions between 18.64 and 15 Ma. The Pohorje pluton intruded at variable depth from ~4 to 16–18 km and experienced ductile stretching, westward tilting, and asymmetric exhumation of its eastern side. Terrestrial early Miocene (Ottnangian to Karpatian, 19–17.25 Ma) syn-rift depositional environment in supradetachment basins evolved to near-shore and bathyal one by the middle Miocene (Badenian, 15.97–12.8 Ma). Deformation subsequently migrated eastwards to the western part of the Transdanubian Range (Keszthely Hills) and to newly formed grabens. In this formerly emerged terrestrial area active faulting started at 15–14.5 Ma and continued through the late Miocene almost continuously up to ~8 Ma but basically terminated in the Mura-Zala Basin by ~15 Ma (early Badenian). These observations suggest a ~200 km shift of active faulting, basin formation, and related syn-tectonic sedimentation from the SW (Pohorje and Mura-Zala Basin) toward the Pannonian Basin center. Building on the above described observational and modeling data makes the Pannonian Basin an ideal natural laboratory for understanding the coupling between deep Earth and surface processes.

* Corresponding author at: Department of Geology, Eötvös University, Budapest, Hungary.
E-mail address: imre.laszlo.fodor@ttk.elte.hu (L. Fodor).

https://doi.org/10.1016/j.gloplacha.2021.103475
Received 15 July 2020; Received in revised form 15 February 2021; Accepted 19 March 2021
Available online 24 March 2021

1. Introduction

Stretching and thinning of the continental lithosphere is a first-order plate tectonic process, which creates a wide spectrum of extensional structures and sedimentary basin geometries. The style of rifting is driven by the links between multiple inherited compositional and thermal properties of the lithosphere and local or external forcing factors (e.g., Brun, 1999; Lavier and Manatschal, 2006). The classical pure shear models assumed that crustal and lithospheric stretching is accommodated symmetrically (McKenzie, 1978). Availability of high resolution marine seismic and geological data suggests that most extensional basins including passive margins and continental back-arc basins show pronounced asymmetry of their crustal and lithospheric structures (Péron-Pinvidic and Manatschal, 2009) despite that plate divergence is a symmetrical process (Jolivet et al., 2018). Classical models proposed strain localization along lithospheric-scale simple shear zones (Lister et al., 1986; Wernicke, 1985) cutting through the entire crust and mantle. However, in most cases weak ductile layers decouple the deformation in the upper and lower crust or in the lithospheric mantle (Balázs et al., 2017; Burov, 2011).

Rift initiation often occurs along weak crustal or lithospheric structures inherited from preceding orogenic evolution (e.g., Dunbar and Sawyer, 1988; Duretz et al., 2016; Heron et al., 2016; Ustaszewski et al., 2010). From a mechanical point of view reactivation of former thrusts as normal faults is not an easy task due to the low angle nature of the thrust structures (Faccenna et al., 1995; Windhoffer et al., 2005). However, weak zones, such as inherited suture zones in the mantle (Tommasi and Vauchez, 2001) or major nappe contacts provide sufficiently weak rheological contrasts to localize deformation, where extensional normal faults could cross-cut the pre-existing thrusts or partially reactivate their segments (as proposed by Tari et al., 2021, for the Pannonian Basin).

Following rift initiation and the activation of low-angle detachments and rotating normal faults exhuming mid- to lower crustal rocks at the basin margins, further deformation is accommodated by sequential normal faulting in the upper crust (Ranero and Perez-Gussinye, 2010) and the locus of high strain deformation migrates hundreds of kilometers towards the new depocenter (Naliboff and Buiter, 2015). Migration of active deformation is a general process affecting extensional basins at multiple spatial and temporal scales. Basin migration can reflect variation of slow extension or tectonic quiescence and subsequent increased stretching or constant low rate stretching and associated time-dependent strengthening of the old rift zone that is inferred for the multiphase rifting in the mid-Norwegian and Galicia margins (van Wijk and Cloetingh, 2002). In extensional back-arc basins, where the rate of rifting is substantially higher than in most continental rifts the migration of active lithospheric extension is proposed to be linked to trench dynamics and slab-induced and external mantle flow effects, for instance in the case of the Liguro-Provencal and Tyrrhenian Sea extension in the Central Mediterranean (Faccenna et al., 2014). It has been shown by numerical models that rift asymmetry and the migration of active deformation is inherently linked to the asymmetrical ascent and lateral motion of the asthenosphere (Balázs et al., 2017; Brune et al., 2014). Sequential faulting and depocenter migration within one basin system is also controlled by the lateral differences of thermal or mechanical weakening effects supported by shear stresses from the asthenosphere (Jolivet et al., 2018).

In this study, we review and complement with unpublished structural data the evolution of Miocene structures related to the formation of the southwestern Pannonian Basin of Central Europe (Fig. 1). The paper aims to investigate the role of low-angle detachment faults and the connecting transfer faults in rifting. We review the formerly published thermochronological and stratigraphic data and supplemented with new data and interpretation. The compilation of such data enabled us to propose a robust fine-resolution temporal evolution of faulting and basin subsidence, which shows a clear spatial migration from the southwestern margin toward the basin center. In addition, the paper investigates how modern modelling results are in accordance with the observations, and how the model-predicted deep Earth processes explain the migration of near-surface processes, such as faulting and basin subsidence.

2. Geological setting

2.1. Tectonic framework of the Pannonian Basin

The Pannonian Basin (PB) of Central Europe is a large extensional

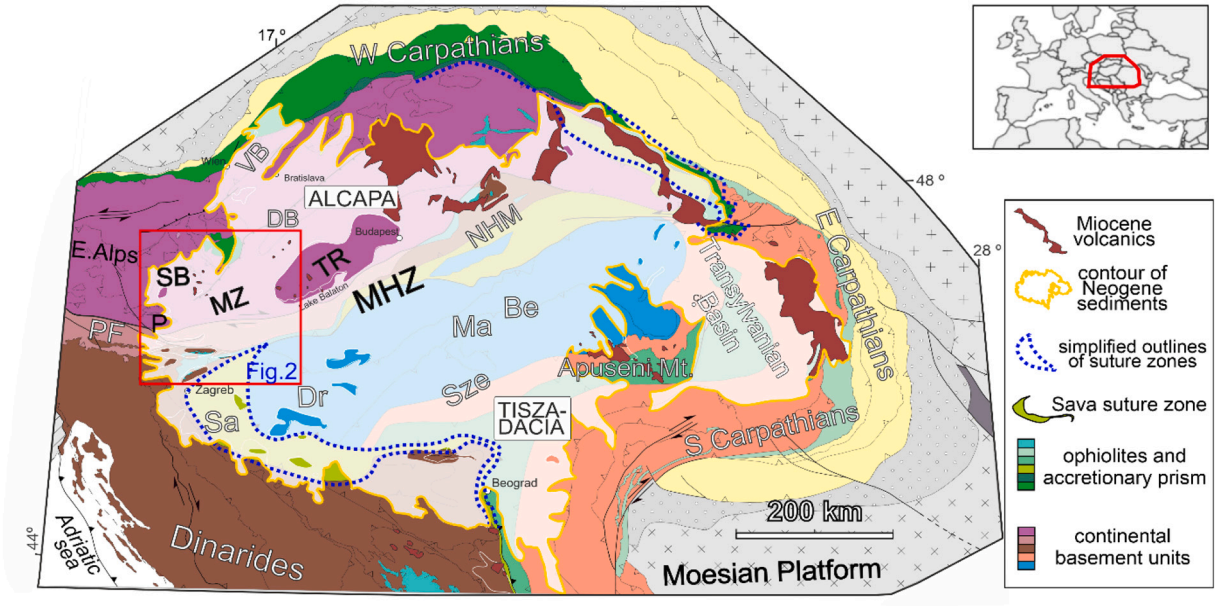

Fig. 1. The Pannonian Basin within the Alpine-Carpathian-Dinaridic orogen. Basement map is after Schmid et al. (2020). Be = Békés Basin, DB = Danube Basin, Dr = Drava Basin, Ma = Makó Basin, MHZ = Mid-Hungarian Shear Zone, MZ = Mura-Zala Basin, NHM = North Hungarian Mountains, P = Pohorje Mts., PF = Periadriatic Fault, Sa = Sava Basin, SB = Styrian Basin TR = Transdanubian Range, VB = Vienna Basin. Note the suture zones at the Dinaridic and Carpathian margins of the basins, partially highlighted by simplified dotted lines.

basin system within the partly coeval orogenic arcs of the Eastern Alps, Carpathians, and Dinarides (Fig. 1; Royden et al., 1983; Horváth et al., 2015). Basin formation started in the early Miocene and subsidence lasted up to the end of Miocene in many sub-basins. The PB is composed of diverse structural elements including, but not limited to, low-angle normal shear zones, exhumed mid-crustal rocks, high-angle normal faults, and transfer strike-slip faults. Its history also involved vertical-axis rotation events (Márton and Márton, 1996, 1999; Márton et al., 2002b, 2015). The onset of extensional faulting and graben formation varies widely across the basins system, starting at ~25 Ma in the southern parts of the basin (Ustaszewski et al., 2010; Matenco and Radivojević, 2012) and as late as ~11–9 Ma in its central-eastern part (Balázs et al., 2016). The extensional setting was progressively overprinted by contraction and transpression during the latest Miocene resulting in basin inversion and uplift in large parts of the PB (Horváth and Cloetingh, 1996; Bada et al., 2007). Persistent subsidence in some depocenters lead to differential vertical motions and denudation of elevated areas (Ruszkiczay-Rüdiger et al., 2020).

Within the western and southern PB, a number of sub-basins developed, reaching a maximum depth of ~7.5 km (Royden et al., 1983; Royden and Horváth, 1988; Fodor et al., 2013; Horváth et al., 2015). Many of them are bounded by low-angle detachment faults or shear zones which exhumed metamorphic rocks from depths corresponding to ~250–450°C (Dunkl and Demény, 1997; Tari et al., 1999; Ustaszewski et al., 2010; Matenco and Radivojević, 2012; Cao et al., 2013). These metamorphic domes often show antiformal shapes and are connected by NE-SW striking faults, the role of which will be discussed later.

The timing of the transition from syn-rift to post-rift deformation was debated for a long time. Tari (1994) correctly recognized a major early middle Miocene unconformity in the western PB, which seals most of the normal faults and constrains the end of faulting between 15 and 14 Ma. However, in certain areas of the western PB, similarly to the most extended central parts of the basin (Matenco and Radivojević, 2012; Balázs et al., 2016), faulting and half-graben formation did not terminate before 8.7–8 Ma.

Extension in the eastern part of the Eastern Alps was accommodated by major low-angle detachment faults along the Tauern and Rechnitz windows, minor normal faults, and high-offset strike-slip faults (Genser and Neubauer, 1989; Ratschbacher et al., 1991a; Tari, 1996; Frisch et al., 2000; Rosenberg et al., 2018; van Gelder et al., 2020). The ensemble of these structures resulted in the eastward extrusion of the eastern part of the Eastern Alps from earliest Miocene time (Ratschbacher et al., 1989; Frisch et al., 2000; Wölfler et al., 2011). The southern boundary of the extruding wedge is the dextral Periadriatic Fault (Schmid et al., 1989) that initiated in the Oligocene (~32–30 Ma). Its continuation is found within the wide Mid-Hungarian Shear Zone (MHZ), a lithospheric-scale tectonic boundary separating the two main Cenozoic crustal blocks of the PB; the northern ALCAPA and southern Tisza-Dacia (Fig. 1; Balla, 1988; Csontos et al., 1992; Tari, 1994; Csontos and Nagymarosy, 1998). Although this shear zone is dominantly Miocene in age, its role as a Mesozoic to Paleogene transfer zone between the major Carpathian and Dinaric suture zones is probable (Handy et al., 2015; Schmid et al., 2020). The MHZ separated the major syn-rift basins and itself hosted several very deep (> 5 km) and narrow depressions (Haas et al., 2010; Horváth et al., 2015).

Extension of the Pannonian Basin was superimposed on the generally contractional Alpine–Carpathian–Dinaridic orogenic belt. Deep lithospheric structure, derived mostly from seismic tomographic data is still debated and can be interpreted as southward subduction of the European plate (Mitterbauer et al., 2011; Qorbani et al., 2015), northward subduction of the Adriatic plate (Lippitsch et al., 2003; Zhao et al., 2016) or a combination of both subductions (Kästle et al., 2020).

2.2. Main structural features in the SW Pannonian Basin

2.2.1. Basement units

The crustal part of the Eastern Alps is composed of nappes derived from (bottom to top) the subducted European plate (exposed in the Tauern window, Scharf et al., 2013; Rosenberg et al., 2018), oceanic crust and related sediments of the Alpine Tethys (Penninic unit), and the Adria-derived Austroalpine nappes as the highest unit which have several subdivisions varying between authors (Neubauer et al., 2000; Schuster et al., 2004; Schmid et al., 2004, 2020). The Penninic units composed of a dismembered ophiolite (Koller and Pahr, 1980) and deep-marine sediments are the lowermost ones exposed in the Rechnitz windows (Fig. 2a).

The overlying nappe stack comprises the Austroalpine nappe system, most of which are consisted of pre-Permian metamorphic rocks and overlying Permian to Mesozoic successions and were stacked together during the Eoalpine orogeny during the late Early to Late Cretaceous (Neubauer et al., 2000; Schmid et al., 2004). The Lower Austroalpine nappes (in the sense of Schmid et al., 2004, 2008; Schuster et al., 2004) appears only in the northern part adjacent to the Penninic windows (Fig. 2a) (Willingshofer and Neubauer, 2002; Neubauer et al., 2020). The overlying thick Upper Austroalpine nappe system (UAA) is composed of various metamorphic rocks; the most extensively distributed one is the Koralpe-Wölz (KW) unit, occupying a central position within the UAA (Froitzheim and Schuster, 2008). It comprises amphibolite to eclogite facies metamorphic rocks (Schuster et al., 2004), exhibiting high to ultrahigh-pressure conditions within the study area, in the Pohorje Mts. (Janák et al., 2015; Li et al., 2021). These (ultra) high-pressure rocks could form during intra-continental subduction (Schuster and Stüwe, 2008; Stüwe and Schuster, 2010) and thus represent a major crustal-scale weakness zone. They were exhumed by a large-scale isoclinal antiform and related shear zones (Kirst et al., 2010; Janák et al., 2015). Above the eclogitic rocks, the metamorphic degree is decreasing and frequently a sharp jump appears in the metamorphic grade. The low-grade to very low-grade metamorphic rocks and metasediments are part of the Drauzug-Gurktal (DG) unit (Schmid et al., 2004). The best outcropping part of this upper nappe complex is the Graz Paleozoic (Flügel and Neubauer, 1984), but other units are present below the Miocene fill of the Styrian and Mura-Zala Basins (Kröll et al., 1988). The highest tectonic unit is the Transdanubian Range (TR), composed of Variscan very low-grade rocks and non-metamorphosed Permian to Mesozoic sequences. Although a long time disputed, its nappe position above other Austroalpine units is confirmed by structural studies (Tari, 1994; Fodor et al., 2003; Tari and Horváth, 2010).

A great number of geochronological data constrain nappe emplacement to the Cretaceous (~100 – ~70 Ma, Frank et al., 1987; Dallmeyer et al., 1996, 1998;), while some of the oldest contractional deformations took place around 113 Ma in the highest TR unit (Szives et al., 2018). Late Cretaceous sediments with depositional age from ~85–70 Ma occur on top of the Drauzug-Gurktal and TR units (Fig. 2a) (Willingshofer et al., 1999). Although these basins were formed in an overall contractional setting of the entire Eoalpine orogen (Ortner et al., 2015; Tari and Linzer, 2018), near the study area the Late Cretaceous basin subsidence coincided with the exhumation of the high-pressure Koralpe-Wölz unit from below low-grade units along low-angle shear zones (Neubauer et al., 1995). Such structures include the Plattengneis mylonitic shear zone (Kurz et al., 2002), and the detachments below the Graz Paleozoic (Fig. 2) (Neubauer et al., 1995; Krenn et al., 2008; Herg and Stüwe, 2018).

2.2.2. Miocene basins, faults, and metamorphic domes

The westernmost studied sub-basin within the western PB is the *Slovenj Gradec Basin*. Its stratigraphy was recently updated (Ivančič et al., 2018) and contains late early to middle Miocene sediments (Ottnangian–Karpatian and early Badenian, ~18–13.8 Ma, see local chronostratigraphy in Hohenegger et al., 2014; Sant et al., 2017; Kováč

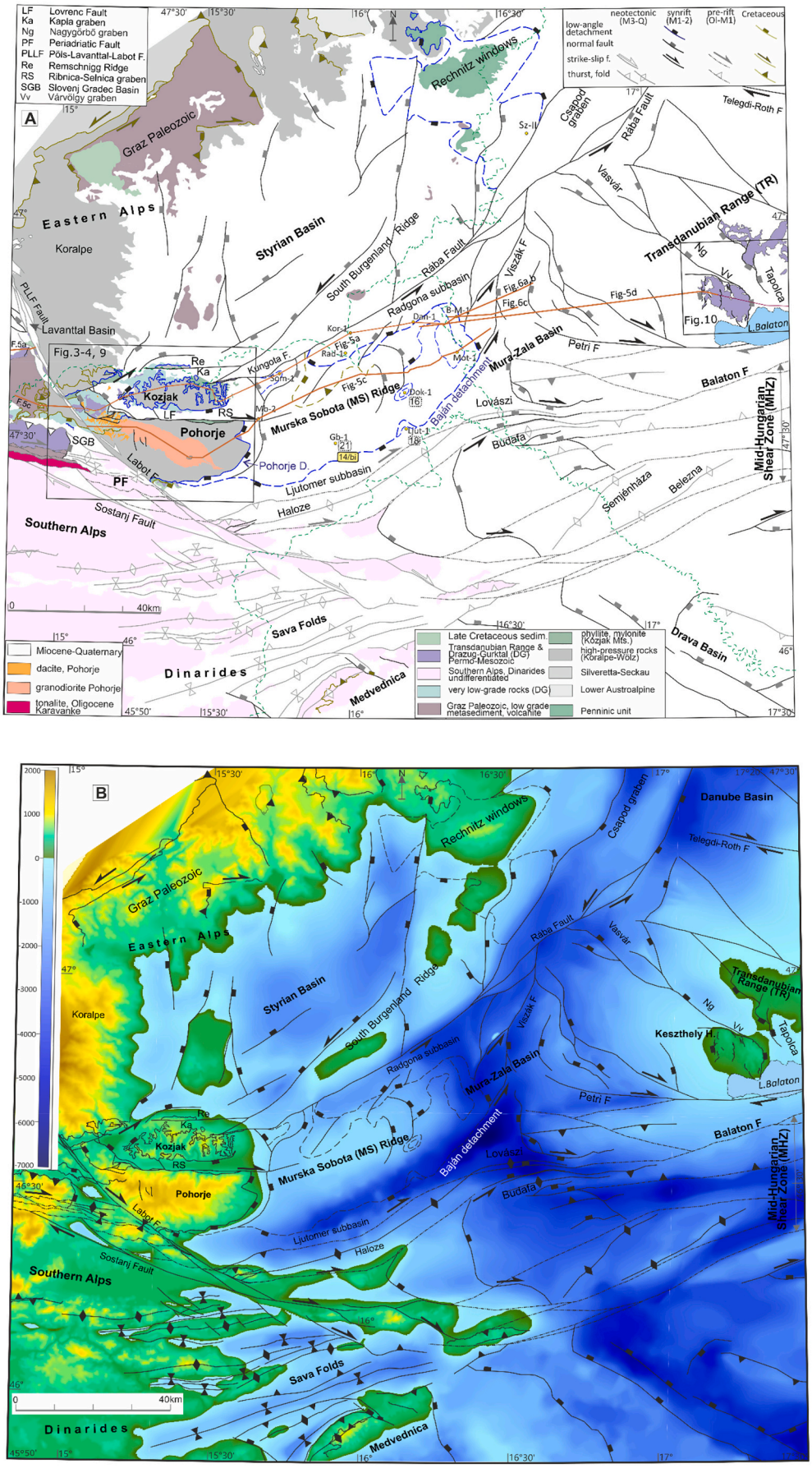

Fig. 2. a) Pre-Miocene units and Miocene to Quaternary structures of the study area, the western Pannonian Basin (based on maps of Flügel and Neubauer, 1984; Tomljenović and Csontos 2001; Fodor et al., 2013; Schmid et al., 2020). b) Morphology of the area shown in sub-figure a) integrating two surfaces; the base of syn-rift sediments and the present-day topography (when syn-rift sediments are missing). (Flügel et al., 1988; Gosar, 1995; Fodor et al., 2013; Haas et al., 2010; Cvetković et al., 2019; modified).

et al., 2018). Initially, the basin could probably be a part of the Ljutomer branch of the Mura-Zala Basin, later separated from the main part by the uplift of the Pohorje Dome and by the dextral offset on the Labot Fault (Fodor et al., 1998; Ivančič et al., 2018) (Fig. 2). This NW–SE striking fault is part of the long-lived *Pöls-Lavanttal-Labot Fault* system (PLLF). NW of the Pohorje Mts. branches of this dextral fault zone form the boundary of several small basins (Strauss et al., 2001; Kurz et al., 2011; Reischenbacher and Sachsenhofer, 2013).

Pohorje Mts. is a metamorphic dome that mainly consists of the Koralpe-Wölz nappe and is surrounded by low-grade metamorphic rocks or directly by non-metamorphosed nappes, belonging to the Drauzug-Gurktal and the Transdanubian Range units, respectively. The boundaries of these units were originally Cretaceous thrusts (Schmid et al., 2004), but now exhibit sharp changes in metamorphic degree (Trajanova, 2002; Herg and Stüwe, 2018). In the core of the dome, the granodioritic Pohorje pluton and subvolcanic dacite bodies intruded the host metamorphic rocks in the Miocene (Fig. 3) (Fodor et al., 2008; Trajanova et al., 2008; Poli et al., 2020). Intrusive rocks penetrate mostly into the KW nappe but in the northwest also into the Drauzug-Gurktal unit. The north-westernmost part of the Pohorje Mts., situated north of the main dacite body has a distinct structure, where only low-grade metamorphics, non-metamorphosed Permo-Mesozoic rocks and Miocene sedimentary and dacitic volcanic formations occur (Mioč and Žnidarčič, 1976).

The *Kozjak Dome* and the E–W trending *Remschnigg ridge* (bounding the Styrian Basin) have a similar structure as the Pohorje Dome but lacks Miocene magmatic rocks (Fig. 2). Here, Miocene syn-rift sediments occur in small patches on top of the low-grade Paleozoic or non-metamorphic Permo-Mesozoic rocks. Slivers of Permo-Mesozoic rocks are incorporated as small lenses within the ENE-trending *Kungota Fault* which merges with the NE corner of the Kozjak Dome (Fig. 3) (Žnidarčič and Mioč 1988) and continue to the South Burgenland Ridge more to the NE.

The *Ribnica-Selnica* and *Kapla* troughs are two synformal structures filled with late early Miocene (Ottnangian? to Karpatian) sediments, occurring on two sides of the Kozjak Dome (Figs. 2, 3) (Mioč, 1977; Stingl, 1994). The E–W strike turns to NW trend in the western segment of the RS trough (Fig. 3). The two structures can be considered as syn-rift grabens, but the steep dip values, locally exceeding 40°, and fault-slip data indicate later modification by contractional deformation (see

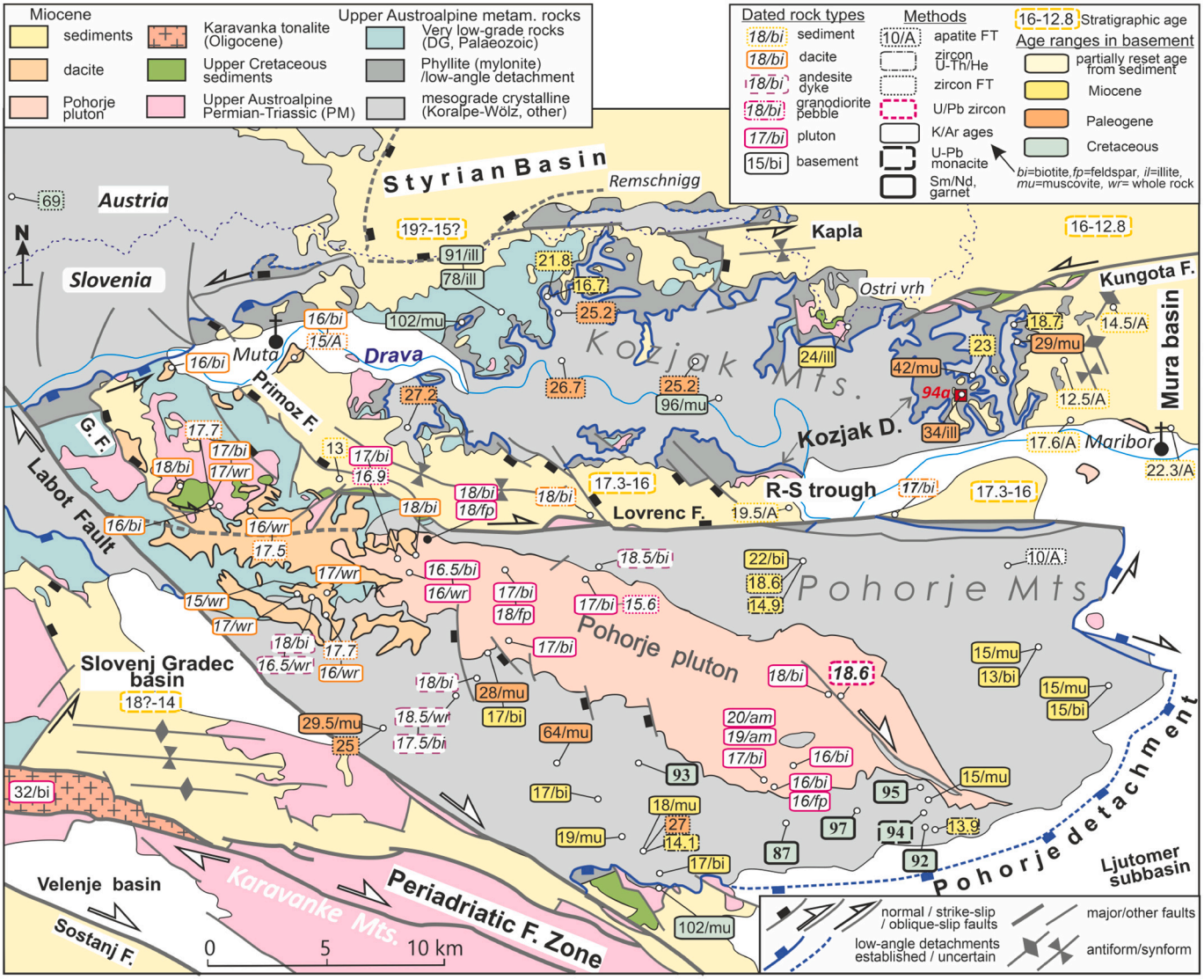

Fig. 3. Geochronological ages from the Pohorje-Kozjak Mts. (after Fodor et al., 2003, 2008; Thöni, 2006; Trajanova et al., 2008; Sandmann et al., 2016; Li et al., 2021). Base map after Mioč and Žnidarčič, 1976; Žnidarčič and Mioč, 1988, modified. Red squares indicate two sites with exposed contact of syn-rift sediments and the metamorphic basement. Detailed age data for newly published (U-Th)/He ages are available in the Supplementary Material 1. (For interpretation of the references to color in this figure legend, the reader is referred to the web version of this article.)

Chapter 3). The conglomeratic infill interfingers with sandstone and siltstone and dacitic volcanoclastic.

In the eastward subsurface continuation of the Pohorje Dome, the *Murska Sobota (MS) Ridge* is composed of the same KW medium-grade rocks as the Pohorje itself (Lelkes-Felvári et al., 2002; Fodor et al., 2013). Thin sheets of greenschist-facies rocks can be interpreted as either retrograde Koralpe-Wölz rocks or separate nappe slices. Small slivers of low-grade Paleozoic rocks and also of non-metamorphosed Permo-Triassic sediments encountered by several boreholes occur sporadically on the top of the medium-grade rocks (Fig. 2, Som-1, Rad-1, Dok-1, Dan-1, Ljut-1; Fodor et al., 2013). The ridge has an antiformal shape surrounded by the Miocene basins on all sides and was gradually flooded during the late middle or late Miocene (Gosar, 1995). The MS Ridge is bounded to the NE by the *Baján Detachment* which is a low-angle shear zone imaged by seismic data and penetrated by the borehole Baján B-M-1 (Fodor et al., 2013; Lelkes-Felvári et al., 2002; Fodor et al., 2013; Nyíri et al., 2021). In map view, the detachment turns westward and bounds the Radgona and Ljutomer sub-basins (Fodor et al., 2003).

The large basin between the Transdanubian Range and the Pohorje Mts. has the common name *Mura-Zala Basin*, with several sub-basins (Fig. 2, detailed by Márton et al., 2002a, and references therein). In its central part it is composed of Miocene half-grabens tilted mostly to the SW, while the two ENE-trending Radgona and Ljutomer sub-basins have synformal shapes. The deepest half-grabens appear in the immediate hanging wall of the Baján Detachment. The normal faults are connected to prominent steeply-dipping N–S to NE–SW trending faults which could have acted as transfer strike-slip faults between different extensional domains. These are the Rába and Viszák Faults in the NW and the Petri and Periadriatic–Balaton Fault in the SE (Fig. 2). During the Miocene basin evolution the *Transdanubian Range (TR)* formed the tilted block edge with respect to the Baján and Rechnitz detachments (Fig. 2) (Tari et al., 1992; Fodor et al., 2013). At its SW end, the range is terminated by several Miocene basins which surround the Keszthely Hills, a horst built of Triassic carbonates. N–S trending faults bound the Keszthely Hills, and they are connected to NW–SE trending grabens from the Tapolca graben up to the Vasvár graben.

The *South Burgenland Ridge* separates the Mura-Zala and Styrian basins (Fig. 2) (Kröll, 1988; Friebe, 1991). It is mostly composed of low-grade metamorphic rocks locally exposed on surface and has a very thin Miocene cover, often only late Miocene in age. The *Styrian Basin* is superimposed on the Austroalpine units and its northern part even on top of the Rechnitz windows (Ebner and Sachsenhofer, 1995). The basin is characterized by N–S to NE–SW trending faults (Fig. 2) and related deep half-grabens (Friebe, 1991; Sachsenhofer et al., 1997). The infill incorporates thick early Miocene (Ottnangian? to Karpatian, ~19–16 Ma, Stingl, 1994; Hohenegger et al., 2009), mostly in its western part, while the middle Miocene sequences can be up to 2 km thick.

Several studies constrained the time of cooling and exhumation of Penninic rocks of the *Rechnitz windows* between ~23 and 17 Ma (Dunkl and Demény, 1997; Ratschbacher et al., 1990). Tari (1994, 1996), Tari et al. (1992, 2020b) and Cao et al. (2013) interpreted these domes as metamorphic core complexes bounded by simple shear detachments and having been exhumed by rolling hinge type deformation due to NE–SW extension. Ratschbacher et al. (1990) connected the ductile extensional structure to lateral extrusion phase of the ALCAPA unit. They also suggested and intervening compression phase resulted in folded character of the domes which was interpreted as antiformal corrugations by Tari (1996) and Tari et al. (2020b). The main detachment has been penetrated by the well Sz-II and the fault zone contained variable tectonites from mylonites to fault breccias (Lelkes-Felvári, 1994).

3. Extension and exhumation in the south-western Pannonian Basin

Several arguments demonstrate considerable extension and related exhumation in the Pohorje and Kozjak Mts., along the Murska Sobota Ridge and in the Mura-Zala Basin (Figs. 3–9). In the first subchapter, we revise the available radiometric ages constraining the footwall exhumation. Although most of the data have been published, and only a few new zircon FT and the (U-Th)/He data are shown here, their integration into a coherent picture is needed to explain time constraints of the local structural evolution and its comparison with the TR. Then we describe structural features indicating extensional deformation, and finally provide a model for interpretation of these data. We use structural maps, cross-sections, magnetic anisotropy data, stereoplots, field photos, and microphotographs. Published 1:100.000 scale maps of former Yugoslavia (Mioč and Žnidarčič, 1976; Mioč et al., 1981; Žnidarčič and Mioč, 1988) represent the base map for the Pohorje and Kozjak domes and the simplified and unified version was first published in Fodor et al. (2008) and refined in detail in this work (Figs. 3, 4). The cross-sections of Fig. 5a and c reflect the concept of a sub-parallel section of Fodor et al. (2003) but the locations are different, and the metamorphic rocks are subdivided on the MS Ridge using the maps of the TJAM and TransEnergy geothermal research projects (Maros and Maigut, 2011; Nádor et al., 2012; Fodor et al., 2013). Magnetic anisotropy and fault-slip data were partly published in Fodor et al. (2002, 2008, 2020) but a few new data were also added.

3.1. Exhumation in the Pohorje, Kozjak Domes and Murska Sobota Ridge

The exhumation of the Pohorje and Kozjak Domes is constrained by diverse geochronological data, including K-Ar ages on variable mineral separates, zircon and apatite fission-track ages, and new zircon (U-Th)/He ages (Fig. 3, Supporting material 1). Cretaceous Sm/Nd ages on garnets and a monazite age mark the time of metamorphism of the (ultra)high-pressure rocks between 97 and 87 Ma in the southeastern Pohorje (Thöni, 2006; Sandmann et al., 2016; Li et al., 2021). Muscovite K-Ar ages from mesograde rocks of the Kozjak Dome, and from low-grade rocks of the northern Kozjak and from the southern Pohorje Domes are Cretaceous suggesting that cooling of the structurally higher units below ~420–350°C (Harrison et al. 2009) already happened during the Eoalpine orogeny (Fodor et al., 2008).

In the western Pohorje Dome, few muscovite K-Ar ages indicate Oligocene cooling. Similar cooling ages, but at a lower temperature, appear from zircon FT data of the Kozjak Dome which are all between 27 and 22 Ma (Fig. 3). This cooling can be interpreted as having followed the thermal input derived from the Paleogene Periadriatic, mostly tonalitic magmatism (Rosenberg, 2004; Schulz, 2012; Neubauer et al., 2018). This cooling could also be connected to the earliest stage of lateral extrusion of the Eastern Alps (Rosenberg et al., 2018). On the other hand, the Miocene zircon FT ages are close to the possible onset of sedimentation (~19–17.3 Ma) and the somewhat younger zircon (U-Th)/He ages (18.7–16.7 Ma) are coeval with the earliest sediments (Fig. 3). Therefore we prefer connecting these ages to extensional exhumation of the Kozjak Dome, although the exact onset cannot be better constrained than ~25–23 Ma.

Miocene exhumation is clearly documented by muscovite and biotite K-Ar ages from the mesograde metamorphic rocks in the eastern and southern part of the Pohorje Dome; the ages range from 22 to 13 Ma (Fig. 3) (Fodor et al., 2003, 2008). New zircon (U-Pb)/He ages constraint the late stage of cooling around ~15–14 Ma (Fig. 3, Supplementary material 1). We have to admit that all these thermochronological ages are in contrast to apatite (U-Th)/He ages ranging from 20.4 to 13.9 Ma (Legrain et al., 2014), a contradiction to be resolved by future studies.

The eastern part of the Kozjak Detachment show a complex picture; the shear zone and the underlying rocks exhibit muscovite and illite K-Ar ages between 42 and 24 Ma (Fig. 3). In site 94a illite K-Ar age of 34 Ma of a fault gouge located between syn-rift sediments and mylonites is a good example of such samples. One zircon FT and one zircon (U-Th)/He age fall in the early Miocene (23 and 18.7 Ma, respectively). In the syn-rift sediment, located just above the shear zone, detrital apatite grains show partially reset ages (Fig. 3; Sachsenhofer et al., 1998a). Therefore,

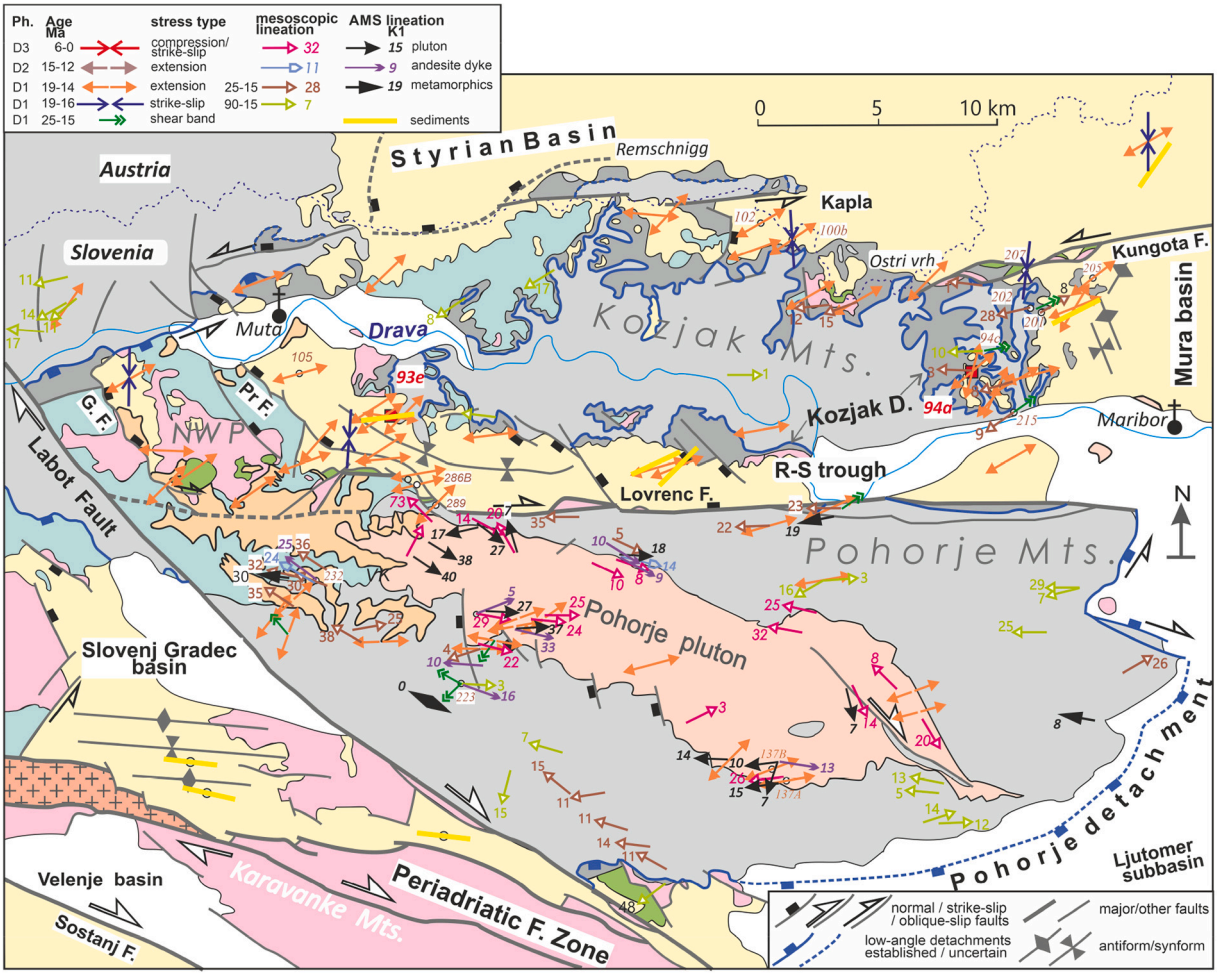

Fig. 4. Cretaceous and Miocene syn-rift extensional structures in the Pohorje and Kozjak Domes. Note coherence between different indices (ductile lineation, AMS and brittle extensional axes). Base map is the same as on Fig. 3. Partly after Fodor et al., 2008, 2020). G.F: Golarjev Peak Fault, NW P: northwestern Pohorje, Pr F.: Primož Fault, R-S trough: Ribnica-Selnica trough. Numbers near arrows indicate the plunge of lineations.

we interpret the Paleogene K-Ar ages as mixed ages derived from the Cretaceous post-orogenic cooling and the Miocene exhumation along the eastern Kozjak Detachment.

In the pluton, biotite, feldspar and whole-rock K-Ar ages scatter between 18.1 and 15.7 Ma and the FT ages are in the same range (Dolenec, 1994; Fodor et al., 2003, 2008; Trajanova et al., 2008). Both are interpreted as cooling ages, postdating the intrusion which is dated with a zircon U-Pb age of 18.64±0.11 Ma (Fodor et al., 2008). Fast cooling is also indicated by biotite K-Ar ages of 18–17 Ma from pebbles of the Miocene sediments of the RS trough having almost the same depositional age as the cooling of the source granodiorite (Fig. 3). In the dacite body, and in few isolated intrusions along the Drava river the biotite and whole-rock K-Ar age ranges is 18.2–15.8, Ma and this may be close to formation age because of shallower emplacement depth. The andesitic and rhyolitic dykes show a K-Ar age range similar to the main dacite body (18.5–16 Ma; Fodor et al., 2008), with the exception of a single rhyodacite dyke being dated as young as 14.9 Ma (Trajanova et al., 2008).

Three new zircon FT data from mesograde rocks and one published biotite K-Ar age from a micaschist (Fodor et al., 2003) from three boreholes of the MS Ridge indicate Miocene cooling (Fig. 2; 20.8–16.1 and 14 Ma, respectively). On the other hand, mica separates from the footwall of the Baján Detachment yielded a latest Cretaceous age (65 Ma, Lelkes-Felvári et al., 2002). Although this latter age is younger than other ages in the Eastern Alps, we leave open the possibility of Late Cretaceous exhumation along the low-angle Baján Detachment. This would be in good agreement with the presence of high-angle Late Cretaceous normal faults observed in the hanging wall (Héja, 2019).

3.2. *Extension in the Pohorje, Kozjak and Murska Sobota domes*

Evidence for Miocene extensional deformation of the area will be presented under the following points; (1) the existence of sub-horizontal to low-angle detachment zones, (2) disposition and geometry of Permo-Mesozoic and low-grade rocks above and around the domes, (3) large-scale tilting of the entire Pohorje Dome, (4) eastward younging of thermochronological ages, (5) anisotropy of magnetic susceptibility (AMS) data, interpreted together with (6) mesoscale ductile structures in the Miocene plutonic and host metamorphic rocks, (7) omnipresent brittle extensional structures, and variable tilt of syn-rift sediments together with AMS data, (8) exposed basal contact of the exhumed metamorphic rocks and syn-rift sediments, and (9) high vitrinite reflectance values, and clay mineral alteration near the Kozjak Detachment.

(1 and 2) In the Kozjak Mts. a completely flat tectonic contact occurs at the top of the medium-grade rocks (Figs. 4, 5a, b). Above this contact, the very low-grade Paleozoic and tilted Permo-Mesozoic sequences are all truncated and only occur in reduced thicknesses. At Ostri vrh, strongly tilted Upper Triassic carbonate rocks (Hauptdolomit Fm.) are almost directly in flat-lying contact with medium-grade rocks (Figs. 4, 5a). The ~200 m thick contact zone was mapped as a separate phyllite unit (Mioč and Žnidarčič, 1976) but was later interpreted as a mylonitic

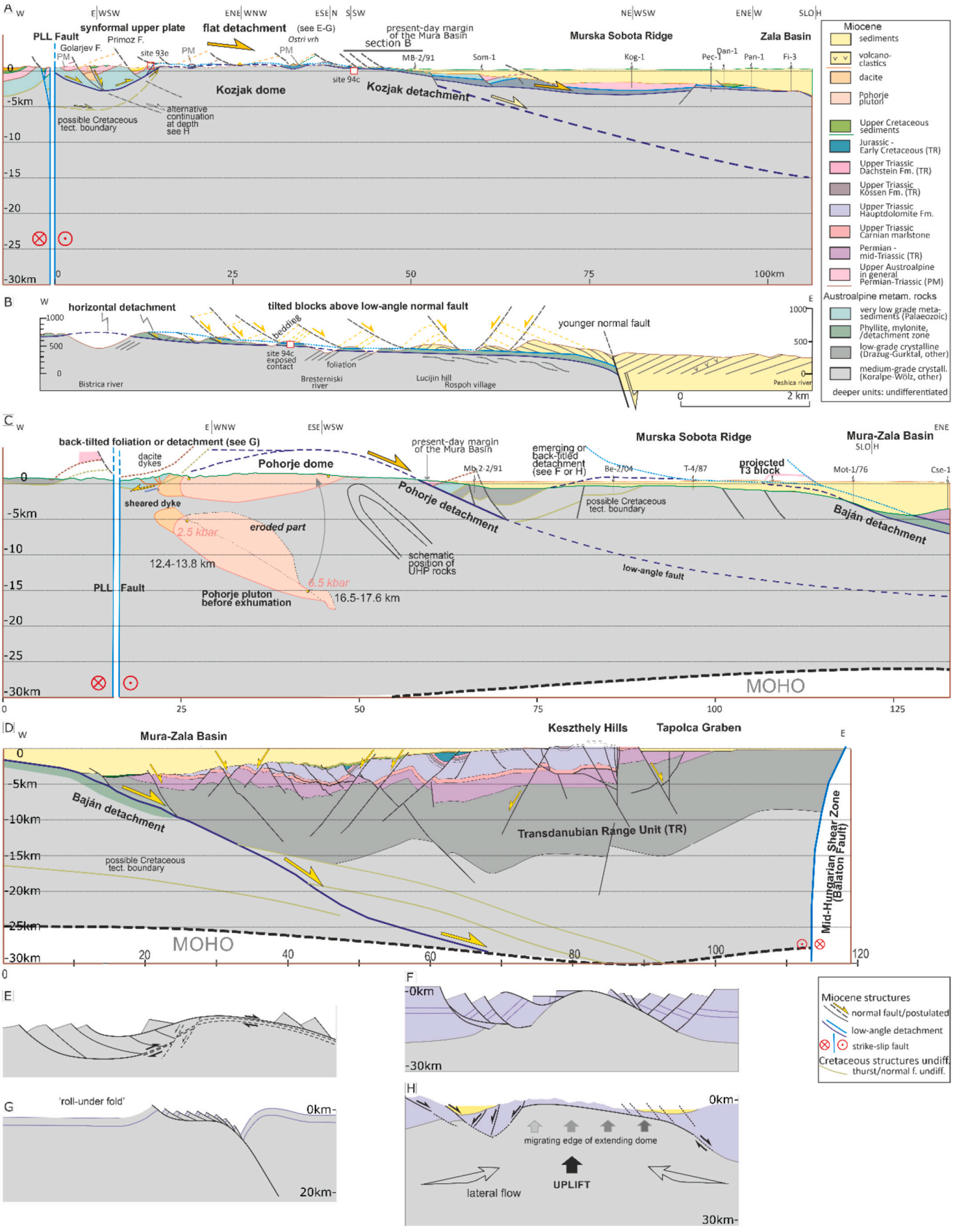

(caption on next page)

Fig. 5. Cross sections in the western PB. a) Across the Kozjak Dome to the NE corner of the MSR. b) Detailed section of the gently dipping part of the Kozjak Detachment. c) Cross section from the Pohorje Dome to the MS Ridge (partly after Fodor et al., 2003, 2013). d) Continuation of section 5c through the Zala Basin to the Keszthely Hills. The section is based on interpretation of seismic reflection profiles and cross section balancing (Héja, 2019; modified). For the detailed view of the Baján Detachment, see Fig. 6. Moho depth is from Horváth et al. (2015) and Kalmár et al. (2018). Insets show possible models for interpretation, after (e) Reynolds and Lister (1990); (f) Brun et al. (1994); (g) Buck (1988); (h) Miller et al. (1999). Note references to these models on Fig. 5a–c. Note slight changes in section directions.

shear zone (Trajanova, 2002; Fodor et al., 2002, 2008). We refer to this structure as the Kozjak Detachment. The sub-horizontal segment slightly bends to a gently ENE-dipping orientation below the Mura Basin (Fig. 5a, b; Fodor et al., 2003). Stretching lineations are broadly ENE-trending within the mylonite. Shear bands within the mylonite and in the underlying medium-grade rocks both exhibit top-to-the-NE displacement along the eastern Kozjak Detachment (Fig. 7d, e; Fodor et al., 2008).

Above the flat part of the detachment, the reduced thickness of the mylonitic phyllite and very low-grade units or even their complete omission indicates a very large amount of extension. Mesozoic rocks occur only at one place, at the Ostri vrh, where direct contact of Upper Triassic carbonate rocks with the mylonitic-phyllitic deformation zone indicate at least 4–6 km of stratigraphic omission. The detachment remains very gently dipping at the present-day erosional margin of the Mura Basin. The strongly tilted syn-rift sequences corroborate large extensional deformation along this segment (Fig. 5b).

At the eastern boundary of the MS Ridge seismic sections show that the Baján Detachment is composed of a thick, parallel reflection package (Fig. 6; Nyíri et al., 2021) which probably indicates a mylonitic foliation within the detachment zone, seen also in cores from the Baján-M-1 borehole (Lelkes-Felvári et al., 2002). The detachment zone is imaged near and below of an asymmetric hanging wall graben with a syn-rift fill of 1.5–3 km that is the deepest part of the Zala Basin. Applying a reasonable time-depth conversion of the 3D seismic data, the shear zone exhibits a dip angle of 15–30°. This zone separates the footwall medium-grade rocks of the Koralpe-Wölz unit from the non-metamorphosed Transdanubian Range sequence in the hanging-wall, therefore ~6–10 km of rock pile, corresponding to the Bundschuh and Drauzug-Gurktal nappes is missing.

The disposition of the Permian-Triassic sequence around the domes also indicates differential uplift and large exhumation of the central part of the domes. In the Pohorje, these units crop out in small patches along the northern, eastern, and southern boundaries, although their continuation could be covered by Miocene or Quaternary sediments. Sharp (unfortunately covered) tectonic contact with metamorphic rocks is particularly clear in the eastern Pohorje, where retrogressed eclogitic amphibolite is in contact with Triassic carbonates (Fig. 4). In the south of the Pohorje a very thin sheet of low-grade metasediments and a mylonitic shear zone are present. One muscovite K-Ar age obtained from the hanging wall of the shear zone is Cretaceous while published zircon FT ages and new (U-Th/He) ages are Miocene from the footwall (Fig. 3, Fodor et al., 2008). This can suggest a twofold evolution: Cretaceous post-metamorphic cooling in the hanging wall and Miocene footwall exhumation.

(3) Four independent data sets provide the pressure conditions at the time of the Pohorje granodiorite formation (Altherr et al., 1995; Fodor et al., 2008; Sotelšek et al., 2019; Poli et al., 2020). All datasets agree with the structural scenario that the entire massive has been tilted westward after pluton emplacement. Uplift of the eastern tip of the intrusion ranges from 15 to 20 km, depending on the uncertainty range of the pressure estimates (Fig. 5c). Data are more variable for the emplacement depth of the upper part of the pluton in the west; estimates range between ca. 7.5 km (2.5 kbar) to 12 km (Sotelšek et al., 2019; Poli et al., 2020). As the upper and lower parts of the pluton are presently at the same topographic level, this means that the amount of westward tilt reaches up to 25°.

(4) Fodor et al. (2008) demonstrated that low-temperature thermochronological data exhibit a trend of eastward younging ages (Fig. 3). This is most prominently seen for K-Ar white mica ages, which are Oligocene (29.5–25 Ma) in the south-western and Miocene (19–15 Ma) in the eastern and southern parts of the Pohorje Dome. The two available zircon FT ages from the basement corroborate this observation while the three (U-Th)/He ages are also Miocene (14.9–13.9 Ma, Supplementary material 1). Fodor et al. (2008) interpreted these data as an argument for the westward tilt of the pluton and here we additionally suggest that Miocene exhumation also occurred in the southern part of the Pohorje dome (Fig. 5c).

(5) AMS is a measure of the ductile strain of the measured rocks and mostly indicate ~E–W ductile stretching within the pluton (Fodor et al., 2020). Mesoscopic stretching lineations in the pluton and in some early dykes are also trending in the same direction as AMS axes (Fig. 4). Since mesoscopic lineations are associated with extensional structures (e.g. shear bands) AMS can probably be interpreted as having been related to extension rather than to pluton emplacement (Fodor et al., 2020). This deformation is clearly of Miocene age in the pluton, where K-Ar and fission-track cooling ages constrain both the crystal plastic deformation and the acquisition of the AMS signal between 18.6 and ~15.5 Ma. E–W Extension was associated with vertical flattening and formation of gently dipping foliation in most parts of the pluton (Fig. 7g) while shear bands indicate top-to-east slip (Fig. 7f).

(6) In the host metamorphic rocks, prominent stretching lineations and frequent extensional shear bands occur both in the Pohorje and Kozjak Domes (Fig. 4). However, the age of extension is not so well constrained. Part of the ductile structures could form already during the Late Cretaceous when exhumation of the mid-crustal medium-grade rocks of the Austroalpine nappe pile was a common process just north of the Kozjak Dome (Neubauer et al., 1995; Kurz et al., 2002) and a similar process has been suggested for the Pohorje (Kirst et al., 2010). We consider lineations in medium-grade rocks, which potentially formed near peak-metamorphic conditions, as being of Cretaceous age. However, K-Ar ages on muscovite and biotite seem to suggest that at least in the eastern Pohorje Dome the extensional structures could be Miocene in age (Figs. 3, 4); temperature conditions above 350°C would permit the activity of crystal plastic deformation within shear zones. The same can be assumed for extensional shear bands of the eastern Kozjak, where the formation conditions of the brittle-plastic structures were close to the retention temperature for fission tracks in zircon.

(7) Brittle extensional structures occur in map- and outcrop-scale (Fig. 4). West of the Ribnica-Selnica trough, in the NW Pohorje, east-northeast dipping normal faults cut across a km-thick very low-grade metamorphic suite and its Permo-Mesozoic stratigraphic cover. Dip data in both the Miocene and Permian rocks demonstrate the existence of westward-tilted domino-style blocks between the Primož and Golarjev Peak Faults (Figs. 4, 5a). They merge into a ~E–W trending postulated fault zone concealed by the dacite body, which itself could join the Lovrenc Fault further eastward Fig. 4).

Above the Kozjak Detachment, and particularly at its eastern segment, the Miocene sediments are moderately to strongly tilted to the west (Fig. 5b) while east-dipping normal faults are postulated between the west-tilted blocks. The lack of normal faults in the footwall medium-grade rocks indicates that these secondary normal faults merge into the sub-horizontal detachment. The westward and occasionally eastward-dipping beds indicate the presence of antiforms which can be interpreted as fault-related folds (Fig. 5b, north of Maribor). The whole Ribnica-Selnica and Kapla synforms can be considered as large fault-

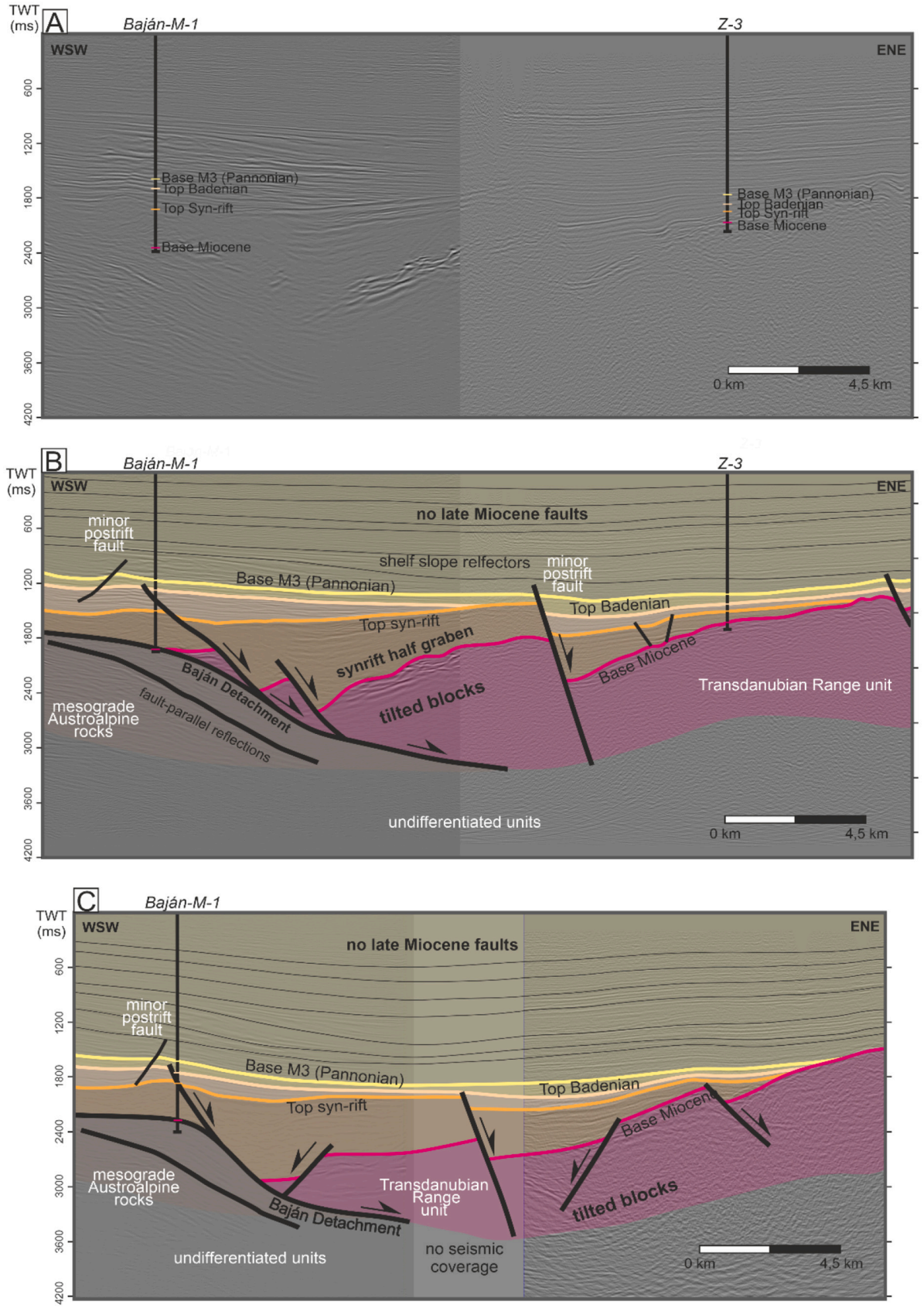

Fig. 6. Interpretation of the structural geometry along the Baján Detachment. For section locations see Fig. 2. These time-migrated sections are the combination of a 3D survey (Bajánsenye) and several vintage 2D lines. The 3D seismic data were acquired in 2008 and the processing was done by Geoinform Ltd. For the interpretation DecisionSpace Geosciences software was used which was developed by Halliburton. For an early interpretation of a section parallel to A-B, see Fodor et al. (2013). Additional seismic sections across the detachment are shown in Nyíri et al. (2021).

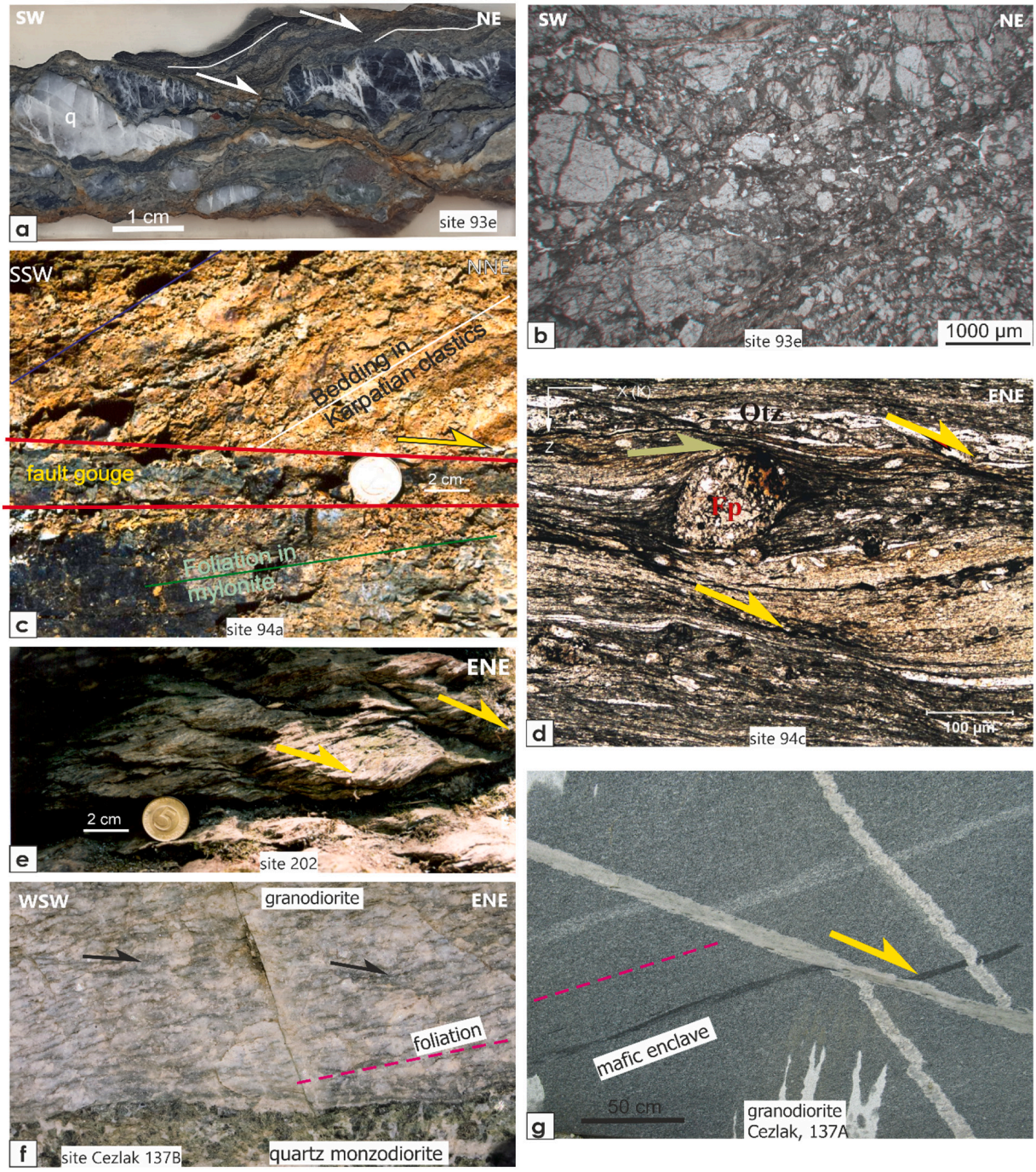

Fig. 7. a) Polished surface of a sample from strongly deformed syn-rift sediments in the western Kozjak (site 93e), b) Microphotograph of the same site, with strong cataclasis, extensional veins in quartz grains. c) Contact of the Karpatian sediments with a fault gouge and mylonitic basement, mapped as phyllite (site 94a). d) Microphotograph of the site 94c, just below site 94a. Note that top-to-ENE shear indicated by feldspar porphyroclast could be Cretaceous in age. e) Shear bands in the eastern Kozjak Detachment zone, site 202, close to sites 94a and 94c. f) Gently tilted foliation and top-to-E shear zones in the pluton, site 137B. g) Foliated granodiorite, flattened mafic enclaves cut by aplite dykes and crosscut by east-dipping late fault.

related synforms.

Fault-slip data document a complex evolution which has 3 main phases (Figs. 4, 8, 9a, b) (Fodor et al., 2002, 2008, 2020). The main deformation was characterized by a NE–SW to E–W directed extensional stress field designated as D1 phase (Figs. 4, 8). A great number of striated faults were formed when layers were still horizontal because the symmetry plane of conjugate faults are perpendicular to the now tilted beds. Such pre-tilt faults were also observed in the pluton in which the foliation has been tilted (Fig. 7g). The directions of σ_3 axes derived from brittle faults are parallel to measured K1 axes of the AMS (Fig. 4). Sediments having been still in non-cemented state acquired AMS as the earliest deformation event. Tilt test demonstrates that this event happened when beds were in horizontal position (Fodor et al., 2020). This observation, and the lack of such faults and of the tectonic AMS signal in rocks younger than ~14 Ma indicate that the deformation occurred before 15 or 14 Ma.

This extensional phase was overprinted by the D2 phase characterized by E–W to SE–NW extension. In sediments, overprinting criteria are clear; D2 is always post-tilt in relative age, and frequently reactivated the previously formed NW–SE trending normal faults with oblique slip

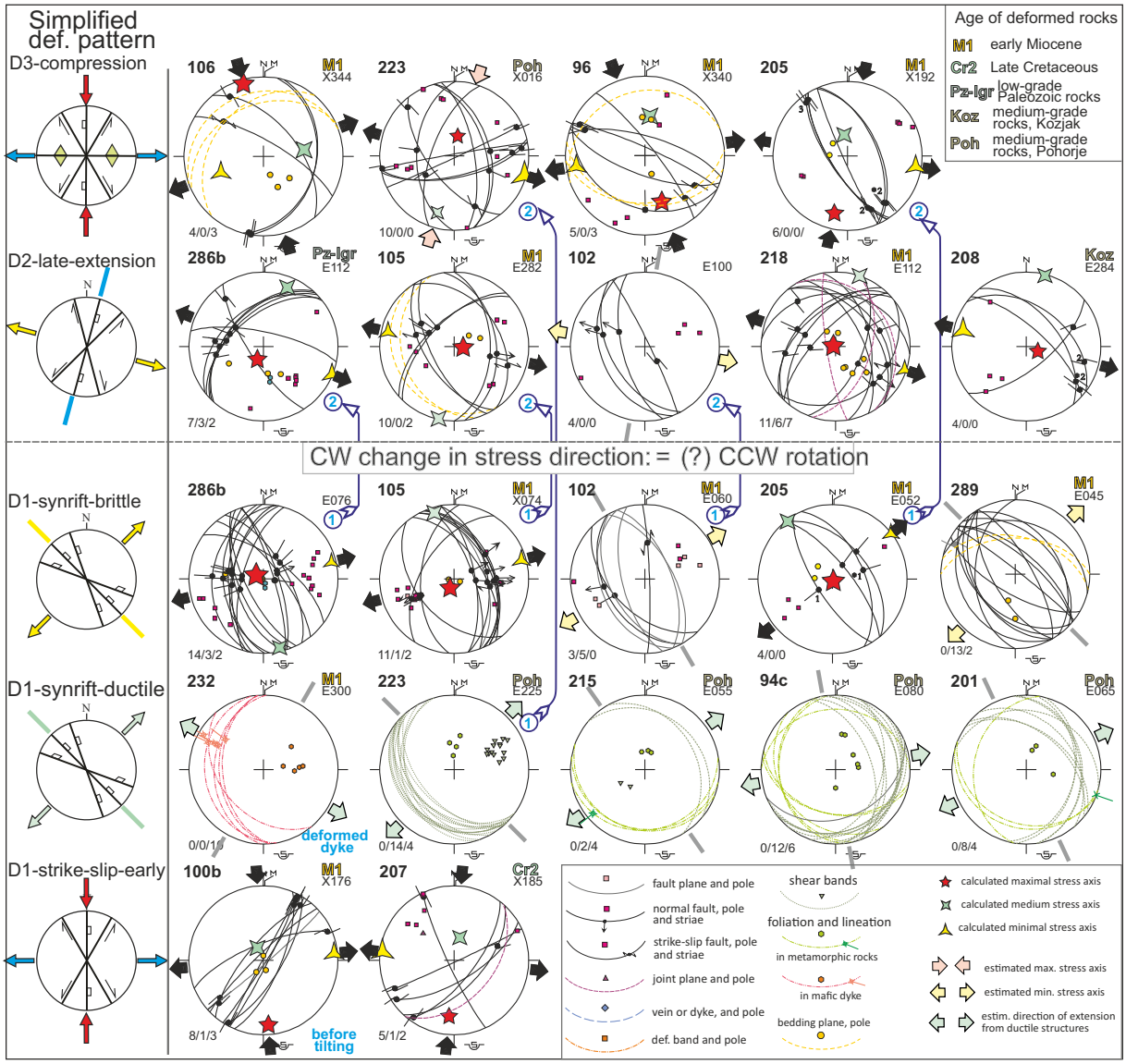

Fig. 8. Stereonets of fault-slip data and mesoscale ductile structures from the Pohorje, Kozjak Mts., RS and Kapla grabens. Partly after Fodor et al. (2008, 2020). Note the presence of N–S compression having affected beds both at horizontal and tilted position, attributed to D1 and D3 phases, respectively. Left column shows the simplified deformation patterns of each deformation phase. Left upper corner: number of sites shown on Figs. 4, 9. Upper right corner: age of the rocks, and type of stress field (E= extensional, X= strike-slip) with the main direction of S_{Hmax} or S_{Hmin} and estimated direction of extension for ductile structures; lower left corner: data numbers; striated faults/other fractures/bedding or foliation. Paleostress calculations were made by the software package of Angelier (1984). Blue circled numbers and arrows show the relative chronology between phases based on superposing structures.

(sites 102, 208 on Fig. 8). The extensional deformation was overprinted by strike-slip faults attributed to the Pliocene-Quaternary neotectonic D3 phase (Fig. 9b) (Fodor et al., 1998, 2008). Tilted syn-rift normal faults, reactivated as strike-slip and oblique-reverse faults were documented at several sites (Fig. 8). D3 compression could have enhanced the synform structures of the Miocene grabens and the domes. Dextral reactivation of the Labot fault and folding in the southern part of the Slovenj Gradec basin are also attributed to this phase (Fig. 2a). Stress fields similar to D1–D3 phases were recognized in the Eastern Alps, and authors noted the same clockwise change in the extensional direction (Pischinger et al., 2008; Reischenbacher and Sachsenhofer, 2013; Brosch and Pischinger, 2014). The amount of rotation of the minimal stress axis σ_3 between phases D1 and D2 is close to the amount of CCW rotation documented in the Miocene rocks of the RS trough (Márton et al., 2006). We, therefore, assume that the change in stress field is only apparent and reflects vertical axis rotation (Fig. 8). This then implies that the extension was oriented roughly E–W through the Miocene evolution.

(8) The site 94c in the eastern Kozjak Dome (Figs. 4, and 7c) exposes the tilted Miocene syn-rift sediments above a 10 cm thick fault gouge and the underlying mylonitic metamorphic rocks. Just below the brittle fault, mylonitic basement rocks exhibit top-to-the-NE shear bands (Fig. 7d). In the western part, the Kozjak Detachment dips below the NW branch of the Ribnica-Selnica synform (site 93e, Fig. 4). Here, the exposed basal syn-rift beds exhibit strong cataclastic deformation with a dense network of fractures with rigid clasts cut by extensional quartz veins (Fig. 7a, b). The rotated decimeter-scale dominoes and intervening low-angle faults dip both to NE and W-SW and show no definite shear direction although top-to-the-west shear dominates. AMS data also point to WNW–ENE elongation when restored to horizontal bed position (Fodor et al., 2020).

(9) Vitrinite reflectance values are very high (up to 2.5% Rr) around the eastern termination of the Kozjak Dome and also around the Remschnigg Ridge (Sachsenhofer et al., 1998a). Together with clay

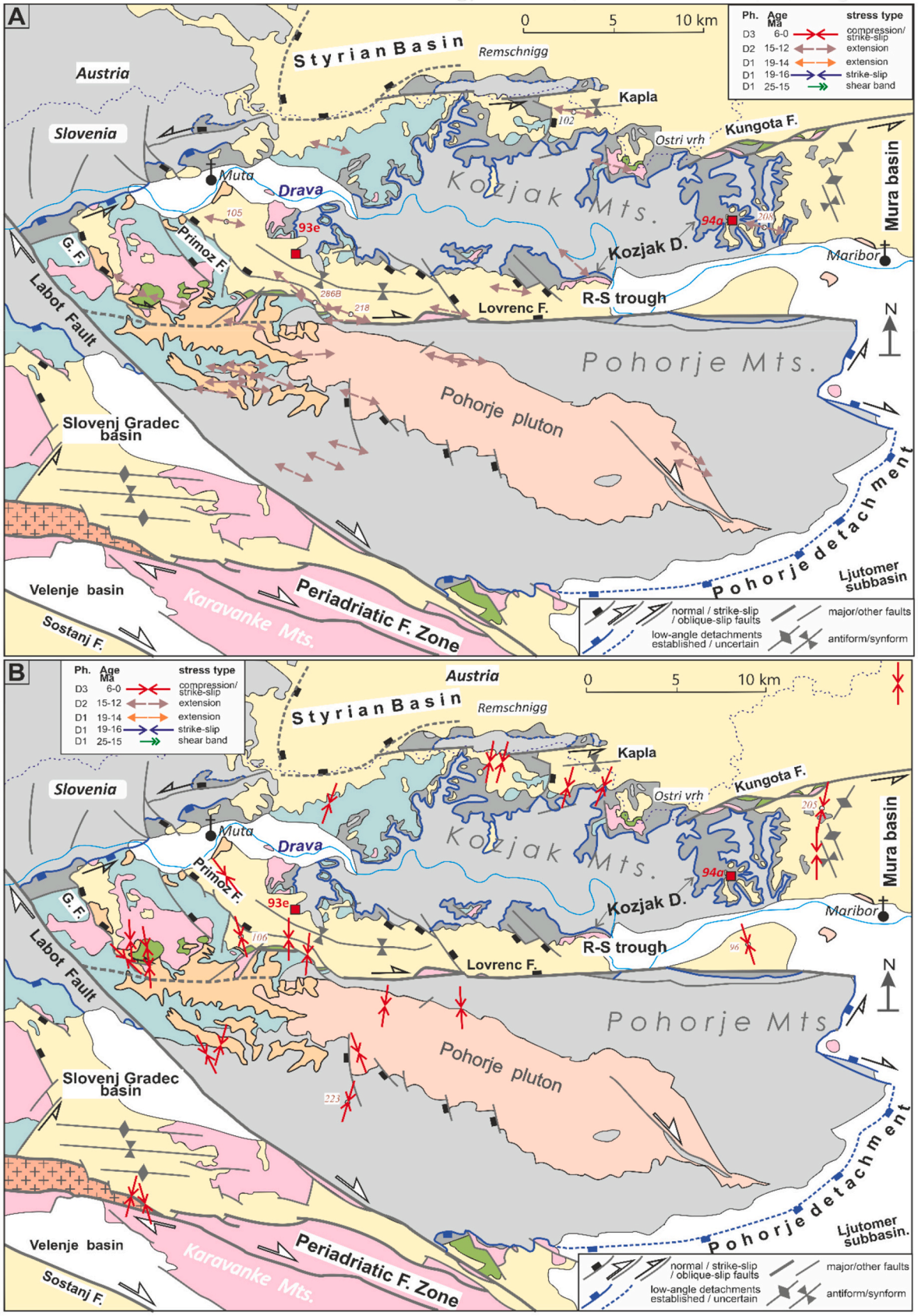

Fig. 9. a) Late extensional stress axes indicating post-15 Ma deformation, b) Plio-Quaternary strike-slip faulting of the D3 phase. Base map is the same as on Fig. 3. Partly after Fodor et al. (2008, 2020).

mineral alteration up to thermally anchizonal conditions (Sachsenhofer et al., 1998b) the vitrinite anomaly indicates significant thermal input which was originally considered as magmatic in origin. Fodor et al. (2002, 2008) interpreted these indices as the sign of advective heat transport from the footwall of the Kozjak Detachment implying important Miocene fault-related exhumation; a situation analog to those one modeled by Dunkl et al. (1998) around the Rechnitz windows. This is in line with partially reset apatite FT ages from the sediments overlying the shallow part of the detachment (Fig. 3).

3.3. Interpretation of the fault geometry in the western PB

Two cross-sections show the structural characteristics of the Pohorje and Kozjak Domes, the Murska Sobota Ridge, and the Mura-Zala Basin up to the Transdanubian Range (Fig. 5). Both sections are oriented subparallel to the local direction of extension, indicated by fault-slip, AMS, and stretching lineation data. The westernmost portions of both sections are shifted by 10–18 km, to account for the dextral slip along the PLL fault system. The observations can be compiled into several conceptual models and we will discuss alternative scenarios.

Across the Kozjak Dome, the fault pattern seems to agree with the typical fault geometry in a rolling hinge-type metamorphic core complex (Buck, 1988; Lavier et al., 1999; Wernicke and Axen, 1988, Fig. 5g). The tilted blocks at the western part of the section (NW Pohorje) would be located above a back-tilted segment of a folded detachment with top-to-the-east-northeast simple shear mechanism (a synformal upper plate, Fig. 5e, g; Spencer, 1984; Brun et al., 2018). The breakaway fault would have been located west of the PLL fault but has been displaced during the D3 phase. In this simple shear model the small outcrop at the western Kozjak Detachment (site 93e, Fig. 4) can reflect top-to-the-NE simple shear back-tilted to the SW, or alternatively, a late-stage top-to-the-SW shear on the western side of the emerging Kozjak Dome (like suggested by Reynolds and Lister, 1990; Figs. 5e).

Alternatively, the east-dipping faults west from the dome would not merge to a folded detachment but would continue eastward below the Kozjak Dome, like suggested for the Northern Snake Range décollement and seen on analog models (Figs. 5a, f, h) (Brun et al., 1994, 2018; Miller et al., 1999, respectively). In this case, the thick low-grade suite would have a continuous transition to higher-grade metamorphics (Brun et al., 2018) and the mylonitic front would be located much below the base of the low-grade suite (Davis and Lister, 1988). Finally, we can consider the western part of the Kozjak Detachment as a top-to-west shear zone. In this sense, the Kozjak would be a more symmetric dome with double-verging shear zones at both ends, like the model suggested by Platt et al. (2015) for the Shuswap Dome. In this case, the faults west of the dome would join this detachment as antithetic faults; however, the lack of east-tilted blocks discredits this scenario.

In cross-section, the Pohorje Dome (Fig. 5c) forms a strongly west-tilted block, which was bounded in the east by a low-angle shear zone where abundant extensional shear bands document top-to-NE displacement (Fodor et al., 2003). About 25–30 km of extension can be postulated along this shear zone by connecting the base of the tilted low-grade unit (west, footwall cutoff) to its displaced equivalent below the Miocene sediments (east, hanging wall cutoff).

Along the western margin of the dome, a jump in metamorphic degree is present at the base of the very-low-grade suite, but the contact zone lacks outcrops. However, near the contact, and parallel to it, two observed andesite dykes exhibit penetrative deformation, including foliation, stretching lineation, and a large degree of anisotropy of susceptibility (Fodor et al., 2020). Kinematic data from one of the dykes suggest top-to-west normal shear (Fig. 5c). Despite this localized deformation, the westward dipping contact of the very-low-grade and medium-grade rocks does not seem to be the back-tilted segment of an originally east-dipping simple shear detachment. The geometry resembles the synclinal fold of the detachment footwall, called roll-under fold (Fig. 5g; Brun et al., 2018). In summary, the Pohorje Dome can be considered as a metamorphic core complex using the criteria of Platt et al. (2015).

In a third scenario, the uplift of the pluton could be interpreted as a simple double-plunging fold where exhumation was mainly achieved by erosion. However, this interpretation does not account for the asymmetry of the dome and the predominance of extensional structures, and indicators of N–S contraction are scarce. Nevertheless, a component of folding-related uplift cannot be ruled out.

Above the low-angle Baján Detachment the entire Zala Basin seems to be a large-scale tilted block, with a width of ca. having ~80 km width (Fig. 5c, d). Several smaller normal faults, mostly north-east dipping, bound small half-grabens (Figs. 6, 5d). The TR in the hanging wall represents the highest unit in the Austroalpine nappe pile, and the highest (most distal) among the tilted blocks (Fig. 5d). The tilted edge was located in the southwestern TR, in the Keszthely Hills, the structure and stratigraphy of which will be discussed in detail.

Up-dip, the Baján Detachment zone may continue along thin slivers of low-grade metamorphic rocks carpeting the medium-grade rocks all along the MS Ridge. The northern section suggests that the Baján Detachment is connected directly to the Kozjak Detachment along a wide flat segment since most of the boreholes reveal Permo-Mesozoic rocks (including Late Cretaceous carbonates in Dan-1, Gosar, 1995) truncated at the base, and the phyllite or the medium-grade rocks are at a shallow depth below the base of the Miocene sediments (Fig. 5c). Slivers of Permian to Mesozoic rocks were interpreted as extensional allochtons, belonging to the hanging wall TR unit, scattered along the Baján Detachment (Fodor et al., 2003, 2013). In the southern section, the detachment reaches the former surface and exhibits Mesozoic units in its footwall. However, since the Mesozoic rocks are always truncated from below (lacking Permian to early Triassic strata), a tectonic contact should be postulated below these occurrences, too. A direct connection to the Pohorje Detachment (implying folding of the detachment surface) is not excluded (Fig. 5c). The fault geometry of the MS Ridge resembles the structure described in the Northern Snake Range (Fig. 5h; Miller et al., 1999). As the metamorphic history of the MS Ridge is not well-known and the data are scattered, an unequivocal solution cannot be given.

The preserved fault geometry is different between the southern and northern sides of the Lovrenc Fault, therefore a discussion of the kinematics and the role of this structure is required. Map view of the fault implies its steep to sub-vertical dip (Fig. 4). In the eastern part, the fault has a few parallel branches which join the N–S trending gently dipping main Pohorje Detachment. In the west, the Lovrenc Fault is connected to the NW-trending normal fault system of the north-western Pohorje (Primož and Golarjev faults), via direct fault segments, relay ramps, and a postulated E–W trending branch concealed by the dacite body (Fig. 4). In this transitional area, the fault could change laterally to a monocline because the contacts between Paleozoic, Cretaceous and Miocene rocks are steeply dipping or sub-vertical and just slightly disrupted. The fault's displacement varies along strike and seems to follow the amount of exhumation of the Pohorje Dome because Triassic rocks occur at the same elevation all along the hanging wall.

Stress data from the hanging wall of the Lovrenc Fault (the R-S trough) indicate two extensional deformation phases with the σ_3 axes trending NE–SW to E–W (D1 phase) and E–W to ESE–WNW (D2 phase) (Figs. 4, 9a). These data imply that the Lovrenc Fault acted as a steep dextral fault with a normal slip component during the main syn-rift phase, while kinematics during the D2 phase is less clear. Alternatively, the fault could also act as a reverse fault or would represent the vertical limb of a contractional fold that could develop during the D3 phase of N–S compression (Fig. 9b). However, fault slip data of the D3 phase always exhibit a strike-slip component and never dip-slip reverse faulting, which makes a single-phase contractional character of the Lovrenc Fault much less viable.

In our opinion, the most plausible kinematic scenario for the Lovrenc Fault is a syn-rift transfer fault, superimposed by contraction and

verticalization of the fault (Fig. 10). Because the Lovrenc Fault accommodates the exhumation of the Pohorje Dome, it could also be a stretching fault, like those observed around the eastern Tauern window (Kurz and Neubauer, 1996; Schmid et al., 2013).

Two E- to ENE-trending steep faults join the mesograde rocks of the Kozjak Dome and Remschnigg ridge (Fig. 4). The strike-slip character of the Kungota fault is supported by the occurrence of small lenses of Mesozoic rocks (strike-slip duplexes) inside the shear zone, and we postulate similar kinematics for the parallel southern boundary fault of the Remschnigg ridge (Figs. 4, 10). Like the Lovrenc Fault, these fault zones could be interpreted as transfer or stretching faults because the Kungota Fault clearly merges with the Kozjak Detachment and do not cut across. The RS and the Kapla synforms can be considered as synclinal corrugations. Later during the evolution, their synformal shape could be enhanced by D3 shortening (Fig. 10).

The structural geometry in the western PB is marked by metamorphic domes elongated in ENE direction, bounded by the subhorizontal Kozjak or gently dipping Pohorje Detachments (Fig. 10). It is still a matter of interpretation if the domes are also bounded by oppositely verging shear zones, or represent metamorphic core complexes under a folded east-verging simple shear detachment. Because of their domal shape, they are similar to antiformal corrugations frequently occurring in extensional domains (review of Platt et al., 2015). The domes are separated by Miocene basins which can be considered as synformal corrugations.

A marked feature of the area are the numerous ENE-trending faults at the boundary of the domes and intervening synformal basins (Fig. 10). Although the existence of the faults has been known for a long time, they are interpreted here as transfer or stretching faults, which are subparallel to the extensional direction. Such faults commonly occur in metamorphic core complexes worldwide (e.g., North Aegean, Brun and Sokoutis, 2018).

4. Miocene topography and basin formation in the Keszthely Hills (TR)

The Mesozoic carbonate blocks of the Keszthely Hills are surrounded by Miocene sediments and Pliocene basalt volcanoes, maars, and diatremes (Budai et al., 1999; Martin and Németh, 2004). To the north and east, boreholes revealed marine sedimentation during part of the middle Miocene, when two connected grabens, the Tapolca and Várvölgy grabens developed (Fig. 11). Their NW–SE oriented boundary fault can be followed to the NW, where the deeper Nagygörbő and Vasvár grabens formed (Dudko et al., 1992; Tari, 1994; Fodor et al., 2013). The lower part of the middle Miocene sequence (Badenian) is missing for 10–20 km to the west and south from the present-day hills demonstrating terrestrial exposure in large areas lasting up to the late Miocene.

4.1. Miocene infill of the syn-rift grabens

The Miocene stratigraphy can be discussed using the data of few key boreholes arranged in a ~N–S section which reveals the architecture of the basin fill (Fig. 12). We will focus on the Badenian (15.97–12.8 Ma) formations and the onset of sedimentation. Near the Keszthely Hills the sequence starts with shallow marine limestone which gradually passes to the fine-grained siliciclastic Tekeres Formation. The fossil content documents a gradually deepening depositional environment from shoreface to offshore while the overlying Szilágy Fm. indicates gradual

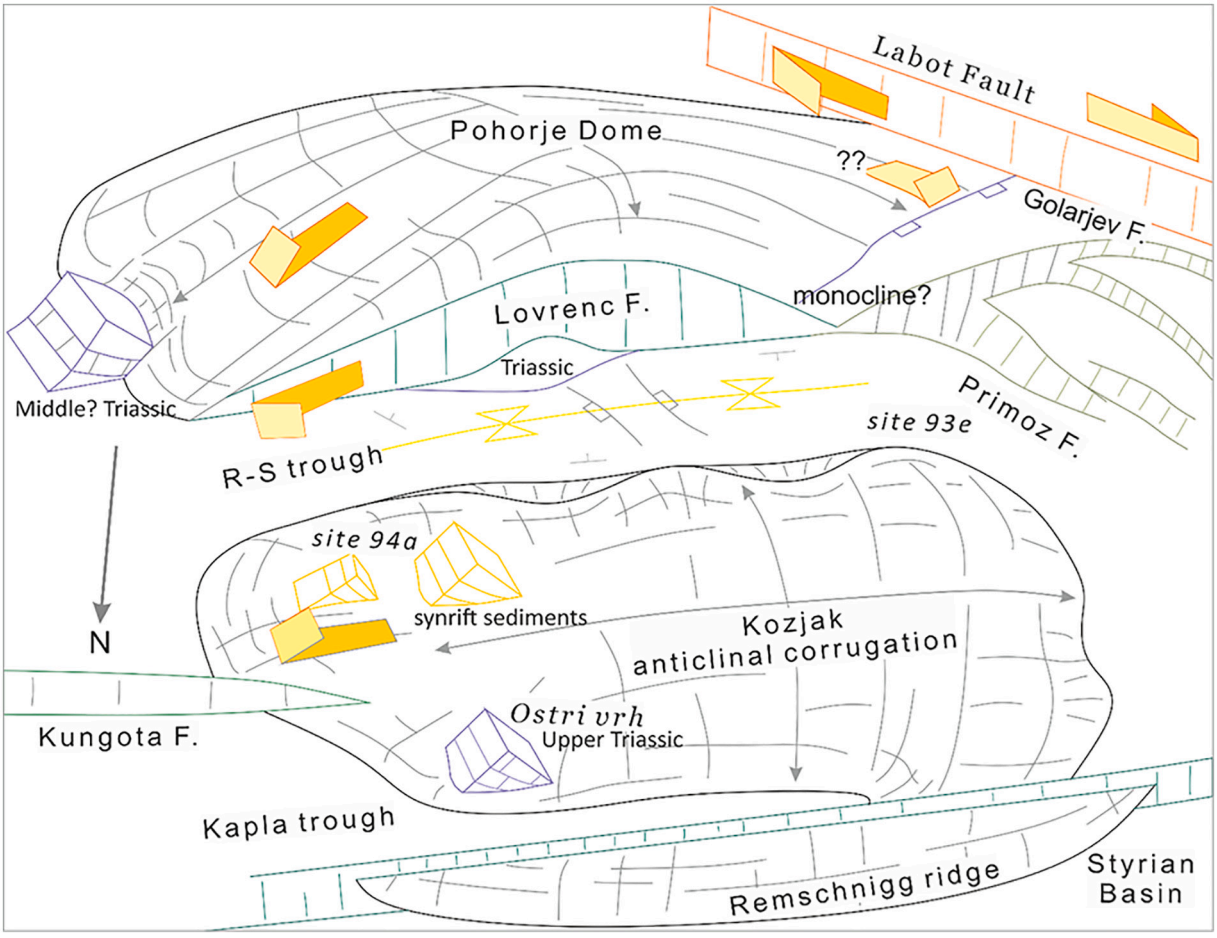

Fig. 10. 3D model of the connection of detachment faulting, and transfer faults in the study area. It shows the same area as Fig. 4, looking from the north.

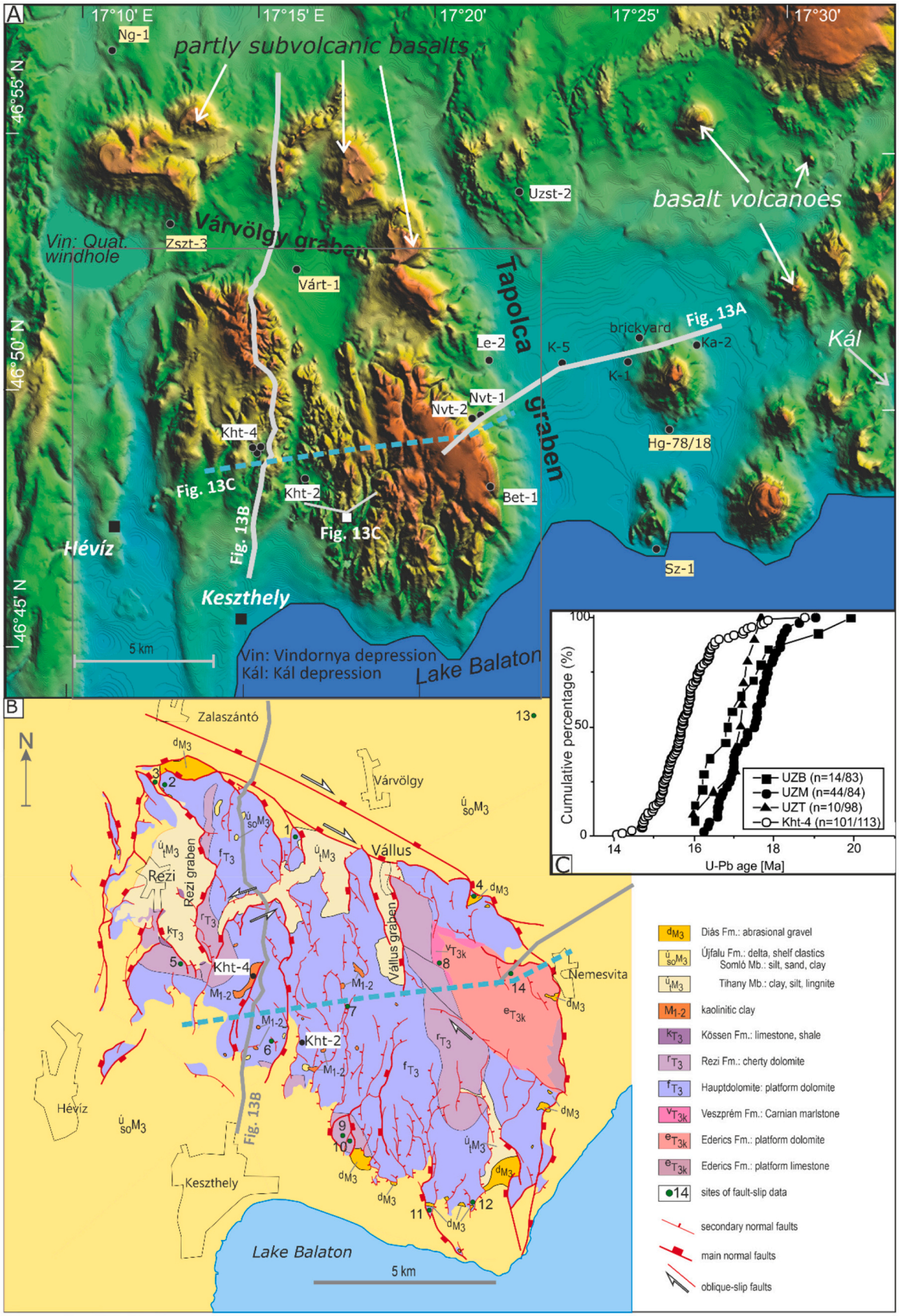

Fig. 11. a) Morphology of the Keszthely Hills and surrounding grabens with geological (solid grey line) and topographic sections (dashed blue) and boreholes (black dots). b) Pre-Pliocene map of the Keszthely Hills with sites for fault-slip analyses, partly after Budai et al. (1999). For location see grey rectangle on a. c) Miocene part of the U-Pb age spectrum of zircon crystals in the sinkholes near the Keszthely Hills (Kelemen et al., 2021). UZB, UZM, UZT samples from Uzsa Uzst-2 borehole. (For interpretation of the references to color in this figure legend, the reader is referred to the web version of this article.)

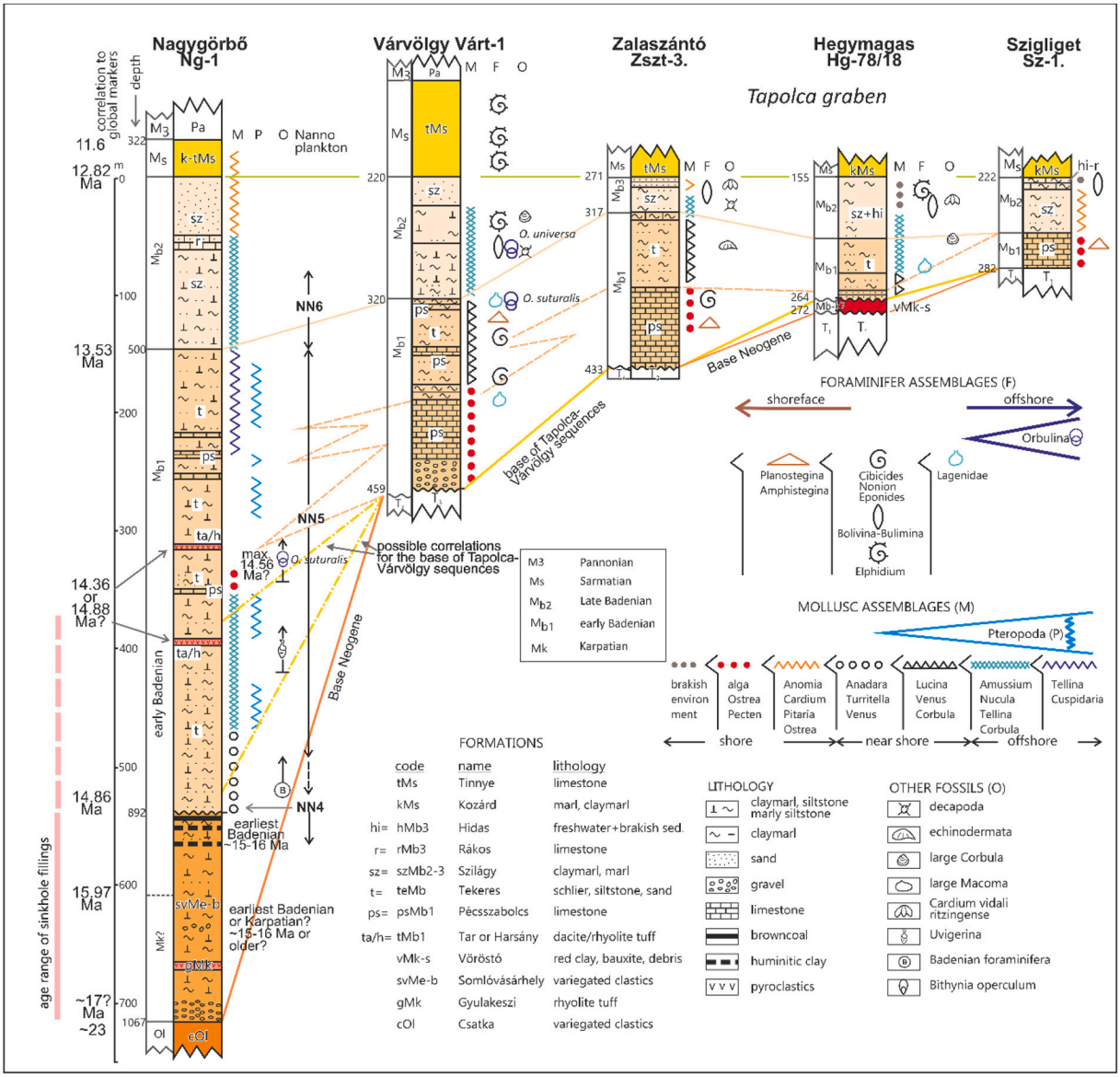

Fig. 12. Stratigraphy and correlation of sedimentary units in the Tapolca, Várvölgy and Nagygörbő grabens around the Keszthely Hills (after Jámbor and Korpás, 1974 and Selmeczi et al., 2004 modified). Note that the correlation of the base of Tapolca-Várvölgy sequences is not unequivocal to the continuous Ng-1 borehole.

shallowing conditions, terminated by limestone or brackish to freshwater layers (Sz-1, Hidas Fm., Kókay, 1985). In the northern Ng-1 borehole the basal limestone is missing, and only occasional intercalations occur, probably redeposited by gravity flows. Below the Tekeres Fm. variegated clastic formations occur which contain coal seams at the upper part (Jámbor and Korpás, 1974; Fig. 12).

The presence of Lagenid foraminifers and the *Orbulina suturalis* indicate late early Badenian age for the Tekeres Fm., potentially deposited after 14.56 Ma (Hohenegger et al., 2009). This is in agreement with NN5 nannoplankton assemblage in the Ng-1 borehole, while the overlying Szilágy Fm. belongs to the NN6 zone corresponding broadly to the late Badenian (Selmeczi et al. 2004). The pyroclastic intercalations within the Tekeres Fm. of the Ng-1 borehole can be tentatively correlated with the Tar or Harsány Fm. of NE Hungary; their U-Pb ages correlate well with the NN5 zone (14. 88 and 14.36 Ma, Lukács et al., 2018).

No fossils belonging to the NN4 zone were documented except in the northernmost Ng-1 borehole where NN4 zone nannofossils are present just above the coal seams, within the first unambiguously marine layers (Báldi-Beke, pers. comm.) These layers indicate an earliest Badenian age (older than ~14.9 Ma, Hohenegger et al., 2009), and the underlying clastics could still be Badenian (~15–16 Ma) or belong to the late early Miocene (Karpatian, 17.25–16 Ma).

This older part of the Ng-1 sequence has no correlative sediments near the Keszthely Hills and the basal layers of the marine syn-rift sequence of the Tapolca and Várvölgy grabens can be correlated to the NN4–NN5 boundary of the Ng-1 borehole (Fig. 12). In these grabens the lowermost Badenian was marked by terrestrial conditions locally preserved as red clay and clastics (Fig. 12, Vöröstó Fm. in Hg-78/18). A similar terrestrial formation was deposited on the top of the Keszthely horst as sinkhole infillings up to ~14.5 Ma (Kelemen et al., 2021). We, therefore, conclude that the marine sedimentation around the Keszthely Hills started and the sinkhole fillings ended sometimes between 15 and 14 Ma, probably at 14.5 Ma.

The late middle Miocene (Sarmatian, 12.8–11.6 Ma) is marked by shallow marine sedimentation (limestone and marls), but the completeness of the sequence is questionable. Boreholes demonstrate that fine-grained sedimentation occurred in the earliest late Miocene (Pannonian) from 11 Ma up to ~10 Ma (sM3 on Fig. 13). Lacustrine sedimentation started only in the late Miocene on top of the Keszthely

Hills (Budai et al., 1999). A wave of flooding occurred around 10 Ma when sediments started to fill up the deepest part of the Keszthely horst. This flooding was associated with the formation of small-scale, locally sourced deltas (Csillag et al., 2010; Sztanó et al., 2016; referred to as klM3 Kálla Fm. on Fig. 13). The transgression was soon followed by normal regression because the shelf-slope of the western Pannonian Basin reached the elevated TR. Biostratigraphic data suggest 9.7–8.7 Ma for this process (Magyar et al., 1999; Hably, 2013). The deltas and subsequent fluvial sedimentation had aggradational character so the area continued to subside. This was the time when the Keszthely horst was almost completely flooded; small erosional remnants of this cover sequence are still preserved on the high plateau.

4.2. *Structures and morphology of the Keszthely Hills – the story of rifting "on land"*

4.2.1. *Landforms and deformation*

Landforms and small remnants of the Miocene succession on the elevated Keszthely Hills are the key elements for understanding the local structural evolution. The Paleozoic-Mesozoic successions suffered terrestrial denudation during several phases since the Cretaceous. This denudation resulted in an originally sub-horizontal surface which is dissected by vertical dolines (sinkholes) reaching max. 120m depth (Csillag and Nádor, 1997). The sinkholes were filled with sediments, mostly kaolinic clays, and underwent in-situ weathering. The infill was dated by zircon crystals deriving from airborne volcanic ash originated from the Carpathian-Pannonian Neogene volcanism; the most probable source of the ash is in NE Hungary where the recent results prove the same ages (Lukács et al., 2018). The age spectrum of Miocene zircons is between ~16 to 14.5 Ma in the borehole Kht-4 (Keszthely Hills) while it is somewhat older in a nearby borehole Uzsa Uzst-2 (~20–16 Ma, fig. 11C; Kelemen et al., 2021).

Topographic cross-sections demonstrate that the entire Keszthely Hills were tilted to the west–southwest (Fig. 13c) (Csillag and Nádor, 1997). The tilting and concurrent to subsequent denudation resulted in a three-fold subdivision of the morphology. The western–southwestern segment of the Keszthely Hills still shows the almost intact mid-Miocene denudation surface, where the infilled dolines are preserved in their nearly original depth. In the middle part of the hills, the terrain is rugged, and only the peaks of the hills correspond to the former mid-Miocene denudation surface. Here the valley incision possibly evolved during the tilting, and the steep dolines were eroded to their maximum depth. In the eastern segment, no Miocene dolines can be detected, probably because they were eroded during or after the tilting (Fig. 13c).

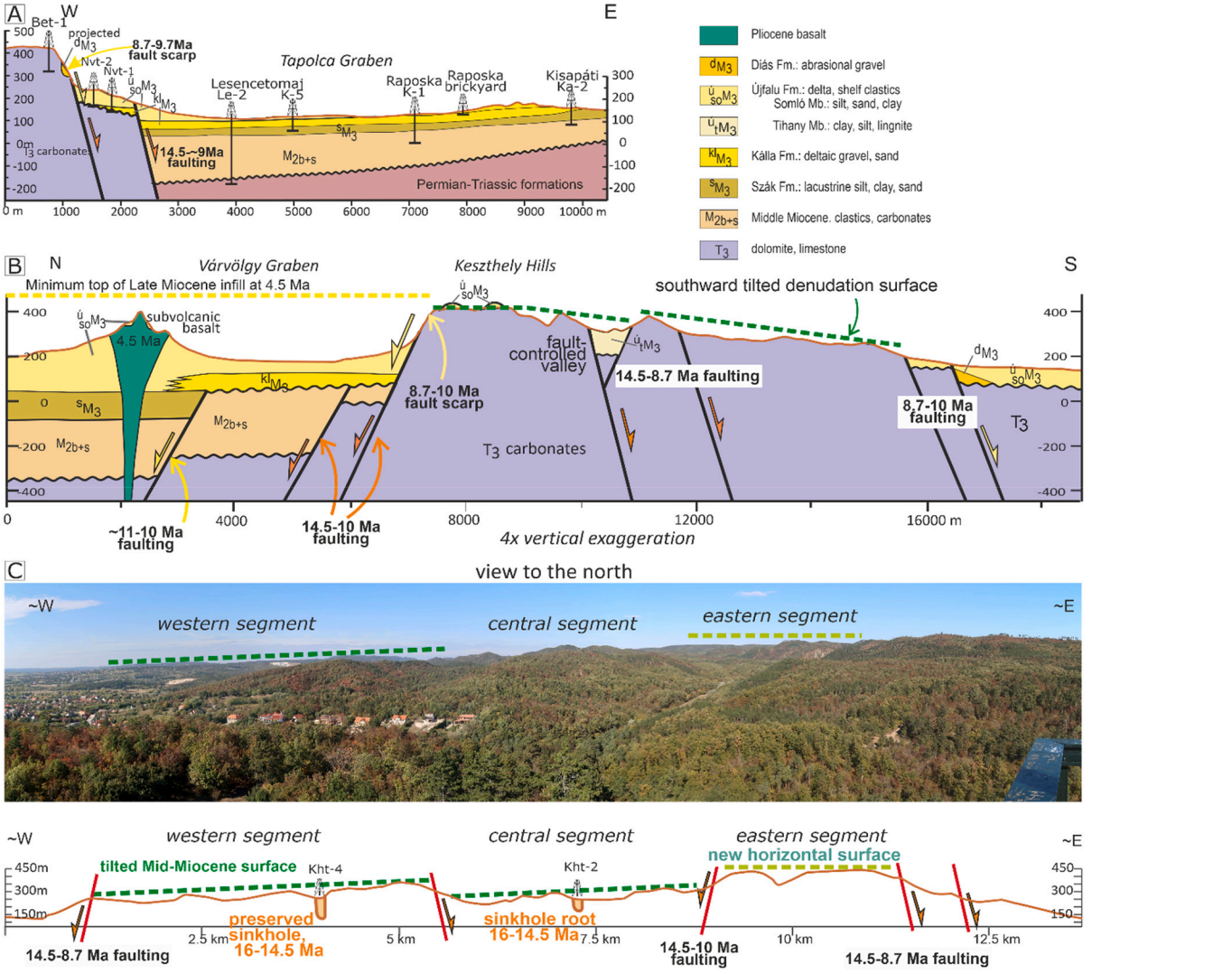

Fig. 13. a and b) Cross sections across the Keszthely Hills (southwestern TR) and surrounding grabens. Note tilted and faulted denudation surface and the variable, partly late Miocene age of deformation. c) View and simplified topographic cross section showing the pre-14.5 Ma denudation surface and its disintegration by faulting. For location of sections and the viewpoint, see Fig. 11. Note 4-fold vertical exaggeration.

Instead, a new sub-horizontal denudation surface developed which remained intact and was not dissected by valleys (Fig. 13c). We interpret this surface as a new denudation surface having cut the former tilted surface. All these processes should have occurred between ~14.5 and ~10 Ma because the basal late Miocene sequence sometimes covers eroded sinkholes (Keszthely Hills, Kht-2, Fig. 11).

4.2.2. Fault pattern

The map-scale fault pattern of the Keszthely Hills consists of NW–SE, N–S, and NE–SW trending elements. The faults show a gradual change in direction, frequent debranching, and relay ramps with locally developed connecting fault splays. The tectonic boundary of the horst itself is prominent along the northern and eastern margin. Boreholes demonstrate 0.5–0.7km offsets along these margins. The northern boundary fault extends much further to the NW, where displacement increases up to ~1.5 km in the Vasvár graben.

Several ~N–S trending faults, dipping east or west, displace the former denudation surface (Fig. 11b). Csillag and Nádor (1997) estimated the displacement of the faults, using the infilled dolines and the denudation surface as markers; the separation values reach 20–100 meters, so the crustal stretching remained modest. This faulting should postdate the formation of the surface because the infill of dolines was partly transported from a large distance. Thus faulting could have happened during or partly after the tilting. It is to note that tilting affected the Tapolca graben because it is also asymmetric and the infill is thickening toward the eastern boundary fault of the Keszthely Hills (Fig. 13a). We, therefore, suggest that the tilting of the elevated plateau and the major sedimentary graben was coeval. As we presented above, the cessation of sinkhole filling and the onset of graben sedimentation are coeval within a ~0.5 Ma interval.

Along the N–S-trending faults several small grabens filled with late Miocene sediments dissect the Keszthely Hills; the largest one is the Rezi graben (Fig. 11). These narrow grabens partly correspond to erosional valleys, but the steep and linear valley sides, and the different elevation of the tilted plateau fragments in the footwall and hanging wall suggest that faulting preceded valley incision.

4.2.3. Kinematics

Fault-slip data suggest that most faults have normal kinematics proved by conjugate "Andersonian" geometry and striae. NW- to N-trending faults exhibit oblique-dextral to almost purely dextral kinematics (Fig. 14). The estimated or calculated stress fields can be subdivided into three types; NE–SW, E–W to ESE–WNW, and (S)SE–(N)NW extension. The E–W tensional stress field tends to change toward a strike-slip type stress field with decreasing plunge of the striae. The (S)SE–(N)NW extension is occurring only sporadically and has no impact on map-view structures, therefore we interpret it as being a local variation of the general stress field, or a minor event.

4.2.4. Timing of denudation, faulting and basin subsidence around the Keszthely Hills

Although most of the data were measured in Triassic carbonates, faults, and joints post-date the Cretaceous folding and should, therefore, be of latest Cretaceous to Cenozoic age. A few data from late Miocene

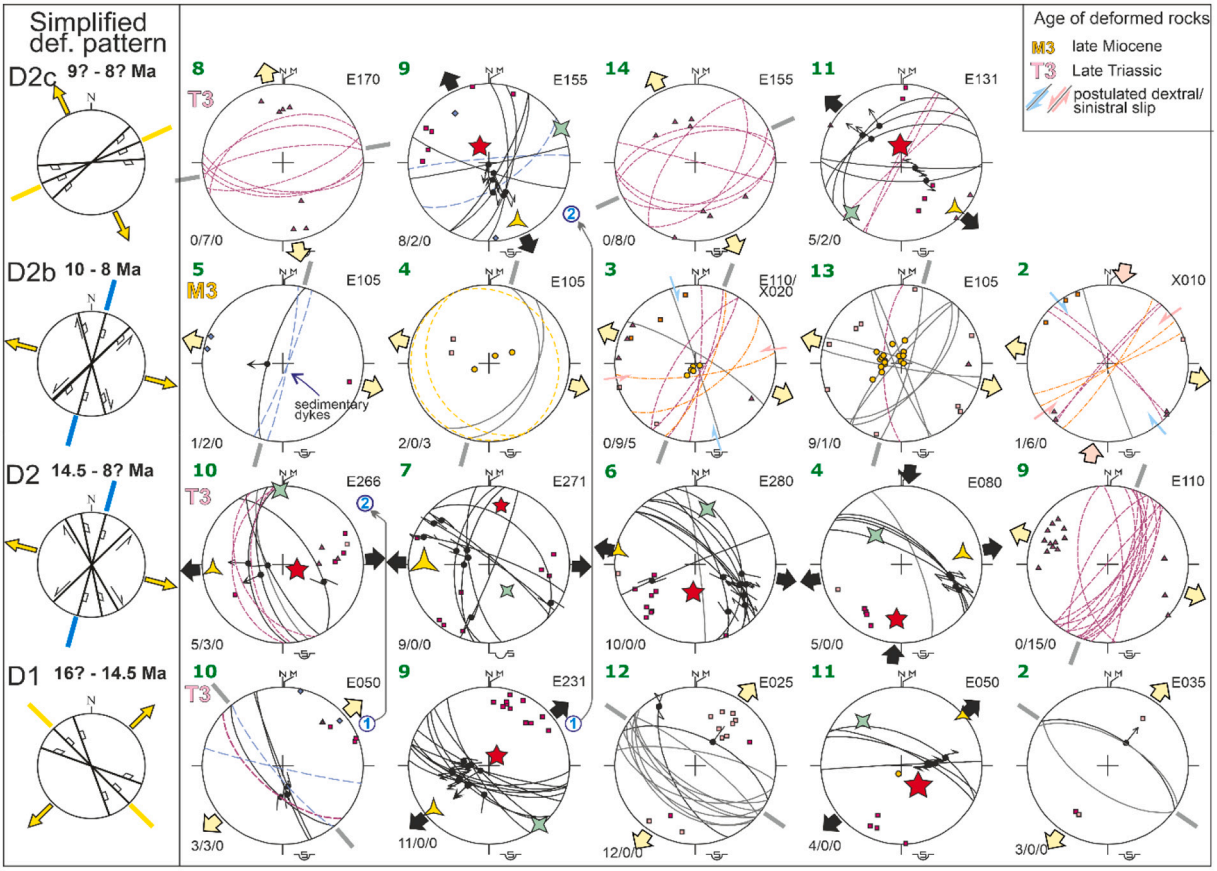

Fig. 14. Stereograms for outcrop-scale faulting in the Keszthely Hills. Note similar data for D2 phase measured in Triassic (T3) and late Miocene (M3) rocks. Left column shows the simplified deformation patterns for each deformation phase. For locations see Fig. 11b. Legend is on Fig. 8. Blue encircled numbers and arrows indicate relative chronology between phases. (For interpretation of the references to color in this figure legend, the reader is referred to the web version of this article.)

sediments clearly show that N–S to NNE–SSW trending fractures are at least partly late Miocene in age (Fig. 14). Oblique striae on NW-trending faults suggest a relative chronology between NE–SW extension (being older) and E–W extension, the latter having reactivated the former normal faults with dextral-normal slip (Fig. 14). This relative chronology is in agreement with regional data (Fodor et al., 1999; Márton and Fodor, 2003), which suggest a clockwise change of the extensional direction during Miocene rifting. This change was apparent and reflects the counterclockwise rotation of the Pannonian part of the ALCAPA unit including the Pohorje-Kozjak area (Márton and Fodor, 2003; Márton et al., 2006). The rotation and induced stress field change probably occurred in the 15–14 Ma time span (Fodor et al., 2020; Márton and Pécskay, 1998).

The age of detrital material within the sinkholes demonstrates a continuous terrestrial denudation phase during the late early to early middle Miocene from ~18 to 14.5 Ma. The general scarcity of earliest Miocene sediments in the entire TR extends the time span of terrestrial environment down to ca. 23 Ma. During this time span only outcrop-scale NW–SE oriented faults formed and this fault direction is poorly expressed within the Keszthely horst so the role of such early syn-rift faults are can be minor. The only exception could be the northern boundary fault; this was active in the west, near the Ng-1 borehole, and further northward, in the Vasvár graben, where initial subsidence started in the earliest middle Miocene (~16 Ma). The horst itself, and a larger area around it formed an elevated karstic plateau dominated by terrestrial sedimentation during the early middle Miocene. The Uzst-2 borehole constraints this paleogeographic interpretation at least up to 16 Ma placing the earliest possible faulting event around the turn of early to mid-Miocene. The Kht-4 borehole argues for the continuation of terrestrial environment and lack of faulting up to 14.5 Ma.

The tilting and the dissection of the mid-Miocene ("syn-rift") denudation surface argues for considerable deformation after ~14.5 Ma. The tilting also affected the syn-tectonic fill of the surrounding grabens (Fig. 13). The 14.5–12.8 Ma time span corresponds to the initial subsidence phase of the Tapolca and Várvölgy grabens; the sequences register a gradual deepening to few hundred meters. This subsidence and related faulting represent locally the rift initiation phase. Some of the late middle Miocene faults remained active in the earliest late Miocene from 11 to ~10 Ma when the oldest late Miocene formations were locally deposited in the fault-controlled grabens. Some faults seem to be sealed by the ~10 Ma old sedimentary package (Fig. 13b); this punctuates faulting into pre- and post-10 Ma events. Continuation of faulting after ~10 Ma is suggested by the distribution of the late Miocene stratigraphic units. Sediments of the ~10 Ma flooding filled up small grabens or tectonically controlled valleys dissecting the Keszthely Plateau. In the large grabens sedimentation continued at least up to 8.7 Ma and finally almost the whole plateau was covered by the distally-sourced delta sediments (Sztanó et al., 2016). Basin-margin faulting is corroborated by the presence of abrasional gravels all along the eastern fault scarps of the Keszthely Hills facing the Tapolca Graben.

These constraints suggest the following subdivision of deformation events and associated sedimentation following the nomenclature of Prosser (1993) describing the interplay between normal fault activity and synkinematic depositional systems. It has to be noted that the original description was applied to the marine North Sea basins, while its recent modifications were applied to the PB by Balázs et al. (2016) or to the Dinaridic extensional basins by Andrić et al. (2017). The onset of local normal fault activity indicating the rift initiation phase is dated as 16–14.5 Ma. Tectonically induced transgression and the rift climax period lasted between 14.5 and 10 Ma. Subsequent suppressed normal faulting marks the transition from late rift climax to immediate post-rift times between 10 and 8.7 Ma, followed by the overall late post-rift regression.

5. 3D thermomechanical modeling of the deformation migration in the western Pannonian Basin

5.1. Numerical model setup

Rift initiation and the structural style of extensional basin formation are influenced by a large number of parameters including the initial compositional layering and thermal properties of the lithosphere (e.g., Buck, 1988; Le Pourhiet et al., 2004; Tirel et al., 2008; Dias et al., 2015), rates of extension (Brune et al., 2014; Naliboff and Buiter, 2015) and are also controlled by surface processes, such as erosion and sedimentation (Andrés-Martínez et al., 2019; Balázs et al., 2021). A noteworthy observation in the Pannonian Basin system is the presence of early to middle Miocene exhumation of extensional domes at the western basin margin (Tari, 1996; Fodor et al., 2008; Ustaszewski et al., 2010) and the subsequent gradual migration of deformation towards the basin center (Tari et al., 1999; Matenco and Radivojević, 2012; Balázs et al., 2016). Our study proposes a new kinematic evolutionary model from the extension inception until the termination of extensional deformation and its spatial and temporal migration in the western part of the PB that here we address by the means of high resolution 3D coupled thermo-mechanical numerical modeling (Fig. 15). The initial model setup approximates in a simplified manner the pre-extensional crustal structure of the western PB focusing on the negative structural inversion of an inherited structural contact, which can be the equivalent the Cretaceous thrust or low-angle normal faults within the Austroalpine units (Fig. 15). While previous similar models for the PB analyzed its overall lithospheric evolution or the dynamics of the transfer zone between the extending units (Balázs et al., 2017, 2018), here we conduct high resolution modeling focused on the crustal-scale structural evolution of the western PB.

We use the numerical code I3ELVIS (Gerya and Yuen, 2007) that is based on the staggered finite differences and marker-in-cell techniques which solves the mass, momentum and energy conservation equations. We use visco-plastic rock rheologies that combine ductile diffusion and dislocation creep flow laws with the brittle/plastic Drucker-Prager yield criterion to determine whether viscous or brittle/plastic deformation occurs. Partial melting of the mantle is modeled by using the common parametrization of batch mantle melting processes of Katz et al. (2003). Further description of the applied numerical method (Gerya, 2013; Gerya et al., 2015) can be found in the Supplementary material 2.

The setup involves a volume of 404 × 180 × 228 km^3 with 1 km horizontal and vertical resolution. The frontal and rear sides of the model are free slip. A 15 km sticky air layer is imposed in the upper part of the model which mimics the internal free upper surface and enables the analysis of surface subsidence and uplift. Constant 2.5 cm/yr divergent velocity is imposed on the right model side simulating the slab roll-back and background extension from the Carpathians subduction zone. The initial temperature field is horizontally uniform and the temperature linearly increases from 0 °C at the surface, to 740 °C at Moho depth and 1330 °C at 100 km depth defining the base of the lithosphere. The setup consists of a 23 km thick upper crust (wet quartzite flow law), 19 km thick lower crust (diabase flow law) and mantle (both lithospheric and asthenospheric, dry olivine flow law). Furthermore, an inclined weakened zone representing an inherited thrust contact is defined in the upper crust in the middle of the model domain between 0 and 90 km in the Z direction until 23 km below the surface (Fig. 15). The sticky air layer is changed to water 15 km below the upper model boundary defining a water level. The parameter test is shown in the Supplementary material 2.

5.2. Structural features shown in the numerical model

During the initial stages of extension, deformation is localized in the close vicinity of the inherited thrust contact associated with footwall uplift and hanging wall subsidence in a half-graben geometry (Fig. 15d).

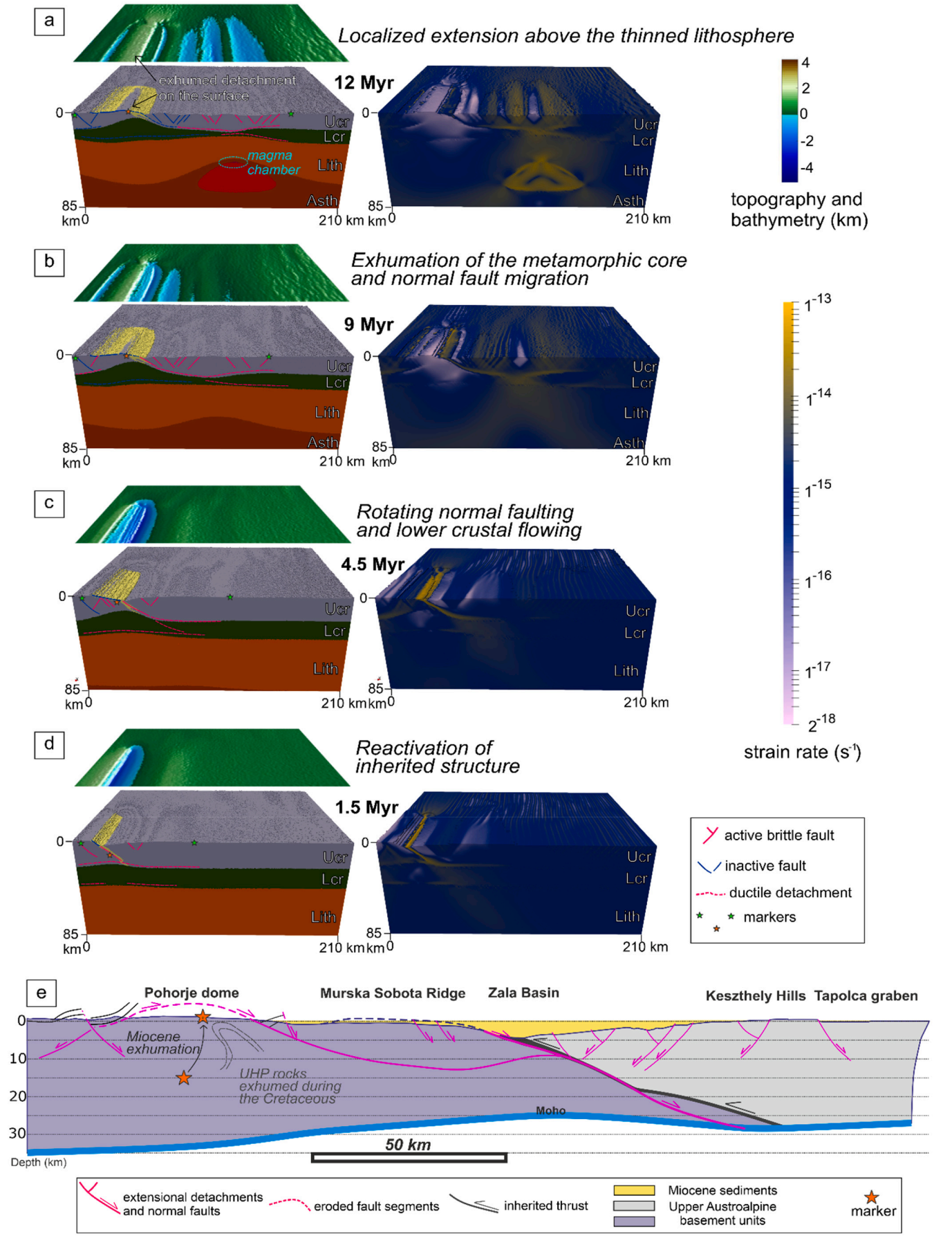

(caption on next page)

Fig. 15. a–d) 3D thermomechanical model showing the extensional reactivation of an inherited thrust contact (tilted yellow layers) within the upper crust and its temporal evolution. The model consists of an initially 23 km upper crust (Ucr), 19 km lower crust (Lcr), 58 km thick lithospheric mantle (Lith) and the underlying 113 km thick asthenosphere (Asth). Two green marker points are plotted at the sides of the extending domain, while another orange marker point at an initial depth of 17 km indicates extensional exhumation. Note the partially molten peridotites (red domain having low viscosity) and the molten basaltic magma chamber at the base of the lithosphere below the most extended domain after 12 Myr model run. Active and inactive brittle and ductile structures are drawn based on strain rate values. Effective viscosity results with blue color corresponding to low viscosity highlights zones of active deformation. e) Simplified geological cross-section through the Pohorje Dome, Mura-Zala and Tapolca basin area combined from sections of Figs. 5c, d (for location see Fig. 2). Moho depth map is drawn after Horváth et al. (2015) and Kalmár et al. (2018). (For interpretation of the references to color in this figure legend, the reader is referred to the web version of this article.)

The deformation in the upper crust, lower crust, and lithospheric mantle are decoupled by ductile weak layers at the base of the upper crust and base of the lower crust due to the high initial geotherm (Fig. 15c, d). These weak zones accommodate horizontal ductile crustal flow. Subsequent evolution is similar to the flexural rolling hinge type of extension (e.g., Buck, 1988; Axen, 1992), where the active fault zone migrates in the dip direction of the initial fault, while the inactive fault segment is gradually rotating creating a sub-horizontal fault surface. The lower and middle crust flows horizontally towards the uplifting footwall and facilitates updoming and crustal exhumation. A wider, low strain west-dipping retro-shear zone develops beneath the footwall of the reactivated fault zone (Fig. 15b). 9 Ma after the onset of extension the active fault plane has migrated ca. 30 km from the location of fault initiation, furthermore new brittle fault zones are activated and detached in the ductile middle crustal shear zone at 50–70 km from the initial extensional dome. In the area where the inherited thrust contact was not defined, distributed normal faulting affects the upper crust (Fig. 15b). Lithospheric mantle thinning is suppressed until 9 Ma (Fig. 15b versus c, d).

By 12 Ma after the onset of extension that corresponds to the end of the syn-rift phase in the PB the lithosphere is thinned to a minimum of 45 km beneath the most extended area, where also a magma chamber develops at the base of the lithosphere (Fig. 15a). By this time the older extensional dome has become inactive. Middle crustal rocks are exhumed from an initial depth of 18 km. The initial half-graben geometry is completely overprinted by the updoming of the extensional structure destroying the previously developed accommodation space. By this time active extensional deformation has migrated ~120 km eastwards, where upper crustal brittle faults are detached in middle and lower crustal ductile shear zones (Fig. 15a).

6. Discussion

6.1. Extension and contraction around the metamorphic domes

The exhumed metamorphic domes of the western PB are marked by the wavy geometry of the detachments. Penninic rocks of the Rechnitz windows form four NE-trending antiforms while in the three intervening synforms hanging wall units appear (Ratschbacher et al., 1990; Neubauer and Cao, 2021). In Slovenia, the Pohorje, Kozjak and MS Ridge are similar antiformal while the RS, Kapla troughs and Radgona, Ljutomer sub-basins are synformal features.

These folds can be interpreted in three ways; either they are antiformal and synformal corrugations, uniquely related to axis-parallel extension (Cann et al., 1997; Spencer, 1999), or they represent true contractional folds in a constrictional strain field where NE–SW extension and NW–SE contraction coexisted (Braathen et al., 2004; Holm et al., 1994; Singleton, 2013). Finally, contractional domes unrelated to extension are also possible.

Ratschbacher et al. (1990) interpreted the Rechnitz windows as contractional structures, due to their position in front of the foreland spur of the Bohemian massif. In this interpretation a contractional phase disrupted two extensional phases. On the other hand, Tari (1994, 1996) and Tari et al. (2020b) suggested pure extensional origin and suggested that corrugation axes are parallel to the crustal extensional direction and coeval with core complex exhumation. For the Pohorje Dome, Sölva et al. (2005) suggested Pliocene folding separating in time the extension and the contraction. In agreement with ~N–S shortening of the Pohorje Dome, small-scale fault-slip data indicate such deformation in the RS graben. To make the story complex, this stress field was either coeval with extension or post-dating it (Fodor et al., 2008, 2020; Fig. 8 of this study).

Nyíri et al. (this volume) considered as corrugation the small synformal basin above the Baján Detachment; here we apply such interpretation also to the Ljutomer and Radgona sub-basins on both sides of the MS ridge. The main phase of basin formation correlates with the main rifting stage (17–15 Ma) but continued, with modest rate, during the late syn-rift stage, between ~15 and ~13 Ma. The latter may be the continuation of detachment faulting or simply to non-tectonic folding due to differential compaction resulted by the overburden sediment load (Balázs et al., 2021).

In a regional context, contractional structures are present west from the western PB, like the positive flower structure of the entire northern Karawanke Mts. (Polinski and Eisbacher, 1992), the Klagenfurt basin (~13–0 Ma, Nemes et al., 1997) and in a number of Miocene basins within the Eastern Alps (Sachsenhofer et al., 2000; Gruber et al., 2004; Kurz et al., 2011; Reischenbacher and Sachsenhofer, 2013). Deformed syn-rift sediments and low-temperature geochronological data (Wölfler et al., 2010; Neubauer et al., 2018) indicate that the structures mostly post-date the middle Miocene extension and belong to the neotectonic phase, although strike-slip faulting and transtension are an integrated part of the local syn-rift deformation, too.

These data indicate that the contractional structures mostly post-date the main phase of extension. This leads us to favor a complex origin of the corrugations, the early extensional origin could be later modified by contraction after the syn-rift climax, possibly during the “neotectonic phase”. Additional data, mainly for the time constraints, are necessary for definite interpretation.

6.2. Depocenter migration in the western PB

The presented geochronological data, in association with structural data, suggest that extensional deformation at the western part of the PB (Pohorje, Kozjak, Murska Sobota domes, Mura-Zala Basin) could have started in the time span of 25–23 Ma, but was certainly active from ~19 Ma onwards (Fig. 16). This led to the exhumation of the middle part of the Austroalpine nappe pile, although this process could have partly happened already in the Late Cretaceous; the exact proportion of the two phases of exhumation remains questionable for the Kozjak Dome. The suggested time span overlaps with the exhumation of the Penninic rocks in the Rechnitz windows along low-angle detachments (Dunkl and Demény, 1997; Cao et al., 2013; Ratschbacher et al., 1990) (Fig. 16). Post-25 Ma extensional exhumation characterizes the metamorphic domes along the Sava river and in the Tauern windows (Ustaszewski et al., 2010; Stojadinović et al. 2013; Toljić et al., 2013; Scharf et al., 2013), and thus the western PB perfectly fits into this extensional deformation. Cooling ages in the Pohorje Dome clearly constraint the ductile (crystalplastic) deformation regime up to 15 Ma, while the temperature could be around 200–300°C in the Kozjak Dome and MS Ridge within the same time span.

The onset of sedimentation is poorly constrained in the supra-detachment basins because of the terrestrial character of the initial sedimentary sequences. Ottnangian (19–17.25 Ma) or only Karpatian (17.25–15.97 Ma) onset can be considered in the Styrian, Slovenj Gradec

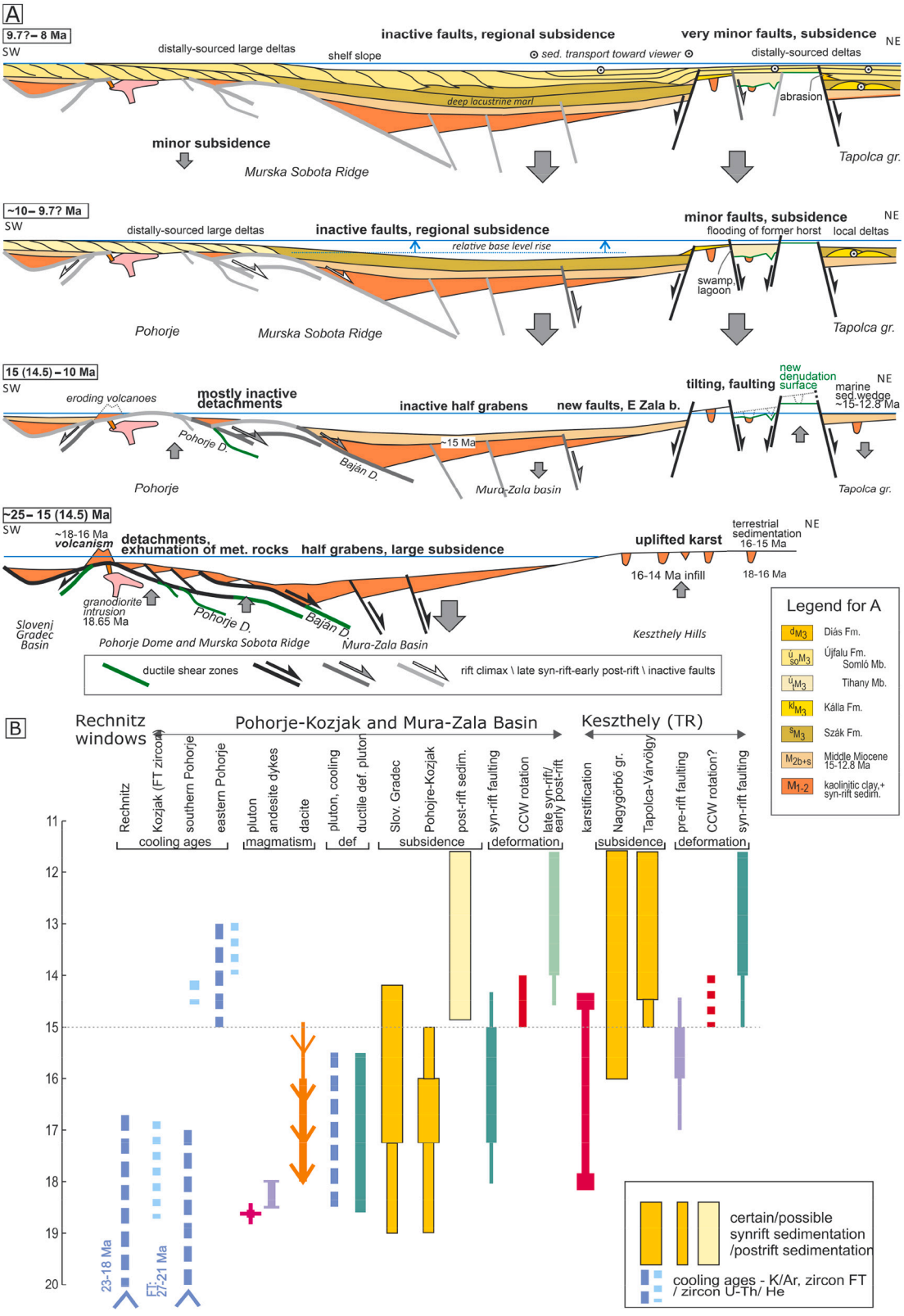

Fig. 16. a) Model for subsidence, exhumation and uplift in the southwestern Pannonian Basin, restricted to the late early and middle Miocene. b) Timing of the main magmatic, structural and sedimentary processes. Thick and thin lines and boxes mark the certain or possible duration of the process.

basins or in the tilted blocks of the NW Pohorje Mts. (Hohenegger et al., 2009; Ivančič et al., 2018; and Sachsenhofer et al., 1997; Stingl, 1994, respectively). The 19–15 or 18–15 Ma time span corresponds to the most important and fastest subsidence of the western Pannonian Basin (Fig. 16). The depositional environment evolved from terrestrial through near-shore to a bathyal one; the latter is indicated by the plankton-benthos ratio of foraminifers (Jelen and Rifelj, 2003). Extensional deformation gradually ceased from 15 Ma onwards, with the

development of an angular discordance (Fig. 6 and Tari, 1994). While 1–2.5 km of sediments were accumulated in the syn-rift grabens, the far-field edge of the largest tilted block, the Keszthely Hills were exposed to terrestrial conditions, and underwent denudation; U-Pb ages indicate doline-filling sedimentation in elevated karst plateaus from at least 18 Ma, up to ~14.5 Ma (Fig. 16).

Rift climax of the Mura-Zala Basin could be coeval with the onset of initial faulting, i.e., rift initiation in the Keszthely Hills, where no sign of subsidence nor sedimentation is preserved. The initiation of subsidence is present only north of the Keszthely Hills (Nagygörbő graben in Figs. 2, 16b) in a location closer to the Rába Fault and Zala Basin. After this first phase of faulting a counterclockwise rotation could have occurred, probably between 15 and 14 Ma (Figs. 8, 14, 16b). The change in the stress field from ~ENE–WSW to ~ESE–WNW extension can be coeval within the study area and was due to the vertical-axes block rotations. The role of this change is different in the western and eastern sub-areas; it separated the syn-rift and immediate post-rift faulting phases in the Pohorje and Mura-Zala Basin, but the same event preceded the subsidence and was just followed by the syn-rift normal faulting in the TR. All these changes could be coeval with a major marine flooding in the Styrian Basin, which was younger than 15.2 Ma based on $^{40}Ar/^{39}Ar$ dating of volcaniclastic horizons (Sant et al., 2020)

The modest deformation from ~15 Ma onwards led to noticeable subsidence in newly formed grabens and to flooding of the TR, the formerly elevated part of the Pannonian Basin. In contrast, post-15 Ma faulting was very modest in the Mura-Zala Basin because only a few faults displace slightly the intra-Badenian unconformity (Figs. 6, 16a). Exhumation continued in the metamorphic domes and the detachments could slightly be reactivated in the brittle field. Active faulting continued in the Keszthely hills through the early late Miocene up to ~8 Ma but was completely terminated in the Mura-Zala Basin. Two main faulting events occurred in the late Miocene lacustrine environment, where at first, the local, then the distally derived deltas filled the accommodation space from the north (Fig. 16a; Csillag et al., 2010; Sztanó et al., 2016). In summary, all these observations suggest a shift of active faulting, basin subsidence, and syn-tectonic sedimentation from the west (Pohorje Dome and Mura-Zala Basin) toward the Pannonian Basin center in the range of ca. 200–250 km.

6.3. *Comparison of field data and modelling results on the style and evolution of deformation*

The structural geometries observed in the field and in the numerical model agree fairly well; flattened detachment with rotated blocks has been observed in the Kozjak dome (Figs. 5 and 15). The west-dipping crustal low strain shear zone seen in the model corresponds to a similarly dipping shear zone inferred at the western boundary of the Kozjak Dome (site 93e, Figs. 5a, c and 15b).

The numerical model assumed an initially thickened (42 km), hot crust resulted from the preceding orogenic evolution. This is in agreement with the reconstructed pre-rift architecture of the Eastern Alps (Rosenberg et al., 2018). Further models with initially thinner and thicker crust are shown in the Supplementary material 2. Our imposed crustal weak zone simplifies an inherited rheologically weak thrust or nappe contact in the upper crust. Its location determines the initial localization of extension, whereas subsequent structures are not predefined, but self-organized.

In the eastern Pohorje dome UHP rocks have been exhumed during the Cretaceous (Janák et al., 2015) from ~100km. UHP rocks subducted below the mantle wedge during peak metamorphism were initially exhumed by slab extraction (Janák et al., 2004). The driving force of exhumation to mid-crustal levels was the negative buoyancy of the subducted material (Janák et al., 2015). This process needs an exhumation channel and a ductile extensional shear zone above the UHP rocks; the geometry of the structures has not yet been precisely determined. The postulated shear zone can be connected to Cretaceous thrusting and could be reactivated by late Cretaceous normal shearing as well (Kirst et al., 2010; Janák et al., 2015). The Pohorje Detachment is located close to this zone while it represents a major gap in metamorphic degree between (ultra)high-pressure and low-grade rocks. Therefore, the Miocene extension can be initiated along the inherited Cretaceous structures.

Thermochronology from the Pohorje-Kozjak Domes and dating of the oldest rift climax syn-kinematic strata from the neighboring depocenters inferred a temporal lag between the onset of extension and syn-rift sedimentation. Numerical models also predict a lag between the onset of extension and the oldest preserved syn-kinematic sedimentary ages. This is due to the fast lithospheric mantle thinning and initially distributed low offset faulting and related initial surface updoming (Balázs et al., 2017). Our model assuming a crustal weak zone also predicts a temporal shift between the onset of extension and the oldest preserved depocenter due to the rotating and updoming detachment that cannibalizes and gradually exhumes the oldest supra-detachment depocenter. This temporal shift between rift initiation and rift climax subsidence in the preserved depocenter is around 5 Ma in the model and the difference between the 25–23 Ma and 19–18 Ma timing for the onset of extension and rift climax sedimentation, respectively, is closely the same. Our model is also in good agreement with the spatial and temporal variation of extension in the Pohorje-Kozjak Domes and its gradual migration eastwards, first, to the Zala Basin with the deepest depocenter (at ~17 Ma), then towards the Keszthely Hills and Tapolca half-graben (~14.5 Ma). 12 Myr after the initiation of extension, at ~11–13 Ma the model predicts still ongoing faulting at the easternmost part of the section, ~100–120 km away from the exhumed domes (Fig. 15a); this is the case in the Tapolca graben where ongoing late Miocene faulting is clear (Figs. 12, 13, 16a). The model predicts the lack of late Miocene faults in the west, which is clearly seen on seismic sections in the Mura-Zala Basin (Fig. 6), and only modest jointing has been observed in upper Miocene outcrops (Márton et al., 2002a).

The parameter tests show that models with thicker and hotter crust would favor a larger 135 km distance from the MCC to the final localization of deformation. Previous, larger lithospheric-scale numerical models analyzed the role of inherited lithospheric suture zones and the role of surface processes in the migration of deformation in the Pannonian Basin. Those models assumed an overall 260 km extension creating a 350 km wide basin system, where deformation migrated ~180 km from the orogenic margin to the most thinned Great Hungarian Plain part of the Pannonian Basin center (Balázs et al., 2017).

Finally, thermochronology of the Pohorje Dome indicates the exhumation of middle crustal rocks from ~15–18 km depth which is reproduced by our model (compare orange markers on Figs. 175d and b). The overall evolution of these structures resembles the formation of metamorphic core complexes. Our parameter study shows that lower initial crustal thickness and lower initial Moho temperature values lead to suppressed lower crustal flow and thus lower amounts of exhumation. Similar results are reported from classical metamorphic core complexes, such as in the Mediterranean (Tirel et al., 2008; Huet et al., 2011). In the Pannonian Basin, the amount of extension is much lower than in the Aegean case. Nevertheless, in both basins exhumation of middle crustal rocks, and the ductile horizontal flow of the lower crust accommodating upper crustal brittle faulting characterized the initially thick and hot crust.

6.4. *Extension, transfer faults and rotation from a Pannonian perspective*

Most of the earlier works recognized that extension in the Pannonian Basin was associated with rotations. For the western margin of the PB, Balla (1984) suggested a simple curved fault passing across the Rechnitz windows and the Styrian Basin; this fault would separate non-rotated and counterclockwise (CCW) rotated domains. Analogue models for the deformation of the Alps suggested CCW rotations mostly because the easily deforming PB permitted this deformation (Ratschbacher et al.,

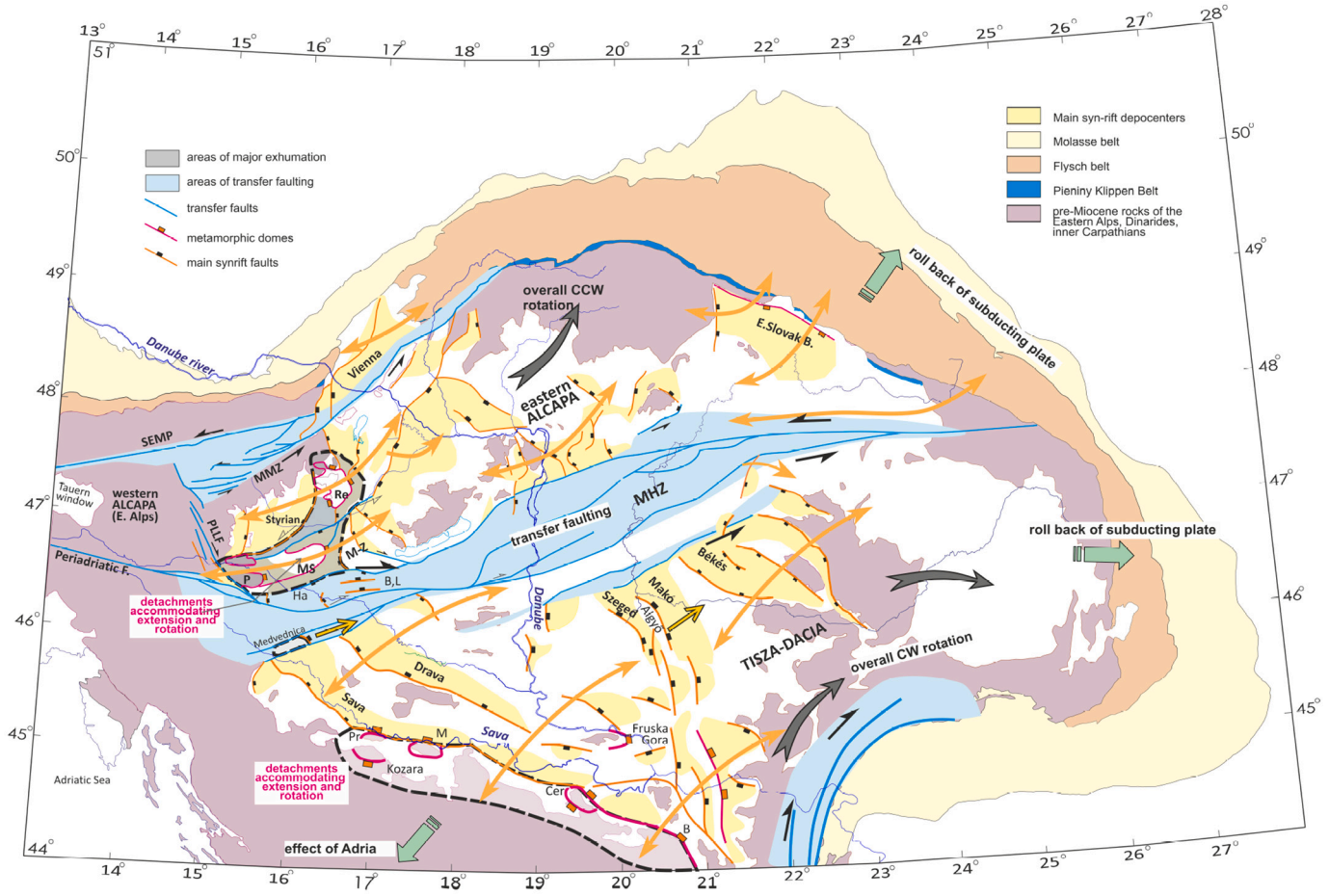

Fig. 17. Model for the distribution and geometry of core complexes, major normal faults, transfer faults in the Pannonian Basin. After Csontos (1995); Balázs et al. (2017); Fodor et al. (1998, 1999); Maţenco and Radivojević (2012); Ustaszewski et al. (2010), following the early idea of Balla (1984, 1988). B: Bukulja; B,L: Budafa, Lovászi grabens; Ha: Haloze; MS: Murska Sobota Ridge; M-Z: Mura-Zala Basin; M: Motajica; MMZ: Mur-Mürz-Zilina fault zone; P: Pohorje; PLLF: Pöls-Lavantal-Labot Fault; Pr: Prosara; Re: Rechnitz windows; SEMP: Salzachtal-Ennstal-Mariazell-Puchberg Fault (Ratschbacher et al., 1991b)

1991b; van Gelder et al., 2017).

This study argues for the presence of large-scale extension in the Pohorje, Kozjak, and Murska Sobota Domes and more to the north, in the Styrian Basin and Rechnitz windows where large-scale extension has already been documented (Ratschbacher et al., 1990; Tari, 1996; Sachsenhofer et al., 1997; Cao et al., 2013; Tari et al., 2020b). More to the north, in the Vienna Basin, NE-SW extension remains modest (Decker, 1996), and this basin is separated from the southern extensional domain by the Mur-Mürz strike-slip (transfer) fault zone (Sachsenhofer et al., 2003; van Gelder et al., 2020). The northward decreasing amount of extension would require a counterclockwise rotation of the hanging wall block, the western basins of the PB itself, with respect to the non- or slightly rotated footwall (Eastern Alps) (Fig. 17). Following Fodor et al. (1998) we emphasize that not a simple steep curved fault zone separated the differently rotating units (Balla, 1984; Ratschbacher et al., 1990) but instead, a wide extensional belt involving low-angle detachment zones and metamorphic core complexes (Fig. 17). Further to the east a system of northward terminating normal faults and northward narrowing grabens is present east from this extensional corridor within the ALCAPA block; good examples are the grabens east of the Danube (Fig. 17). This structural geometry would result in a larger CCW rotation in the eastern than the western part of the ALPACA (Márton and Fodor, 2003).

Paleomagnetic data measured on the pre-rift and early syn-rift rocks seem to be in fairly good agreement with this model. The Pannonian segment of the ALCAPA block suffered up to 80° CCW rotation while this remained modest in the Eastern Alps, west of the extensional domain (Márton and Márton, 1996; Márton et al., 2000a; Márton and Fodor, 2003; Márton et al., 2015). Although good time constraints are scarce, data indicate rotations during the rifting, after 18–17 and before ~15 or ~14 Ma (Márton and Pécskay, 1998; Petrik et al., 2016; Lukács et al., 2018). This short time span falls in the later part of the rift climax phase of the western PB. This rotation can also explain the apparent change in the extension direction from ENE–WSW to ESE–WNW within the study area, between D1 to D2 phases, while the regional direction of extension did not change and could be around E–W (Márton and Fodor, 2003). It is to note that in the northeastern part of the ALCAPA rotation continued after 14 Ma, during the latest middle Miocene (Márton and Pécskay, 1995; Márton et al., 2000b).

A similar combination of rotation and extension is present in the southern Tisza-Dacia block. The low-angle detachments and associated metamorphic domes were almost exclusively described along the southwestern and southern margin of the PB (Ustaszewski et al., 2010; Maţenco and Radivojević, 2012; Stojadinović et al., 2013). The exceptions are the Fruška Gora (Toljić et al., 2013) and possibly the Algyő High where the amount, timing, and structural style of extension is disputed (Fig. 17) (cf., Tari et al., 1999; Balázs et al., 2016). Like along the western margin of the PB, the "southern Pannonian extensional belt" separated domains with different rotations, namely the dominantly CCW rotated Adria and CW rotated southern PB (Fig. 17).

NW–SE trending major depocenters mark the structural geometry from the Sava, Drava Basin, to Szeged, Makó, and Békés half-grabens

(Györfi and Csontos, 1994; Csontos, 1995). The extensional area converges into a narrow stripe between the Dinarides and the Southern Carpathians (Fig. 17) (Maţenco and Radivojević, 2012). Most of these extensional structures are wedging southward, inferring a larger amount of extension towards the north (MHZ) and contributing to the potentially larger CW rotation of the eastern part of the Tisza-Dacia block. This model of wedge-shape grabens strengthens the earlier idea of Balla (1984, 1988) Csontos (1995) and Maţenco and Radivojević (2012) about the rotational deformation of the Tisza-Dacia block. Its CW rotation has an important kinematic consequence, the curved dextral shear zone along the Southern Carpathians and their transition to the Balkan Mts. Map-scale faults and the characteristic stress field were demonstrated by a number of studies (Fügenschuh and Schmid, 2005; Mladenović et al., 2019; Krstekanić et al., 2020). A similar kinematic model has been proposed for other Mediterranean extensional back-arc basins, such as the Aegean (Dewey and Şengör, 1979; Kissel and Laj, 1988; Jolivet et al., 2018) or Tyrrhenian Basins (Faccenna et al., 2014).

In the Tisza-Dacia block, paleomagnetic data seem to show an eastward younging trend; CW rotation in the western part of the Tisza block seems to be older than ~16 Ma (Márton and Márton, 1999) while the Apuseni Mts., the Transylvanian Basin, and the Southern Carpathians were still rotated during the middle to late Miocene (Patrascu et al., 1994; Dupont-Nivet et al., 2005; de Leeuw et al., 2013). Such an "eastward-younging rotation" would fit perfectly to the model. It is to note, however, that the young (post 6 Ma) CCW rotation in the southern margin of the PB (Márton et al., 2002b) complicates the picture for the syn-rift CW rotation of the Tisza-Dacia block.

The MHZ and some parallel shear zones within the Tisza block bound the oppositely rotating major blocks and form the boundaries of the wedge-shaped grabens (Fig. 17) (Balla, 1984, 1988; Csontos, 1995; Fodor et al., 1999). There are no high-angle normal faults or low-angle detachments cutting across the MHZ as all faults terminate against or within the shear zone (Fig. 17) (Fodor et al., 1999). Near the western parts of the MHZ, in the vicinity of the Alpine-Dinaridic junction, the NW-trending Drava, Sava grabens, and the Baján Detachment and high-angle faults in the Zala Basin bend to the MHZ from the south and north, respectively (Fig. 17). Another set of syn-rift extensional faults are within and parallel to the shear zone (Lovászi, Budafa, Haloze grabens on Figs. 2, 17; Dank, 1962; Márton et al., 2002a). Extensional structures which would accommodate NE–SW oriented extension can only be postulated from changes in thickness of Miocene sediments at the eastern margin of pre-Miocene outcrops (Fig. 2, south of Haloze). A noticeable exception is the Medvednica Mts. where extensional structures related to Cretaceous exhumation were reactivated in the Miocene (Fig. 17) (van Gelder et al., 2015). The western part of the MHZ and parallel syn-rift structures were prone to neotectonic reactivation (Fig. 2) (Márton et al., 2002a; Tari et al., 2020a). The situation is similar in the central and eastern part of the PB while no major crosscutting normal faults occur but the extension is parallel to the MHZ and was mostly accommodated by transtensional or pull-apart basins (Royden, 1988; Palotai and Csontos, 2010; Petrik et al., 2016; Balázs et al., 2018; Petrik et al., 2019). In conclusion, it is logical to consider the whole MHZ as a major transfer fault system, which completely separated the two extensional domains, the ALCAPA and Tisza-Dacia blocks and more locally in the southwestern PB, the "Pohorje–Kozjak–Mura-Zala–Rechnitz system" and the "Sava extensional system". This transfer zone represents a lithospheric weakness zone inherited from early Miocene extrusion tectonics (Balla, 1988; Csontos et al., 1992; Fodor et al., 1998) and from Cretaceous deformations, too (Handy et al. 215; Schmid et al., 2020).

Large-scale 3D numerical modeling provided a simple dynamic model for the formation of such basin systems and their separating transfer zone. Extensional reactivation of inherited structures located at the opposite basin margins (Fig. 1), and the diachronous formation of extensional (half-)grabens created a transfer zone between the extensional domains (Balázs et al., 2018). This wide transfer zone mimics the MHZ and consists of a number of diffused dextral and sinistral step overs, oblique rift arms evolving into pull-apart basins, strike-slip duplexes, and discontinuous transform faults. The gradual opening of new sub-basins in the ALCAPA and Tisza-Dacia units results in the episodic switches between the dextral and sinistral kinematics along the MHZ. Therefore, a common kinematic character cannot be ascribed to the entire zone during the rifting, since the kinematics was determined by the balance of extension rate in the two bounded crustal domains; it might have remained dextral in the west and changed to sinistral in the east (Fig. 17). The formation of such transtensional transfer zones is also coupled with rotation of the transfer faults and intervening crustal blocks, similarly to other extensional basins with pronounced along-strike variations, such as the Angola-Gabon passive margin (Péron-Pinvidic et al., 2015), the South China Sea (Franke et al., 2014), or the Northern Afar rift (Illsley-Kemp et al., 2018). When extensional offsets are several hundreds of kilometers, rotation of crustal units within the transfer zone can reach even 80–90 degrees (Gerya, 2013; Liao and Gerya, 2014). In the case of the PB the extension ceased before crustal break-up and before the formation of a mature transform fault, but ~25° rotation is predicted by numerical models between the oblique transtensional fault segments (Balázs et al., 2018).

7. Conclusions

This study combining near-surface observations and thermomechanical modeling brought new observations and ideas about the structural geometry and the temporal evolution of structures and basins in the western part of the Pannonian Basin system. Variable structures, ranging from ductile stretching lineation, detachment faults, and tilted half-grabens characterized the Miocene evolution of the western Pannonian Basin. Detailed stratigraphy demonstrates that the highest edges of tilted crustal blocks experienced exposure and denudation at the same time when the deepest sub-basin, located 80–100 km to west, underwent rapid subsidence, and the footwall of the bounding major detachment faults experienced rapid exhumation. Transfer faults striking obliquely or sub-parallel to the extension direction played an important role and connected domains with different amount or different style of extension. These structural features are integrated into a regional model of the entire Pannonian Basin and can be extrapolated to other extensional basins systems.

Thermochronological and field evidence document the detailed timing of crustal exhumation, ductile stretching, brittle faulting, and basin subsidence and their migration from the Alpine margin toward the basin center. Thermochronological data constraint the transition from ductile to brittle deformation style within the exhuming domes. This change around 15 Ma seems to be coeval with a major step in depocenter migration, counterclockwise block rotation, a concomitant change in extensional stress direction and could be correlated with a tectonically induced transgression and flooding of the formerly terrestrial depositional areas in the TR. Thermomechanical models simulating the extension of a thick and hot crust with a pre-existing weakness zone predict similar deformation migration from the exhumed crustal dome at the margin towards the most thinned basin center. Such models demonstrate the role of mantle processes in the migration of upper crustal faulting, lower crustal shearing, and basin subsidence. Building on the above described observational data makes the Pannonian Basin an ideal natural laboratory for understanding the coupling between deep Earth and near-surface processes.

Declaration of Competing Interest

The authors declare that they have no known competing financial interests or personal relationships that could have appeared to influence the work reported in this paper.

Acknowledgements

The early part of the research in Slovenia was carried out in the frame of numerous bilateral scientific cooperation projects between Slovenia and Hungary. The research was supported by the Slovenian Research Agency (research core funding No. P1-0195), and by a Central European Exchange Program for University Studies (CEEPUS) scholarship for Fodor. The Hungarian research grants of the National Research Development and Innovation Office (NKFIH) OTKA 106197 and K113013 supported the works of Csillag and Fodor, respectively. The manuscript has been finished with the support of the grant NKFI OTKA 134873. Balázs acknowledges financial support from the ETH Zürich Postdoctoral Fellowship program. MOL Plc. is acknowledged for the general support of the research and permission for publication of seismic sections. Taras Gerya (Zürich) is acknowledged for his thorough comments on an early version of the manuscript. 4 anonymous reviewers made very constructive remarks and suggested numerous aspects for improving the manuscript. Editorial support of Liviu Maţenco (Utrecht) helped to complete the revision.

Appendix A. Supplementary data

Supplementary data to this article can be found online at https://doi.org/10.1016/j.gloplacha.2021.103475.

References

Altherr, R., Lugović, B., Meyer, H.P., Majer, V., 1995. Early Miocene post-collisional calc-alkaline magmatism along the easternmost segment of the Periadriatic fault system (Slovenia and Croatia). Mineral. Petrol. 54, 225–247.

Andrés-Martínez, M., Pérez-Gussinyé, M., Armitage, J., Morgan, J.P., 2019. Thermomechanical implications of sediment transport for the architecture and evolution of continental rifts and margins. Tectonics 38, 641–665.

Andrić, N., Sant, K., Matenco, L., Mandic, O., Tomljenović, B., Pavelić, D., Hrvatović, H., Demir, V., Ooms, J., 2017. The link between tectonics and sedimentation in asymmetric extensional basins: inferences from the study of the Sarajevo-Zenica Basin. Mar. Pet. Geol. 83, 305–322.

Angelier, J., 1984. Tectonic analysis of fault slip data sets. J. Geophys. Res. 89 (B7), 5835–5848. https://doi.org/10.1029/jb089ib07p05835.

Axen, G.J., 1992. Pore pressure, stress increase, and fault weakening in low-angle normal faulting. J. Geophys. Res. 97, 8979–8991.

Bada, G., Horváth, F., Dövényi, P., Szafián, P., Windhoffer, G., Cloetingh, S., 2007. Present-day stress field and tectonic inversion in the Pannonian basin. Glob. Planet. Chang. 58, 165–180.

Balázs, A., Matenco, L., Magyar, I., Horváth, F., Cloetingh, S., 2016. The link between tectonics and sedimentation in back-arc basins: new genetic constraints from the analysis of the Pannonian Basin. Tectonics 35, 1526–1559. https://doi.org/10.1002/2015TC004109.

Balázs, A., Burov, E., Maţenco, L., Vogt, K., Francois, T., Cloetingh, S., 2017. Symmetry during the syn- and post-rift evolution of extensional back-arc basins: the role of inherited orogenic structures. Earth Planet. Sci. Lett. 462, 86–98.

Balázs, A., Maţenco, L., Vogt, K., Cloetingh, S., Gerya, T., 2018. Extensional polarity change in continental rifts: inferences from 3D numerical modeling and observations. J. Geophys. Res. Solid Earth 123, 8073–8094. https://doi.org/10.1029/2018jb015643.

Balázs, A., Maţenco, L., Granjeon, D., Vogt, K., Francois, T., Sztanó, O., 2021. Towards stratigraphic thermo-mechanical numerical modelling: integrated analysis of asymmetric extensional basins. Glob. Planet. Chang. 196 https://doi.org/10.1016/j.gloplacha.2020.103386.

Balla, Z., 1984. The Carpathian loop and the Pannonian Basin: a kinematic analysis. Geophys. Trans. 30, 313–353.

Balla, Z., 1988. On the origin of the structural pattern of Hungary. Acta Geol. Hung. 31, 53–63.

Braathen, A., Osmundsen, P.T., Gabrielsen, R.H., 2004. Dynamic development of fault rocks in a crustal-scale detachment: an example from western Norway. Tectonics 23, TC4010.

Brosch, F.J., Pischinger, G., 2014. Small- to meso-scale brittle rock structures and the estimation of "paleostress" axes — a case study from the Koralm region (Styria/Carinthia). Austrian J. Earth Sci. 107, 37–59.

Brun, J.-P., 1999. Narrow rifts versus wide rifts: inferences for the mechanics of rifting from laboratory experiments. Philos. Trans. R. Soc. Lond. 357, 695–710.

Brun, J.-P., Sokoutis, D., 2018. Core complex segmentation in North Aegean, a dynamic view. Tectonics 37, 1797–1830. https://doi.org/10.1029/2017TC004939.

Brun, J.-P., Sokoutis, D., van den Driessche, J., 1994. Analogue modeling of detachment fault systems and core complexes. Geology 22, 319–322. https://doi.org/10.1130/0091-7613(1994)022<0319:AMODFS>2.3.CO;2.

Brun, J.-P., Sokoutis, D., Tireld, C., Gueydane, F., van den Driessche, J., Beslier, M.-O., 2018. Crustal versus mantle core complexes. Tectonophysics 746, 22–45.

Brune, S., Heine, C., Perez-Gussinye, M., Sobolev, S.V., 2014. Rift migration explains continental margin asymmetry and crustal hyper-extension. Nat. Commun. 5 (4014) https://doi.org/10.1038/ncomms5014.

Buck, W.R., 1988. Flexural rotation of normal faults. Tectonics 5, 959–973. https://doi.org/10.1029/TC007i005p00959.

Budai, T., Császár, G., Csillag, G., Dudko, A., Koloszár, L., Majoros, Gy., 1999. Geology of the Balaton Highland. Explanatory Booklet to the Geological Map of the Balaton Highland, 1:50.000. Occasional Papers 197. Geol. Inst. of Hungary, Budapest, 257 p.

Burov, E., 2011. Rheology and strength of the lithosphere. Mar. Pet. Geol. 28, 1402–1443.

Cann, J.R., Blackman, D.K., et al., 1997. Corrugated slip surfaces formed at ridge–transform intersections on the Mid-Atlantic Ridge. Nature 385, 329–332.

Cao, S., Neubauer, F., Bernroider, M., Liu, J., Genser, J., 2013. Structures, microfabrics and textures of the Cordilleran-type Rechnitz metamorphic core complex, Eastern Alps. Tectonophysics 608, 1201–1225.

Csillag, G., Nádor, A., 1997. Multi-phase geomorphological evolution of the Keszthely Mountains (SW-Transdanubia) and karstic recharge of the Hévíz lake. Z. Geomorphol. Suppl. 110, 15–26.

Csillag, G., Sztanó, O., Magyar, I., Hámori, Z., 2010. Stratigraphy of the Kálla Gravel in Tapolca Basin based on multi-electrode probing and well data. Földtani Közlöny 140, 183–196.

Csontos, L., 1995. Tertiary tectonic evolution of the Intra-Carpathian area: a review. Acta Vulcanol. 7, 1–13.

Csontos, L., Nagymarosy, A., 1998. The Mid-Hungarian line: a zone of repeated tectonic inversion. Tectonophysics 297, 51–72. https://doi.org/10.1016/s0040-1951(98)00163-2.

Csontos, L., Nagymarosy, A., Horváth, F., Kováč, M., 1992. Tertiary evolution of the Intra-Carpathian area: a model. Tectonophysics 208, 221–241. https://doi.org/10.1016/0040-1951(92)90346-8.

Cvetković, M., Matoš, B., Rukavina, D., Kolenković Močilac, I., Saftić, B., Baketarić, T., Baketarić, M., Vuić, I., Stopar, A., Jarić, A., Paškov, T., 2019. Geoenergy potential of the Croatian part of Pannonian Basin: insights from the reconstruction of the pre-Neogene basement unconformity. J. Maps 15, 651–661. https://doi.org/10.1080/17445647.2019.1645052.

Dallmeyer, R.D., Neubauer, F., Handler, R., Fritz, H., Müller, W., Pana, D., Putiš, M., 1996. Tectonothermal evolution of the internal Alps and Carpathians: evidence from 40Ar/39Ar mineral and whole-rock data. Eclogae Geol. Helv. 89, 203–227, 0012-9402/96/010203-25.

Dallmeyer, R.D., Handler, R., Neubauer, F., Fritz, H., 1998. Sequence of thrusting within a thick-skinned tectonic wedge: evidence from $^{40}Ar/^{39}Ar$ and Rb-Sr ages from the Austroalpine Nappe Complex of the Eastern Alps. J. Geol. 106, 71–86.

Dank, V., 1962. Sketch of the deep geological structure of the south Zala basin. Földtani Közlöny 92, 150–159.

Davis, G.A., Lister, G.S., 1988. Detachment faulting in continental extension; perspectives from the southwestern U.S. Cordillera. In: Clark Jr., S.P., Burchfield, B. C., Suppe, J. (Eds.), Processes in Continental Lithospheric Deformation, Geol. Soc. Amer. Spec. Papers, Vol. 218, pp. 133–159.

de Leeuw, A., Filipescu, S., Maţenco, L., Krijgsman, W., Kuiper, K., Stoica, M., 2013. Paleomagnetic and chronostratigraphic constraints on the Middle to Late Miocene evolution of the Transylvanian Basin (Romania): implications for Central Paratethys stratigraphy and emplacement of the Tisza–Dacia plate. Glob. Planet. Chang. 103, 82–98. https://doi.org/10.1016/j.gloplacha.2012.04.008.

Decker, K., 1996. Miocene tectonics at the Alpine-Carpathian junction and the evolution of the Vienna Basin. Mitt. Ges. Geol. Bergbaustud. 41, 33–44.

Dewey, J., Şengör, C., 1979. Aegean and surrounding regions: complex multiplate and continuum tectonics in a convergent zone. Geol. Soc. Am. Bull. 90, 84–92.

Dias, A.E., Lavier, L.L., Hayman, N.W., 2015. Conjugate rifted margins width and asymmetry: The interplay between lithospheric strength and thermomechanical processes. J. Geophys. Res. Solid Earth 120, 8672–8700. https://doi.org/10.1002/2015JB012074.

Dolenec, T., 1994. New isotopic and radiometric data related to igneous rocks of the Pohorje Mountains. Rudarsko-metalurški zbornik 41, 147–152.

Dudko, A., Bence, G., Selmeczi, I., 1992. The tectonic origin of Miocene basins on the south-western edge of the Transdanubian Central Range. Ann. Rep. Geol. Inst. Hung. 1990, 107–124.

Dunbar, J.A., Sawyer, D.S., 1988. Continental rifting at pre-existing lithospheric weakness. Nature 333, 450–452.

Dunkl, I., Demény, A., 1997. Exhumation of the Rechnitz Window at the border of Eastern Alps and Pannonian basin during Neogene extension. Tectonophysics 272, 197–211.

Dunkl, I., Graseman, B., Frisch, W., 1998. Thermal effects of exhumation of a metamorphic core complex on hanging wall syn-rift sediments: an example from the Rechnitz Window, Eastern Alps. Tectonophysics 297, 31–50.

Dupont-Nivet, G., Vasilieva, J., Langereis, C.G., Krijgsman, W., Panaiotu, C., 2005. Neogene tectonic evolution of the southern and eastern Carpathians constrained by paleomagnetism. Earth Planet. Sci. Lett. 236, 374–387.

Duretz, T., Petri, B., Mohn, G., Schmalholz, S.M., Schenker, F.L., Muntener, O., 2016. The importance of structural softening for the evolution and architecture of passive margins. Sci. Rep. 6, 38704. https://doi.org/10.1038/srep38704.

Ebner, F., Sachsenhofer, R., 1995. Paleogeography, subsidence and thermal history of the Neogene Styrian Basin (Pannonian basin system, Austria). Tectonophysics 242, 133–150.

Faccenna, C., Nalpas, T., Brun, J.-P., Davy, P., 1995. The influence of pre-existing thrust faults on normal fault geometry in nature and in experiments. J. Struct. Geol. 17, 1139–1149.

Faccenna, C., Becker, T.W., Auer, L., Billi, A., Boschi, L., Brun, J.P., Capitanio, F.A., Funiciello, F., Horváth, F., Jolivet, L., 2014. Mantle dynamics in the Mediterranean. Rev. Geophys. 52, 283–332. https://doi.org/10.1002/2013RG000444.

Flügel, W., Neubauer, F. (Eds.), 1984. Geologische Karte der Steiermark, 1:200.000. Geol. Bundesanstalt, Wien.

Flügel, W., Kröll, A., Weber, F., 1988. Geologische Karte des prätertiären Untergrundes, Steierisches Becken-Südburgenlandische Schwelle, 1:200.000. Geol. Bundesanstalt, Wien.

Fodor, L., Jelen, B., Márton, E., Skaberne, D., Čar, J., Vrabec, M., 1998. Miocene-Pliocene tectonic evolution of the Slovenian Periadriatic Line and surrounding area – implication for Alpine-Carpathian extrusion models. Tectonics 17, 690–709. https://doi.org/10.1029/98TC01605.

Fodor, L., Csontos, L., Bada, G., Györfi, I., Benkovics, L., 1999. Tertiary tectonic evolution of the Pannonian basin system and neighbouring orogens: a new synthesis of paleostress data. In: Durand, B., Jolivet, L., Horváth, F., Séranne, M. (Eds.), The Mediterranean Basins: Tertiary Extension within the Alpine Orogen, Geol. Soc. London, Spec. Publ., Vol. 156, pp. 295–334.

Fodor, L., Jelen, B., Márton, E., Rifelj, H., Kraljić, M., Kevrić, R., Márton, P., Koroknai, B., Báldi-Beke, M., 2002. Miocene to Quaternary deformation, stratigraphy and paleogeography in Northeastern Slovenia and Southwestern Hungary. Geologija 45, 103–114.

Fodor, L., Koroknai, B., Balogh, K., Dunkl, I., Horváth, P., 2003. Nappe position of the Transdanubian Range Unit ('Bakony') based on new structural and geochronological data from NE Slovenia. Földtani Közlöny 133, 535–546.

Fodor, L.I., Gerdes, A., Dunkl, I., Koroknai, B., Pécskay, Z., Trajanova, M., Horváth, P., Vrabec, M., Jelen, B., Balogh, K., Frisch, W., 2008. Miocene emplacement and rapid cooling of the Pohorje pluton at the Alpine-Pannonian-Dinaric junction: a geochronological and structural study. Swiss J. Earth Sci. 101 (Supplement 1), 255–271. https://doi.org/10.1007/s00015-008-1286-9.

Fodor, L., Uhrin, A., Palotás, K., Selmeczi, I., Tóthné, Makk Á., Riznar, I., Trajanova, M., Rifelj, H., Jelen, B., Budai, T., Muráti, J., Koroknai, B., Mozetič, S., Nádor, A., Lapanje, A., 2013. Geological and structural model of the Mura–Zala Basin and its rims as a basis for hydrogeological analysis. Ann. Rep. Geol. Inst. Hung. 2011, 47–91.

Fodor, L., Márton, E., Vrabec, M., Koroknai, B., Trajanova, M., Vrabec, M., 2020. Relationship between magnetic fabrics and deformation of the Miocene Pohorje intrusions and surrounding sediments (Eastern Alps). Int. J. Earth Sci. 109, 1377–1401. https://doi.org/10.1007/s00531-020-01846-4.

Frank, W., Kralik, M., Scharbert, S., Thöni, M., 1987. Geochronological data from the Eastern Alps. In: Flügel, H.W., Faupl, P. (Eds.), Geodynamics of the Eastern Alps. Deuticke, Vienna, pp. 272–281.

Franke, D., Savva, D., Pubellier, M., Steuer, S., Mouly, B., Auxietre, J., et al., 2014. The final rifting evolution in the South China Sea. Mar. Pet. Geol. 58, 704–720. https://doi.org/10.1016/j.marpetgeo.2013.11.020.

Friebe, J.G., 1991. Neotektonik an der Mittelsteirischen Schwelle (Österreich). In: Die "Steirische Phase". Zbl. Geol. Paläontol. Teil I, pp. 41–54.

Frisch, W., Dunkl, I., Kuhlemann, J., 2000. Post-collisional orogen-parallel large-scale extension in the Eastern Alps. Tectonophysics 327, 239–265.

Froitzheim, N., Schuster, R., 2008. Alpine tectonics of the Alps and Western Carpathians: the Alps. In: McCann, T. (Ed.), The Geology of Central Europe, Geol. Soc. London, Vol. 2, pp. 1141–1181. Chapter 18.

Fügenschuh, B., Schmid, S.M., 2005. Age and significance of core complex formation in a very curved orogen: Evidence from fission track studies in the South Carpathians (Romania). Tectonophys 404, 33–53.

Genser, J., Neubauer, F., 1989. Low angle normal faults at the eastern margin of the Tauern Window (Eastern Alps). Mitt. Österr. Geol. Ges. 81, 233–243.

Gerya, T., 2013. Three-dimensional thermomechanical modeling of oceanic spreading initiation and evolution. Phys. Earth Planet. Inter. 214, 35–52.

Gerya, T.V., Yuen, D.A., 2007. Robust characteristics method for modelling multi-phase visco-elasto-plastic thermo-mechanical problems. Phys. Earth Planet. Inter. 163, 83–105.

Gerya, T.V., Stern, R.J., Baes, M., Sobolev, S.V., Whattam, S.A., 2015. Plate tectonics on the Earth triggered by plume-induced subduction initiation. Nature 527, 221–225.

Gosar, A., 1995. Modelling of seismic reflection data for underground gas storage in the Pečarovci and Dankovci structures – Mura depression. Geologija 37-38, 483–549.

Gruber, W., Sachsenhofer, R.F., Kofler, N., Decker, K., 2004. The architecture of the intramontane Trofaiach pull-apart basin inferred from geophysical and structural studies. Geol. Carpath. 55, 281–298.

Györfi, I., Csontos, L., 1994. Structural evolution of SE Hungary and Neogene basins of the Apuseni Mountains (Romania). Rom. J. Tectonics Reg. Geol. 75 (Suppl. 1), 19–20.

Haas, J., Budai, T., Csontos, L., Fodor, L., Konrád, Gy, 2010. Pre-Cenozoic Geological Map of Hungary 1:500000. Geol. Inst. Hung, Budapest.

Hably, L., 2013. The Late Miocene Flora of Hungary. Geol. Hung. Ser. Palaeont. 56, 175 p.

Handy, M.R., Ustaszewski, K., Kissling, E., 2015. Reconstructing the Alps–Carpathians–Dinarides as a key to understanding switches in subduction polarity, slab gaps and surface motion. Int. J. Earth Sci. 104, 1–26.

Harrison, T.M., Julien Célérier, J., Aikman, A.B., Hermann, J., Heizler., M.T., 2009. Diffusion of 40Ar in muscovite. Geochimica et Cosmochimica Acta 73, 1039–1051. https://doi.org/10.1016/j.gca.2008.09.038.

Héja, G., 2019. Mesozoic Deformations of the Western Part of the Transdanubian Range. PhD. thesis. Dept. Geol. Eötvös University, Budapest, Hungary, 154 p.

Herg, A., Stüwe, K., 2018. Tectonic interpretation of the metamorphic field gradient south of the Koralpe in the Eastern Alps. Austrian. J. Earth Sci. 111, 155–170. https://doi.org/10.17738/ajes.2018.0010.

Heron, P.J., Pysklywec, R.N., Stephenson, R., 2016. Lasting mantle scars lead to perennial plate tectonics. Nat. Commun. 7, 11834. https://doi.org/10.1038/ncomms11834.

Hohenegger, J., Rögl, F., Ćorić, S., Pervesler, P., Lirer, F., Roetzel, R., Scholger, R., Stingl, K., 2009. The Styrian basin: a key to the middle Miocene (Badenian/Langhian) Central Paratethys transgressions. Austrian J. Earth Sci. 102, 102–132.

Hohenegger, J., Ćorić, S., Wagreich, M., 2014. Timing of the Middle Miocene Badenian stage of the Central Paratethys. Geol. Carpath. 65, 55–66.

Holm, D.K., Fleck, R.J., Lux, D.R., 1994. The Death Valley turtlebacks reinterpreted as Miocene–Pliocene folds of a major detachment surface. J. Geol. 102, 718–727.

Horváth, F., Cloetingh, S., 1996. Stress-induced late-stage subsidence anomalies in the Pannonian basin. Tectonophysics 266, 287–300.

Horváth, F., Musitz, B., Balázs, A., Végh, A., Uhrin, A., Nádor, A., Koroknai, B., Pap, N., Tóth, T., Wórum, G., 2015. Evolution of the Pannonian basin and its geothermal resources. Geothermics 53, 328–352. https://doi.org/10.1016/j.geothermics.2014.07.009.

Huet, B., Pourhiet, L.L., Labrousse, L., Burov, E., Jolivet, L., 2011. Post-orogenic extension and metamorphic core complexes in a heterogeneous crust, the role of pre-existing nappes. Geophys. J. Int. 184, 611–625. https://doi.org/10.1111/j.1365-246X.2010.04849.x.

Illsley-Kemp, F., Bull, J., Keir, D., Gerya, T., Pagli, C., Gernon, T., et al., 2018. Initiation of a proto-transform fault prior to seafloor spreading. Geochem. Geophys. Geosyst. 19, 4744–4756. https://doi.org/10.1029/2018GC007947.

Ivančič, K., Trajanova, M., Ćorić, S., Rožič, B., Šmuc, A., 2018. Miocene paleogeography and biostratigraphy of the Slovenj Gradec Basin: a marine corridor between the Mediterranean and Central Paratethys. Geol. Carpath. 69, 528–544. https://doi.org/10.1515/geoca-2018-0031.

Jámbor, Á., Korpás, L., 1974. Strukturbohrung von Nagygörbő. Ann. Rep. Geol. Inst. Hung. 1972, 161–166.

Janák, M., Froitzheim, N., Lupták, B., Vrabec, M., Krogh Ravna, E.J., 2004. First evidence for ultrahighpressure metamorphism of eclogites in Pohorje, Slovenia: tracing deep continental subduction in the Eastern Alps. Tectonics 23, 1–6. https://doi.org/10.1029/2004TC0016 41.

Janák, M., Froitzheim, N., Yoshida, K., Sasinkova, V., Nosko, M., Kobayashi, T., Hirajima, T., Vrabec, M., 2015. Diamond in metasedimentary crustal rocks from Pohorje, Eastern Alps: a window to deep continental subduction. J. Metamorph. Geol. https://doi.org/10.1111/jmg.12130.

Jelen, B., Rifelj, H., 2003. The Karpatian in Slovenia. In: Brzobohatý, R., Cicha, M., Kováč, M., Rögl, F. (Eds.), The Karpatian: A Lower Miocene Stage of the Central Paratethys. Masaryk Univ., Brno, pp. 133–139.

Jolivet, L., Menant, A., Clerc, C., Sternai, P., Bellahsen, N., Leroy, S., Pik, R., Stab, M., Faccenna, C., Gorini, C., 2018. Extensional crustal tectonics and crust-mantle coupling, a view from the geological record. Earth Sci. Rev. 185, 1187–1209. https://doi.org/10.1016/j.earscirev.2018.09.10.

Kalmár, D., Süle, B., Bondár, I., AlpArray Working Group, 2018. Preliminary Moho depth determination from receiver function analysis using AlpArray stations in Hungary. Acta Geod. Geophys. 53, 309–321. https://doi.org/10.1007/s40328-018-0218-z.

Kästle, E., Rosenberg, C., Boschi, L., Bellahsen, N., Meier, T., El-Sharkawy, A., 2020. Slab break-offs in the Alpine subduction zone. Int. J. Earth Sci. 109, 587–603. https://doi.org/10.1007/s00531-020-01821-z.

Katz, R.F., Spiegelman, M., Langmuir, C.H., 2003. A new parameterization of hydrous mantle melting. Geochem. Geophys. Geosyst. 4, 1073. https://doi.org/10.1029/2002GC000433.

Kelemen, P., Csillag, G., Dunkl, I., Mindszenty, A., Kovács, I., Eynatten, v. H., Józsa S., 2021. Terrestrial kaolin deposits trapped in Miocene karstic sinkholes on planation surface remnants, Transdanubian Range, Pannonian Basin (Hungary). Geol. Mag. 158, 349–358. https://doi.org/10.1017/S0016756820000515.

Kirst, F., Sandmann, S., Nagel, J.T., Froitzheim, N., Janák, M., 2010. Tectonic evolution of the southeastern part of the Pohorje Mountains (Eastern Alps, Slovenia). Geol. Carpath. 61, 451–461. https://doi.org/10.2478/V1009 6-010-0027-Y.

Kissel, C., Laj, C., 1988. The Tertiary geodynamical evolution of the Aegean arc: a paleomagnetic reconstruction. Tectonophysics 146, 183–201.

Kókay, J., 1985. Central and Eastern Paratethyan interrelations in the light of Late Badenian salinity conditions. Geol. Hung. Ser. Paleont. 48, 7–95.

Koller, F., Pahr, A., 1980. The Penninic ophiolites on the eastern end of the Alps. Ofioliti 5, 65–72.

Kováč, M., Halásová, E., Hudáčková, N., Holcová, K., Hyžný, M., Jamrich, M., Ruman, A., 2018. Towards better correlation of the Central Paratethys regional time scale with the standard geological time scale of the Miocene Epoch. Geol. Carpath. 69 (3), 283–300. https://doi.org/10.1515/geoca-2018-0017.

Krenn, K., Fritz, H., Aberra, M., Schaflechner, J., 2008. Late Cretaceous exhumation history of an extensional extruding wedge (Graz Paleozoic Nappe Complex, Austria). Int. J. Earth Sci. (Geol Rundsch) 97, 1331–1352. https://doi.org/10.1007/s00531-007-0221-z.

Kröll, A., 1988. Reliefkarte des prätertiären Untergroundes, Steirisches Becken Südburgenlandische Schwelle, 1.200.000. Geologischen Bundesanstalt, Wien, Austria.

Kröll, A., Flügel, H.W., Seiberl, W., Weber, F., Wallach, G., Zych, D., 1988. Erläuterungen zu den Karten über den prätertiären Untergrund des Steirischen Beckens und der Südburgenlandischen Schwelle. Geologischen Bundesanstalt Wien, Austria, 49 p.

Krstekanić, N., Matenco, L., Toljić, M., Mandić, O., Stojadinović, U., Willingshofer, E., 2020. Understanding partitioning of deformation in highly arcuate orogenic systems: inferences from the evolution of the Serbian Carpathians. Glob. Planet. Chang. 195, 103361.

Kurz, W., Neubauer, F., 1996. Strain Partitioning during Formation of the Sonnblick Dome (southeastern Tauern Window, Austria). J. Struct. Geol. 18, 1327–1343.

Kurz, W., Fritz, H., Tenczer, V., Unzog, W., 2002. Tectonometamoprhic evolution of the Koralm Complex (Eastern Alps): constraints from microstructures and textures of the 'Plattengneis' shear zone. J. Struct. Geol. 24, 1957–1970.
Kurz, W., Wölfler, A., Rabitsch, R., Genser, J., 2011. Polyphase movement on the Lavanttal Fault Zone (Eastern Alps): reconciling the evidence from different geochronological indicators. Swiss J. Geosci. 104, 323–343.
Lavier, L.L., Manatschal, G., 2006. A mechanism to thin the continental lithosphere at magma-poor margins. Nature 440. https://doi.org/10.1038/nature04608.
Lavier, L.L., Buck, W.R., Poliakov, A.N.B., 1999. Self-consistent rolling-hinge model for the evolution of large-offset, low-angle normal faults. Geology 27, 1127–1130. https://doi.org/10.1130/0091-7613(1999)027<1127:SCRHMF>2.3.CO;2.
Le Pourhiet, L., Burov, E., Moretti, I., 2004. Rifting through a stack of inhomogeneous thrusts (the dipping pie concept). Tectonics 23. https://doi.org/10.1029/2003TC001584. TC4005.
Legrain, N., Stüwe, K., Wölfler, K., 2014. Incised relict landscapes in the eastern Alps. Geomorphology 221, 124–138.
Lelkes-Felvári, Gy, 1994. Penninic and Upper Austroalpine Units (Paleozoic of Graz?) in the Borehole Szombathely-ll (Western Hungary). In: Lobitzer, H., Császár, G. (Eds.), Jubiläumsschrift 20 Jahre Geologische Zusammenarbeit Österreich-Ungarn, Vol. II, pp. 379–384.
Lelkes-Felvári, Gy, Sassi, R., Frank, W., 2002. Tertiary S-C mylonites from the Bajánsenye-B-M-I borehole, Western Hungary. Acta Geol. Hung. 45, 29–44.
Li, B., Massonne, J.-H., Koller, F., Zhang, J., 2021. Metapelite from the high-ultrahigh pressure terrane of the Eastern Alps (Pohorje Mountains, Slovenia) – new pressure, temperature, and time constraints on a polymetamorphic rock. Tectonophysics. https://doi.org/10.1111/JMG.12581.
Liao, J., Gerya, T., 2014. Influence of lithospheric mantle stratification on craton extension: insight from two-dimensional thermomechanical modeling. Tectonophysics 631, 50–64. https://doi.org/10.1016/j.tecto.2014.01.020.
Lippitsch, R., Kissling, E., Ansorge, J., 2003. Upper mantle structure beneath the Alpine orogen from high-resolution teleseismic tomography. J. Geoph. Res. 108 (B8), 2376. https://doi.org/10.1029/2002JB002016.
Lister, G., Etheridge, M.A., Symonds, P.A., 1986. Detachment faulting and the evolution of passive continental margins. Geology 14, 246–250.
Lukács, R., Harangi, Sz., Guillong, M., Bachmann, O., Fodor, L., Buret, Y., Dunkl, I., Sliwinski, J., von Quadt, A., Peytcheva, I., Zimmerer, M., 2018. Early to Mid-Miocene syn-extensional massive silicic volcanism in the Pannonian Basin (East-Central Europe): eruption chronology, correlation potential and geodynamic implications. Earth Sci. Rev. 179, 1–19. https://doi.org/10.1016/j.earscirev.2018.02.005.
Magyar, I., Geary, D.H., Müller, P., 1999. Paleogeographic evolution of the Late Miocene Lake Pannon in Central Europe. Palaeogeogr. Palaeoclimatol. Palaeoecol. 147, 151–167.
Maros, Gy., Maigut, V., 2011. Pre-Cenozoic model horizon geology for Supra-Regional Area. In: Maros, Gy (Ed.), Summary Report of Geological Models. TransEnergy project, 190 p. www.http://transenergy-eu.geologie.ac.at.
Martin, U., Németh, K., 2004. Mio/Pliocene Phreatomagmatic Volcanism in the Western Pannonian Basin. In: Geol. Hung. Series Geol., Vol. 26 Geol. Inst. of Hung., Budapest, 191 p.
Márton, E., Fodor, L., 2003. Tertiary paleomagnetic results and structural analysis from the Transdanubian Range (Hungary); sign for rotational disintegration of the Alcapa unit. Tectonophysics 363, 201–224.
Márton, E., Márton, P., 1996. Large scale rotation in North Hungary during the Neogene as indicated by palaeomagnetic data. In: Morris, A., Tarling, D.H. (Eds.), Paleomagnetism and Tectonics of the Pre Mediterranean Region, Geol. Soc. London, Spec. Publ., Vol. 105, pp. 153–173.
Márton, E., Márton, P., 1999. Tectonic aspects of a paleomagnetic study in the Neogene of the Mecsek Mts. Geophys. Trans. 42, 159–180.
Márton, E., Pécskay, Z., 1995. The Tokay-Vihorlát-Oas-Ignis Triangle: complex evaluation of paleomagnetic and isotope age data from Neogene Volcanics. In: Proceedings XVth C.B.G.A. Congress. Geol. Soc. Greece Spec. Publ., Vol. 30.
Márton, E., Pécskay, Z., 1998. Correlation and dating of the Miocene ignimbritic volcanics in the Bükk foreland, Hungary: complex evaluation of paleomagnetic and K-Ar isotope data. Acta Geol. Hung. 41, 467–476.
Márton, E., Kuhlemann, J., Frisch, W., Dunkl, I., 2000a. Miocene rotations in the Eastern Alps – paleomagnetic results from intramontane basin sediments. Tectonophysics 323, 163–182.
Márton, E., Vass, D., Túnyi, I., 2000b. Counterclockwise rotations of the Neogene rocks in the East Slovak Basin. Geol. Carpath. 51, 159–168.
Márton, E., Fodor, L., Jelen, B., Márton, P., Rifelj, H., Kevrić, R., 2002a. Miocene to Quaternary deformation in NE Slovenia: complex paleomagnetic and structural study. J. Geodyn. 34, 627–651.
Márton, E., Pavelić, D., Tomljenović, B., Avanić, R., Pamić, J., Márton, P., 2002b. In the wake of a counterclockwise rotating Adriatic microplate: neogene paleomagnetic results from Northern Croatia. Int. J. Earth Sci. 91, 514–523.
Márton, E., Trajanova, M., Zupančič, N., Jelen, B., 2006. Formation, uplift and tectonic integration of a Periadriatic intrusive complex (Pohorje, Slovenia) as reflected in magnetic parameters and paleomagnetic directions. Geophys. J. Int. 167, 1148–1159.
Márton, E., Grabowski, J., Tokarski, A.K., Túnyi, I., 2015. Palaeomagnetic results from the fold and thrust belt of the Western Carpathians: an overview. In: Pueyo, E.L., Cifelli, F., Sussman, A.J., Oliva-Urcia, B. (Eds.), Palaeomagnetism in Fold and Thrust Belts: New Perspectives, Geol. Soc. London, Spec. Publ., Vol. 425 https://doi.org/10.1144/SP425.1.
Maţenco, L., Radivojević, D., 2012. On the formation and evolution of the Pannonian Basin: constraints derived from the structure of the junction area between the Carpathians and Dinarides. Tectonics 31 (6), TC6007.
McKenzie, D., 1978. Some remarks on the development of sedimentary basins. Earth Planet. Sci. Lett. 40, 25–32.
Miller, E.L., Dumitru, T.A., Brown, R.W., Gans, P.B., 1999. Rapid Miocene slip on the Snake Range–Deep Creek Range fault system, east–central Nevada. Geol. Soc. Am. Bull. 111, 886–905.
Mioč, P., 1977. Geologic structure of the Drava Valley between Dravograd and Selnica. Geologija 20, 193–230.
Mioč, P., Žnidarčič, M., 1976. Geological Map of Yugoslavia, 1:100 000, Sheet Slovenj Gradec. Geol. Survey of Yugoslavia, Beograd.
Mioč, P., Žnidarčič, M., Jerše, Z., 1981. Geological Map of Yugoslavia, Scale 1:100 000, Sheet Ravne na Koroškem. Geol. Surv. of Yugoslavia, Beograd.
Mitterbauer, U., Behm, M., Brückl, E., Lippitsch, R., Guterch, A., Keller, G.R., Koslovskaya, E., Rumpfhuber, E.-M., Sumanovac, F., 2011. Shape and origin of the East-Alpine slab constrained by the ALPASS teleseismic model. Tectonophysics 510, 195–206.
Mladenović, A., Antić, M.D., Trivić, B., Cvetković, V., 2019. Investigating distant effects of the Moesian promontory: brittle tectonics along the western boundary of the Getic unit (East Serbia). Swiss J. Geosci. 112, 143–161.
Nádor, A., Lapanje, A., Tóth, Gy, Rman, N., Szőcs, T., Prestor, J., Uhrin, A., Rajver, D., Fodor, L., Muráti, J., Székely, E., 2012. Transboundary geothermal resources of the Mura-Zala basin: joint thermal aquifer management of Slovenia and Hungary. Geologija 55, 209–224.
Naliboff, J., Buiter, S.J.H., 2015. Rift reactivation and migration during multiphase extension. Earth Planet. Sci. Lett. 421, 58–67.
Nemes, F., Neubauer, F., Cloetingh, S., Genser, J., 1997. The Klagenfurt Basin in the Eastern Alps: an intra-orogenic decoupled flexural basin? Tectonophysics 282, 189–203.
Neubauer, F., Cao, S., 2021. Migration of Late Miocene to Quaternary alkaline magmatism at the Alpine-Pannonian transition area: significance for coupling of Adria plate motion with the Alpine-Carpathian front. Glob. Planet. Chang. submitted.
Neubauer, F., Dallmayer, R.D., Dunkl, I., Schirnik, D., 1995. Late Cretaceous exhumation of the metamorphic Gleinalm dome, Eastern Alps: kinematics, cooling history and sedimentation response in a sinistral wrench corridor. Tectonophysics 242, 79–88.
Neubauer, F., Genser, J., Handler, R., 2000. Eastern Alps: result of a two-stage collision process. Mitt. Österr. Geol. Ges. 92, 117–134.
Neubauer, F., Heberer, B., Dunkl, I., Liu, X., Bernroider, M., Dong, Y., 2018. The Oligocene Reifnitz tonalite (Austria) and its host rocks: implications for Cretaceous and Oligocene–Neogene tectonics of the south-eastern Eastern Alps. Geol. Carpath. 69, 237–253. https://doi.org/10.1515/geoca-2018-0014.
Neubauer, F., Liu, Y., Chang, R., Yuan, S., Yu, Sh., Genser, J., Liu, B., Guan, Q., 2020. The Wechsel Gneiss Complex of Eastern Alps: an Ediacaran to Cambrian continental arc and its Early Proterozoic hinterland. Swiss J. Geosci. 113, 21. https://doi.org/10.1186/s00015-020-00373-3.
Nyíri, D., Tőkés, L., Zadravecz, Cs., Fodor, L., 2021. Early post-rift confined turbidite systems in a supra-detachment basin: implications for the Early to Middle Miocene basin evolution and hydrocarbon exploration of the Pannonian basin. Glob. Planet. Chang. submitted, this volume.
Ortner, H., Kositz, A., Willingshofer, E., Sokoutis, D., 2015. Geometryof growth strata in a transpressive fold belt in field and analogue model: Gosau Group at Muttekopf, Northern Calcareous Alps, Austria. Basin Res. 1–21. https://doi.org/10.1111/bre.12129.
Palotai, M., Csontos, L., 2010. Strike-slip reactivation of a Paleogene to Miocene fold and thrust belt along the central part of the Mid-Hungarian Shear Zone. Geol. Carpath. 61, 483–493. https://doi.org/10.2478/v10096-010-0030-3.
Patrascu, St., Panaiotu, C., Seclaman, M., Panaiotu, C.E., 1994. Timing of rotational motion of Apuseni Mountains (Romania): paleomagnetic data from Tertiary magmatic rocks. Tectonophysics 233, 163–176.
Péron-Pinvidic, G., Manatschal, G., 2009. The final rifting evolution at deep magmapoor passive margins from Iberia-Newfoundland: a new point of view. Int. J. Earth Sci. 98, 1581e1597.
Péron-Pinvidic, G., Manatschal, G., Masini, E., Sutra, E., Flament, J.M., Haupert, I., Unternehr, P., 2015. Unravelling the along-strike variability of the Angola-Gabon rifted margin: a mapping approach. Geol. Soc. Lond. Spec. Publ. 438, 49–76. https://doi.org/10.1144/SP438.1.
Petrik, A., Beke, B., Fodor, L., Lukács, R., 2016. Cenozoic structural evolution of the southwestern Bükk Mts. and the southern part of the Darnó Deformation Belt (NE Hungary). Geol. Carpath. 67, 83–104.
Petrik, A., Fodor, L., Bereczki, L., Klembala, Zs., Lukács, R., Baranyi, V., Beke, B., Harangi, Sz., et al., 2019. Variation in style of magmatism and emplacement mechanism induced by changes in basin environments and stress fields (Pannonian Basin, Central Europe). Basin Research 31 (2), 380–404. https://doi.org/10.1111/bre.12326. Internal Article ID: 16140691.
Pischinger, G., Kurz, W., Übleis, M., Egger, M., Fritz, H., Brosch, F.J., Stingl, K., 2008. Fault slip analysis in the Koralm Massif (Eastern Alps) and consequences for the final uplift of "cold spots" in Miocene times. Swiss J. Geosci. 101, 235–254.
Platt, J.P., Behr, W.M., Cooper, F.J., 2015. Metamorphic core complexes: windows into the mechanics and rheology of the crust. J. Geol. Soc. 172, 9–27. https://doi.org/10.1144/jgs2014-036.
Poli, G., Christofides, G., Koroneos, A., Trajanova, M., Zupančič, N., 2020. Multiple processes in the genesis of the Pohorje igneous complex: evidence from petrology and geochemistry. Lithos 364–365. https://doi.org/10.1016/j.lithos.2020.105512.

Polinski, R.K., Eisbacher, G.H., 1992. Deformation partitioning during polyphase oblique convergence in the Karawanken Mountains, southeastern Alps. J. Struct. Geol. 14, 1203–1213.
Prosser, S., 1993. Rift related depositional system and their seismic expression, in Tectonics and Seismic Sequence Stratigraphy. In: Williams, G.D., Dobb, A. (Eds.), Geol. Soc. Spec. Publ., 71 10.1144/GSL.SP.1993.071.01.03, pp. 35–66.
Qorbani, E., Bokelmann, G., Bianchi, I., 2015. Slab detachment under the Eastern Alps seen by seismic anisotropy. Earth Planet. Sci. Lett. 409, 96–108.
Ranero, C.R., Perez-Gussinye, M., 2010. Sequential faulting explains the asymmetry and extension discrepancy of conjugate margins. Nature 468, 294–299.
Ratschbacher, L., Frisch, W., Neubauer, F., Schmid, S.M., Neugebauer, J., 1989. Extension in compressional orogenic belts: the Eastern Alps. Geology 17, 404–407.
Ratschbacher, L., Behrmann, J., Pahr, A., 1990. Penninic windows at the end of the Alps and their relation to the intra Carpathian basins. Tectonophysics 172, 91–105.
Ratschbacher, L., Frisch, W., Linzer, H.G., Merle, O., 1991a. Lateral extrusion in the Eastern Alps, part 2.: structural analysis. Tectonics 10, 257–271.
Ratschbacher, L., Merle, O., Davy, P., Cobbold, P., 1991b. Lateral extrusion in the Eastern Alps, part 1: boundary conditions and experiments scaled for gravity. Tectonics 10, 245–256.
Reischenbacher, D., Sachsenhofer, R.F., 2013. Basin formation during the post-collisional evolution of the Eastern Alps: the example of the Lavanttal Basin. Int. J. Earth Sci. 102, 517–543. https://doi.org/10.1007/s00531-012-0807-y.
Reynolds, S.J., Lister, G.S., 1990. Folding of mylonitic zones in Cordilleran metamorphic core complexes: evidence from near the mylonitic front. Geology 18, 216–219.
Rosenberg, J., 2004. Shear zones and magma ascent: a model based on a review of the Tertiary magmatism in the Alps. Tectonics 23. https://doi.org/10.1029/2003TC001526. TC3002.
Rosenberg, C.L., Schneider, S., Scharf, A., Bertrand, A., Hammerschmidt, A., Rabaute, A., Brun, J.-P., 2018. Relating collisional kinematics to exhumation processes in the Eastern Alps. Earth Sci. Rev. 176, 311–344.
Royden, L., 1988. Late Cenozoic Tectonics of the Pannonian Basin System. In: Royden, L. H., Horváth, F. (Eds.), The Pannonian Basin, AAPG Memoir, Vol. 45, pp. 27–48.
The Pannonian basin. A Study in Basin Evolution. In: Royden, L.H., Horváth, F. (Eds.), Am. Assoc. Pet. Geol. Memoir 45.
Royden, L.H., Horváth, F., Rumpler, J., 1983. Evolution of the Pannonian Basin System. 1: Tectonics. Tectonics 2, 63–90.
Ruszkiczay-Rüdiger, Zs, Balázs, A., Csillag, G., Drijkoningen, G., Fodor, L., 2020. Uplift of the Transdanubian Range, Pannonian Basin: how fast and why? Glob. Planet. Chang. 192, 103263. https://doi.org/10.1016/j.gloplacha.2020.103263.
Sachsenhofer, R.F., Lankreijer, A., Cloetingh, S., Ebner, F., 1997. Subsidence analysis and quantitative basin modelling in the Styrian Basin (Pannonian Basin system, Austria). Tectonophysics 272, 175–196.
Sachsenhofer, R.F., Dunkl, I., Hasenhüttl, Ch., Jelen, B., 1998a. Miocene thermal history of the southwestern margin of the Styrian Basin: coalification and fission track data from the Pohorje/Kozjak area (Slovenia). Tectonophysics 297, 17–29.
Sachsenhofer, R.F., Rantitsch, G., Hasenhüttl, C., Russegger, B., Jelen, B., 1998b. Smectite to illite diagenesis in early Miocene sediments from the hyperthermal western Pannonian Basin. Clay Miner. 33, 523–537. https://doi.org/10.1180/000985598545778.
Sachsenhofer, R.F., Kogler, A., Polesny, F., Strauss, P., Wagreich, M., 2000. The Neogene Fohnsdorf Basin: Basin formation and basin inversion during lateral extrusion in the Eastern Alps (Austria). Int. J. Earth Sci. 89, 415–430.
Sachsenhofer, R.F., Bechtel, A., Reischenbacher, D., Weiss, A., 2003. Evolution of lacustrine systems along the Miocene Mur-Mürz fault system (Eastern Alps) and implications on source rocks in pull-apart basins. Mar. Pet. Geol. 20, 83–110.
Sandmann, S., Herwartz, D., Kirst, F., Froitzheim, N., Nagel, T.J., Fonseca, R.O.C., Münker, C., Janák, J., 2016. Timing of eclogite-facies metamorphism of mafic and ultramafic rocks from the Pohorje Mountains (Eastern Alps, Slovenia) based on Lu–Hf garnet geochronometry. Lithos 262, 576–585. https://doi.org/10.1016/j.lithos.2016.08.002.
Sant, K., Palcu, D.V., Mandic, O., Krijgsman, W., 2017. Changing seas in the Early–Middle Miocene of Central Europe: a Mediterranean approach to Paratethyan stratigraphy. Terra Nova 29, 273–281. https://doi.org/10.1111/ter.12273.
Sant, K., Kuiper, K.F., Rybár, S., Grunert, P., Harzhauser, M., Mandic, O., Jamrich, M., Šarinová, K., Hudáčková, N., Krijgsman, W., 2020. 40Ar/39Ar geochronology using high sensitivity mass spectrometry: examples from middle Miocene horizons of the Central Paratethys. Geol. Carpath. 71, 166–182. https://doi.org/10.31577/GeolCarp.71.2.5.
Scharf, A., Handy, M.R., Favaro, S., Schmid, S.M., Bertrand, A., 2013. Modes of orogen parallel stretching and extensional exhumation in response to microplate indentation and roll-back subduction (Tauern Window, Eastern Alps). Int. J. Earth Sci. 102 https://doi.org/10.1007/s00531-013-0894-4.
Schmid, S.M., Aebli, H.R., Heller, F., Zingg, A., 1989. The role of the Periadriatic line in the tectonic evolution of the Alps. In: Coward, M.P., Dietrich, D., Park, R.G. (Eds.), Alpine Tectonics, Geol. Soc. Spec. Publ. London, Vol. 45, pp. 153–171.
Schmid, S.M., Fügenschuh, B., Kissling, E., Schuster, R., 2004. Tectonic map and overall architecture of the Alpine orogen. Swiss J. Geosci. 97, 93–117.
Schmid, S.M., Bernoulli, D., Fügenschuh, B., Maţenco, L., Schuster, R., Schefer, S., Tischler, M., Ustaszewski, K., 2008. The Alpine-Carpathian-Dinaridic orogenic system: correlation and evolution of tectonic units. Swiss J. Geosci. 101, 139–183.
Schmid, S., Scharf, A., Handy, M.R., Rosenberg, C., 2013. The Tauern window (Eastern Alps, Austria): a new tectonic map, with cross sections and a tectonometamorphic synthesis. Swiss J. Geosci. 106, 1–32.
Schmid, S.M., Fügenschuh, B., Kounov, A., Maţenco, L., Nievergelt, P., Oberhänsli, R., Pleuger, J., Schefer, S., Schuster, R., Tomljenović, B., Ustaszewski, K., van Hinsbergen, D.J.J., 2020. Tectonic units of the Alpine collision zone between Eastern Alps and western Turkey. Gondwana Res. 78, 308–374.
Schulz, S., 2012. Zircon (U-Th)/He Thermochronology of the Drauzug and the Carnic Alps. Master thesis. Department Sedim. Envir. Geol., Geoscience Center, Georg-August-Univ., Göttingen.
Schuster, R., Stüwe, K., 2008. Permian metamorphic event in the Alps. Geology 36, 603–606. https://doi.org/10.1130/G24703A.1.
Schuster, R., Koller, F., Hoeck, V., Hoinkes, G., Bousquet, R., 2004. Explanatory notes to the map: metamorphic structure of the Alps - metamorphic evolution of the Eastern Alps. Mitt. Österr. Miner. Ges. 149, 175–199.
Selmeczi, I., Bohn-Havas, M., Szegő, É., 2004. Prepannonian Miocene sequences of the SW edge of the Transdanubian Central Range. Litho- and biostratigraphy. Acta Palaeont. Rom. 4, 463–466.
Singleton, J.S., 2013. Development of extension-parallel corrugations in the Buckskin-Rawhide metamorphic core complex, west-central Arizona. Geol. Soc. Am. Bull. 125, 453–472. https://doi.org/10.1130/B30672.1.
Sölva, H., Stüwe, K., Strauss, P., 2005. The Drava River and the Pohorje Mountain Range (Slovenia): geomorphological interactions. Mitt. Naturwiss. Ver. Steiermark 134, 45–55.
Sotelšek, T., Jarc, S., Zupančič, N., Vrabec, M., 2019. The crystallization depth of quartz monzodiorite from Pohorje Mountains. In: Pirker, L. (Ed.), 3rd Meeting of Slovenian Microscopists, Ljubljana, 2019, 72, COBISS.SI-ID 1481822.
Spencer, J.E., 1984. Role of tectonic denudation in warping an uplift of low-angle normal faults. Geology 12, 95–98. https://doi.org/10.1130/0091-7613(1984)12<95:ROTDIW>2.0.CO;2.
Spencer, J.E., 1999. Geologic continuous casting below continental and deep-sea detachment faults and at the striated extrusion of Sacsayhuaman, Peru. Geology 27, 327–330.
Stingl, K., 1994. Depositional environment and sedimentary of the basinal sediments in the Eibiswalder Bucht (Radl Formation and Lower Eibiswald Beds) Miocene Western Styrian Basin, Austria. Geol. Rundsch. 83, 811–821.
Stojadinović, U., Toljić, M., Matenco, L., Andriessen, P.A.M., Foeken, J.P.T., 2013. The balance between orogenic building and subsequent extension during the Tertiary evolution of the NE Dinarides: Constraints from low-temperature thermochronology. Global Planet. Change 103, 19–38.
Strauss, P., Wagreich, M., Decker, K., Sachsenhofer, R.F., 2001. Tectonics and sedimentation in the Fohnsdorf–Seckau Basin (Miocene, Austria): from a pull-apart basin to a half-graben. Int. J. Earth Sci. 90, 549–559. https://doi.org/10.1007/s005310000180.
Stüwe, K., Schuster, R., 2010. Initiation of subduction in the Alps: continent or ocean? Geology 38, 175–178. https://doi.org/10.1130/G30528.1.
Szives, O., Fodor, L., Fogarasi, A., Kövér, Sz, 2018. Integrated calcareous nannofossil and ammonite data from the upper Barremian–lower Albian of the northeastern Transdanubian Range (central Hungary): stratigraphical implications and consequences for dating tectonic events. Cretac. Res. 91, 229–250. https://doi.org/10.1016/j.cretres.2018.06.005.
Sztanó, O., Kováč, M., Magyar, I., Šujan, M., Fodor, L., Uhrin, A., Rybár, S., Csillag, G., Tőkés, L., 2016. Late Miocene sedimentary record of the Danube/Kisalföld Basin: interregional correlation of depositional systems, stratigraphy and structural evolution. Geol. Carpath. 67, 525–542.
Tari, G., 1994. Alpine Tectonics of the Pannonian basin. PhD. Thesis, Rice University, Texas, USA, 501 pp.
Tari, G., 1996. Extreme crustal extension in the Rába river extensional coridor (Austria/Hungary). Mitt. Gesell. Geol. Bergbaustud. Österreich 41, 1–18.
Tari, G., Horváth, F., 2010. Eo-Alpine evolution of the Transdanubian Range in the nappe system of the Eastern Alps: revival of a 15 years tectonic model. Földtani Közlöny 140, 483–510.
Tari, G., Linzer, H.-G., 2018. Austrian versus Hungarian bauxites in an Alpine tectonic context: a tribute to Prof. Andrea Mindszenty. Földtani Közlöny 148, 35–44.
Tari, G., Horváth, F., Rumpler, J., 1992. Styles of extension in the Pannonian Basin. Tectonophysics 208, 203–219. https://doi.org/10.1016/b978-0-444-89912-5.50016-8.
Tari, G., Dövényi, P., Dunkl, I., Horváth, F., Lenkey, L., Stefanescu, M., Szafián, P., Tóth, T., 1999. Lithospheric structure of the Pannonian basin derived from seismic, gravity and geothermal data. In: Durand, B., Jolivet, L., Horváth, F., Séranne, M. (Eds.), The Mediterranean Basins: Tertiary Extension Within the Alpine Orogen, Geol. Soc. Spec. Publ., Vol. 156, pp. 215–250. https://doi.org/10.1144/gsl.sp.1999.156.01.12.
Tari, G., Arbouille, D., Schléder, Zs, Tóth, T., 2020a. Inversion tectonics: a brief petroleum industry perspective. Solid Earth. https://doi.org/10.5194/se-2020-33.
Tari, G., Gjerazi, I., Graseman, B., 2020b. Interpretation of Vintage 2D Seismic Reflection Data Along the Austrian-Hungarian Border: Subsurface Expression of the Rechnitz Metamorphic Core Complex. Interpretation. (in press).
Tari, G., Bada, G., Beidinger, A., Csizmeg, J., Danišík, M., Gjerazi, B., Grasemann, P., Kováč, M., Plašienka, D., Šujan, M., Szafián, P., 2021. The connection between the Alps and the Carpathians beneath the Pannonian Basin: selective reactivation of Alpine nappe contacts during Miocene extension. Glob. Planet. Chang. 197, 103401.
Thöni, M., 2006. Dating eclogite-facies metamorphism in the Eastern Alps – approaches, results, interpretations: a review. Mineral. Petrol. 88, 123–148. https://doi.org/10.1007/s00710-006-0153-5.
Tirel, C., Brun, J.P., Burov, E., 2008. Dynamics and structural development of metamorphic core complexes. J. Geophys. Res. 113, 215–250.
Toljić, M., Matenco, L., Ducea, M.N., Stojadinović, U., Milivojević, J., Đerić, N., 2013. The evolution of a key segment in the Europe–Adria collision: the Fruška Gora of northern Serbia. Glob. Planet. Chang. 103, 39–62.

Tomljenović, B., Csontos, L., 2001. Neogene-Quaternary structures in the border zone between Alps, Dinarides and Pannonian basin (Hrvatsko zagorje and Karlovac basin, Croatia). Int. J. Earth Sciences 90, 560–578. https://doi.org/10.1007/s005310000176.

Tommasi, A., Vauchez, A., 2001. Continental rifting parallel to ancient belts: an effect of the mechanical anisotropy of the lithospheric mantle. Earth Planet. Sci. Lett. 185, 199–210.

Trajanova, M., 2002. Significance of mylonites and phyllonites in the Pohorje and Kobansko area. Geologija 45, 149–161.

Trajanova, M., Pécskay, Z., Itaya, T., 2008. K–Ar dating and petrography of the Neogene Pohorje Mts. igneous rocks, Slovenia. Geol. Carpathica 59, 247–260.

Ustaszewski, K., Kounov, A., Schmid, S.M., Schaltegger, U., Krenn, E., Frank, W., Fügenschuh, B., 2010. Evolution of the Adria-Europe plate boundary in the northern Dinarides: from continent-continent collision to back-arc extension. Tectonics 29. https://doi.org/10.1029/2010TC002668. TC6017.

van Gelder, I.E., Matenco, L., Willingshofer, E., Tomljenović, B., Andriessen, P.A.M., Ducea, M.N., Beniest, A., Gruić, A., 2015. The tectonic evolution of a critical segment of the Dinarides-Alps connection: kinematic and geochronological inferences from the Medvednica Mountains, NE Croatia. Tectonics 34, 1952–1978. https://doi.org/10.1002/2015TC003937.

van Gelder, I.E., Willingshofer, E., Sokoutis, D., Cloetingh, S.A.P.L., 2017. The interplay between subduction and lateral extrusion: a case study for the European Eastern Alps based on analogue models. Earth Planet. Sci. Lett. 472, 82–94. https://doi.org/10.1016/j.epsl.2017.05.012.

van Gelder, I.E., Willingshofer, E., Andriessen, P.A.M., Schuster, R., Sokoutis, D., 2020. Cooling and vertical motions of crustal wedges prior to, during and after lateral extrusion in the Eastern Alps: new field kinematic and fission track data from the Mur-Mürz fault system. Tectonics 39, e2019TC005754. https://doi.org/10.1029/2019TC005754.

van Wijk, J.W., Cloetingh, S.A.P.L., 2002. Basin migration caused by slow lithospheric extension. Earth Planet. Sci. Lett. 198, 275–288.

Wernicke, B., 1985. Uniform-sense normal simple shear of the continental lithosphere. Can. J. Earth Sci. 22, 108–125. https://doi.org/10.1139/e85-009.

Wernicke, B., Axen, G.J., 1988. On the role of isostasy in the evolution of normal fault systems. Geology 16, 848–851. https://doi.org/10.1130/0091-7613(1988)016<0848:OTROII>2.3.CO;2.

Willingshofer, E., Neubauer, F., 2002. Structural evolution of an antiformal window: the Scheiblingkirchen Window (Eastern Alps, Austria). J. Struct. Geol. 24, 1603–1618. https://doi.org/10.1016/S0191-8141(01)00161-4.

Willingshofer, E., Neubauer, F., Cloetingh, S., 1999. The Significance of Gosau-Type Basins for the Late Cretaceous Tectonic History of the Alpine-Carpathian Belt. Phys. Chem. Earth A 24 (8), 687–695.

Windhoffer, G., Bada, G., Nieuwland, D., Wórum, G., Horváth, F., Cloetingh, S., 2005. On the mechanics of basin formation in the Pannonian basin: inferences from analogue and numerical modelling. Tectonophysics 410, 389–415.

Wölfler, A., Kurz, W., Danisik, M., Rabitsch, R., 2010. Dating of fault zone activity by apatite fission track and apatite (U-Th)/He thermochronometry: a case study from the Lavanttal fault system (Eastern Alps). Terra Nova 22, 274–282.

Wölfler, A., Kurz, W., Fritz, H., Stüwe, K., 2011. Lateral extrusion in the Eastern Alps revisited: refining the model by thermochronological, sedimentary, and seismic data. Tectonics 30, 1–15.

Zhao, L., Paul, A., Malusà, M., Xu, X., Zheng, T., Solarino, S., Guillot, S., Schwartz, S., Dumont, T., Salimbeni, S., Aubert, C., Pondrelli, S., Wang, Q., Zhu, R., 2016. Continuity of the Alpine slab unraveled by high-resolution P wave tomography. J. Geophys. Res. Solid Earth 121. https://doi.org/10.1002/2016JB013310.

Žnidarčič, M., Mioč, P., 1988. Geological Map of the Sheets Maribor and Leibnitz, L 33-56 and L 33-44, 1:100 000. Federal Geol. Surv. of Yugoslavia, Belgrade.